

GENESIS OF SOILS AND CARBONATE ENRICHED HORIZONS
IN A CLIMO-SEQUENCE DEVELOPED OVER CRETACEOUS LIMESTONE
IN CENTRAL AND WEST TEXAS

A Dissertation

by

MARTIN CAPELL RABENHORST

Submitted to the Graduate College of
Texas A&M University
in partial fulfillment of the requirements for the degree of
DOCTOR OF PHILOSOPHY

May 1983

Major Subject: Soil Science

GENESIS OF SOILS AND CARBONATE ENRICHED HORIZONS
IN A CLIMO-SEQUENCE DEVELOPED OVER CRETACEOUS LIMESTONE
IN CENTRAL AND WEST TEXAS

A Dissertation

by

MARTIN CAPELL RABENHORST

Approved as to style and content by:



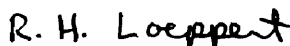
L. P. Wilding
(Chairman of Committee)



B. L. Allen
(Member)



C. T. Hallmark
(Member)



R. H. Loeppert
(Member)



R. Rezak
(Member)



E. C. A. Runge
(Head of Department)

May 1983

1810638

ABSTRACT

Genesis of Soils and Carbonate Enriched Horizons
in a Climo-Sequence Developed Over Cretaceous Limestone
in Central and West Texas. (May 1983)

Martin Capell Rabenhorst, B.S., University of Maryland;

M.S., University of Maryland

Chairman of Advisory Committee: Dr. L. P. Wilding

The Edwards Plateau covers 10 million ha in Central and West Texas (nearly 14% of the state) and is an important agricultural rangeland. A strong climo-gradient extends across the area with annual precipitation decreasing westward from 800 to 300 mm. There is a paucity of information on the shallow and stony soils derived from Cretaceous limestone. Following reconnaissance investigations of 34 sites, 15 pedons were sampled and analyzed for routine physical, chemical, mineralogical and micromorphological data. Four pedons were selected for detailed mineralogical, elemental, and SEM analyses. These data serve for developing pedogenic models.

Carbonate levels in surface horizons were significantly correlated with Thornthwaite's P-E (moisture) index. Soils in the western part of the area commonly had calcic or petrocalcic horizons. Argillic horizons were common in the easternmost part of the study area although illuvial argillans were difficult to verify except in protected areas such as pores within chert fragments.

Euhedral, prismatic quartz grains were identified by SEM to be a prominent component of residues from hard crystalline limestones. These grains were used as marker minerals in identifying parent material discontinuities. Quartz grain morphology, particle size distribution, elemental assay, and mineralogical data indicate a discontinuity between the soil and subjacent limestone. The underlying rock should not, therefore, be considered as the soil parent material. Airborne dusts of uniform quantity and composition are deposited to the surface at the approximate rate of 1 mm/100 yrs. Marker minerals indicate, however, that these dusts are not accumulating on stable land surfaces because erosion presumably exceeds accretion.

Differentiation of lithogenic (limestone) from pedogenic forms of carbonates in soils was accomplished by applying microfabric and stable carbon isotope methodologies. Both methods confirmed that massive indurated carbonate zones and much of the disseminated carbonates were pedogenically derived. Petrocalcic horizons occurring over limestone have formed through in situ pedogenic alteration and reconstitution of limestone. This is distinctly different from the 4-stage model of Gile et al. (1966). A new 3-stage model is proposed to describe the genesis of limestone derived petrocalcic horizons.

DEDICATION

SOLI DEO GLORIA

PREFACE

Every man by nature desires to know, but of what avail is knowledge without the fear of God? A humble farm laborer who serves God is more acceptable to Him than an inquisitive philosopher who, considering the constellations of heaven, willfully forgets himself. He who knows himself well is mean and abject in his own sight, and takes no delight in the vain praise of men. If I knew all things in this world, but knew without charity, what would it avail me before God, who judges every man according to his deeds? Let us, therefore, cease from the desire of such vain knowledge, for often great distraction and deceit of the enemy are found in it, and so the soul is much hindered and blocked from the perfect and true love of God.

Thomas A. Kempis

The Imitation of Christ, 1427

ACKNOWLEDGMENTS

The author is grateful to his major advisor, Dr. Larry Wilding, for his thoughtful and wise counsel and encouragement during the course of this study.

Thanks are also due Drs. Allen, Hallmark, Loeppert, and Rezak for their helpful suggestions and participation in various phases of this project.

The selection of prime sampling locations would not have been possible without the much appreciated assistance of many USDA-Soil Conservation Service personnel. Particular thanks are given Mr. C. L. Girdner for his help in coordinating this effort.

Larry West, Richard Drees, and Ernest Rivers all provided invaluable assistance in the laboratory phase of this study for which the author is grateful.

The author extends thanks to James Rehage, Terry Moore, and Larry West for their help during the installation of dust collection traps and pedon sampling.

The assistance of Mr. Alejandro Ramirez in laboratory analysis and in preparing final drafts of some of the figures is gratefully acknowledged.

The faithful prayers, encouragement, and love of many friends have been instrumental in the completion of this dissertation, but none so much as those of my wife Judy, and my children Annie and Daniel.

TABLE OF CONTENTS

	Page
INTRODUCTION.	1
REVIEW OF LITERATURE.	3
Geology of the Edwards Plateau Region.	3
Climate as a Soil Forming Factor	7
Pedogenesis of Carbonate-Enriched Horizons	8
Dust Contributions and Characterization.	15
METHODS AND MATERIALS	18
Site Selection	18
Field Procedures	20
Laboratory Procedures.	24
RESULTS AND DISCUSSION.	32
Effect of Climate on Soil Properties	32
Parent Material Identification and Uniformity.	43
Differentiation of Pedogenic and Lithogenic Carbonates	85
Pedogenesis of Petrocalcic Horizons.	104
Identification and Genesis of Argillic Horizons.	111
CONCLUSIONS	123
LITERATURE CITED.	128
APPENDIX	
A. PEDON DESCRIPTIONS	135
B. COLLECTION AND CHARACTERIZATION OF AIRBORNE DUST IN TEXAS.	165
C. pH EFFECTS ON CLAY RESIDUES DURING CARBONATE DISSOLUTION.	184
D. IDENTIFICATION OF PEDOGENIC CARBONATES USING STABLE CARBON ISOTOPES	196
E. SOIL CHARACTERIZATION LABORATORY DATA.	225
F. FREE IRON OXIDE LEVELS IN SELECTED PEDONS AND HORIZONS	241
G. PARTICLE SIZE DISTRIBUTION FOR LIMESTONE AND PETROCALCIC RESIDUES	243
H. LITERATURE CITED FOR APPENDICES.	246
VITA.	251

LIST OF TABLES

Table	Page
1. Pedon number, county, and classification of the 15 pedons sampled for detailed analyses during this study	22
2. Estimates of secondary silica content in selected fractions and horizons of the Kinney Co. pedon (#7) based on optical examination	47
3. Semi-quantitative [†] interpretations of XRD analyses of the Kinney Co. pedon.	49
4. Approximate estimates of secondary silica content in selected fractions and horizons of the Pecos Co. pedon (#9). Estimates based on optical examination and/or specific gravity separations.	50
5. Semi-quantitative [†] interpretations of XRD analyses of the Pecos Co. pedon	54
6. Semi-quantitative [†] interpretations of XRD analyses of the Val Verde Co. pedon	69
7. Semi-quantitative [†] interpretations of XRD analyses of the Real Co. pedon.	76
8. Average particle size distribution for dusts (Seven sites and 4 collection periods).	80
9. Semi-quantitative [†] interpretations of XRD analyses of dusts; Summary (Seven sites and 3 collection periods) . .	81
10. Average elemental analysis of the 5-20 μ m fraction of dusts collected.	81
11. Percent calculated pedogenic carbonates in questionable petrocalcic materials based on carbon isotope analysis . . .	103
12. Approximate levels of secondary silica in major horizons of the Pecos Co. pedon (#9) based on optical examination and/or specific gravity separations.	109
13. Plasmic fabrics [†] and major micromorphic features of four pedons containing argillic horizons	115

LIST OF FIGURES

Figure	Page
1. Locations of reconnaissance sites sampled for limestone analyses during preliminary stages of the study.	19
2. Locations of sites selected for detailed sampling, analyses, and pedon descriptions. Site numbers were assigned alphabetically according to county name and then sequentially for counties with more than one pedon. . .	21
3. Annual rainfall (mm) across the Edwards Plateau region. Note the steady decrease from east to west (modified from Texas State Climatologist, 1974)	33
4. Annual class-A pan evaporation (mm) across the Edwards Plateau region. Note the strong east-west gradient (modified from U.S. Dept. Commerce, 1968).	34
5. Values of Thornthwaite's P-E index across the Edwards Plateau region (modified from USDA, 1957).	35
6. Levels of CaCO ₃ occurring in the <2 mm fraction of A horizons of pedons sampled in this study. Note the general though variable trend of increasing levels in an east to west direction.	37
7. Graphs showing Thornthwaite's P-E index versus depth to indurated carbonate and versus percent CaCO ₃ in the A horizons of the 15 pedons sampled.	38
8. Occurrence of petrocalcic horizons in pedons sampled during this study based on field identification.	39
9. Occurrence of argillic horizons in pedons sampled during this study.	41
10. Carbonate-free and carbonate-free, clay-free PSD and sand and silt ratios shown with depth for the Kinney Co. pedon (#7)	46
11. Elemental analyses of carbonate-free silt fractions from soil and residue of the Kinney Co. pedon (#7)	48
12. Carbonate-free and carbonate-free, clay-free PSD and sand and silt ratios shown with depth for the Pecos Co. pedon (#9)	51

Figure	Page
13. Elemental analyses of carbonate-free silt fractions from soil and residue of the Pecos Co. pedon (#9)	53
14. Euhedral prismatic quartz from the medium silt (5-20 μm) fraction of the non-carbonate residue of the limestone underlying the Pecos Co. pedon (#9).	56
15. Prismatic quartz from the carbonate-free residue of the C2cam horizon of the Pecos Co. pedon (#9). Note the partial coating of secondary silica on the lower portion of the grain (arrows).	59
16. General SEM fields showing representative grains from carbonate-free residues of the C1cam (A), C2cam upper (B), C2cam lower (C), and R (D) horizons of the Pecos Co. pedon (#9). Note quartz prisms present in all horizons but especially abundant in the R horizon. Note also the abundance of spongy opaline materials (o) in the lower C2cam field (C). Line scale is 20 μm	61
17. Representative quartz grains from the silt fractions of the A11 (C and D) and the A12 (A and B) horizons of the Pecos Co. pedon (#9). Note the rounded edges and rough pitted surfaces.	63
18. Rare prismatic quartz grains from the A horizons of the Pecos Co. pedon (#9). Note the well preserved euhedral morphology	65
19. Carbonate-free and carbonate-free, clay-free PSD and sand and silt ratios shown with depth for the Val Verde Co. pedon (#15).	66
20. Elemental analyses of carbonate-free silt fractions from soil and residue of the Val Verde Co. pedon (#15).	68
21. General SEM fields showing representative grains of carbonate-free silts from the A horizon (A) and residue of the laminar cap (B) and underlying limestone bedrock (C and D). Note scarcity of quartz prisms in the A1 horizon (arrow), common occurrence in the laminar cap, and prominence (with kaolinite) in the bedrock. Both euhedral quartz prisms (q) and euhedral hexagonal kaolinite plates (k) are considered to be authigenic. Line scales are 10 μm	71

Figure	Page
22. Carbonate-free and carbonate-free, clay-free PSD and sand and silt ratios shown with depth for the Real Co. pedon (#11).	73
23. Elemental analyses of carbonate-free silt fractions from soil and residue of the Real Co. pedon (#11).	74
24. General SEM fields showing representative silt grains from the B22t horizon (A), B3tca horizon (B), and the limestone residue (C and D) of the Real Co. pedon (#11). Note the abundance of quartz prisms marked by prominent striations in the limestone residue. Prismatic quartz crystals are rare in the B3tca (arrows) and absent from the B22t. Line scale is 10 μ m	78
25. Examples of convoluted microfabrics in petrocalcic horizons: C1cam horizon (A and D) and the R1ca/C2cam horizon (C) from pedon #12; A13 & Ccam horizon (B) of pedon #13. Both pedons are in Sutton Co. The line scale is 1 mm. Cross-polarized light.	87
26. Examples of nodular microfabrics in petrocalcic horizons: C1cam (A) and C2cam (B) horizons of Pecos Co. pedon #9; Ccam horizon (C) of the Crockett Co. pedon (#2); Rca/Ccam horizon (D) of the Kerr Co. pedon (#5). Line scale is 1 mm. Cross-polarized light.	90
27. Examples of pisolitic (A and B) and recrystallized (C and D) microfabrics in petrocalcic horizons: Ccam&A1 horizon (A) of the Crockett Co. pedon (#2); C1cam horizon (B) from Pecos Co. pedon #10; C2cam (C) and C1cam (D) horizons from Pecos Co. pedon #9. D shows a few zones of micritic convolutions (mc). Line scale is 1 mm. A and B under plane light. C and D under cross-polarized light.	92
28. Progressive stages in the formation of micritic convoluted fabric through the weathering of limestone. Well crystallized limestone (A) shows slight micritic zones around some pores (arrows). B and C show further development of micritic zones around growing pores which begin to coalesce. D shows nearly complete development of convoluted fabric. R horizon from Gillespie Co. pedon #4. Line scale is 0.5 mm. Cross-polarized light	96

Figure	Page
29. Formation of convoluted fabric through the growth of calcite needles. The higher magnification of A and B reveals growth and coalescing of needles to form a network. C and D show the network at a more advanced stage of formation with a distinctly convoluted appearance. Note in D the presence of Fossils (f) still remaining in the yet unaltered soft limestone material. A, B, and C are from the Cr2 horizon and D from the Cr3 horizon of a soil in the Real series in Hays Co. (not from this study). Line scale is 0.5 mm. Cross-polarized light.	99
30. Formation of nodular microfabric. A and B show alteration of crystalline limestone (ls) (R horizon of Medina Co. pedon #8) to a nodular material (n). Note how in B a limestone remnant has been engulfed by the encroaching nodular matrix. C shows the highly calcareous (44% CaCO ₃) A1 horizon from the Terrell Co. pedon (#14). It has a similar appearance to some nodular fabrics and might be considered a "proto-nodular" or "neo-nodular" fabric. Line scale is 1 mm. Cross-polarized light.	101
31. Fluorite percentages in the carbonate-free residues and fluorite PSD for Pecos Co. pedon #9.	108
32. Clay distribution depth functions for the 4 pedons containing argillic horizons. The B3tca horizon (65-80cm) of pedon #11 was reported on a carbonate-free basis. All other horizons were non-calcareous	113
33. Illuviation argillans present in rhombahedral pores vacated by dissolved dolomite crystals. A and B are from the B22t horizon of the Gillespie Co. pedon (#4) under cross-polarized and plane light respectively. C and D are from the A11 horizon of the Comal Co. pedon (#1) under cross-polarized and plane light respectively. E and F are from the A1 and B21t horizons respectively of the Gillespie Co. pedon (#4) as photographed under plane light. Note in C the band extinction of the argillans (arrows). Note also in A the striated argillan (sa) around the chert fragment.	121
34. Schematic diagram illustrating the weathering of numerous strata of limestone during the accumulation of a residual solum. One or more of the overlying strata may have contrasting residues from the limestone underlying the solum. Soils in the more humid eastern portion of the area tend to have deeper sola while soils in the more arid region tend to have shallower sola which may overlies petrocalcic horizons	124

Figure	Page
35. Four sequential stages in the formation of petrocalcic horizons by <u>in situ</u> pedogenic alteration of limestone and enrichment with pedogenic carbonates. Stage 0 shows the unaltered limestone precursor to the petrocalcic horizon. Stage 3 shows the completely formed petrocalcic horizon.	127

INTRODUCTION

Cretaceous rocks cover about 28 percent of the exposed land area in Texas and approximately one-half of that (10 million hectares) occurs in the Edwards Plateau region. Nearly all of this region is rangeland and is an important area for the production of wool and mohair. A strong climatic gradient exists across the region with the annual precipitation decreasing from about 800 mm at the easternmost edge to 300 mm at its western extreme. Such a pronounced moisture gradient should be clearly reflected in both the genesis and morphology of the soils of the area.

The land surface of the Edwards Plateau is comprised of soils overlying lower to mid Cretaceous limestone, dolomite, and marl, and some calcareous shale and sandstone. The soils of this region are shallow and commonly skeletal, and are generally considered to be residual in origin. The Edwards Plateau is in proximity to extensive desert regions both to the south and west which provide a possible source for airborne dusts carried into the area. While dust additions as storm events have been documented and more gradual additions have been postulated, the actual rates of additions or long-term impact on pedogenesis in this region have not heretofore been established.

Many of the soils in the western part of the Edwards Plateau show evidence of carbonate enrichment. While some of the carbonate

This dissertation conforms to the format and style guidelines of the Soil Science Society of America Journal.

features are obviously of pedogenic origin, it is not clear whether other carbonate forms have formed through pedogenic processes or if they were inherited from the parent lithology (lithogenic). This differentiation is clearly important from the standpoint of genesis and classification of the soils but may also hold implications for soil chemistry and fertility.

The objectives of this study were therefore to: 1) investigate the development of pedogenic features as a function of climate in soils formed over hard Cretaceous limestone on the Edwards Plateau; 2) identify parent materials of soils occurring on the Edwards Plateau and estimate the contributions of eolian material and evaluate the magnitude of its effect on soil formation; and 3) investigate the formation and identification of carbonate enriched horizons including the differentiation of pedogenic from lithogenic forms of carbonates.

REVIEW OF LITERATURE

Geology of the Edwards Plateau Region

Toward the close of the Jurassic about 135 million years ago, nearly all of North America was exposed as dry land (Adkins, 1978). As a result of eustatic changes in sea level, generally thought to be glacially controlled (Jacka, 1977), the Cretaceous seas began advancing northward across Texas as far as Colorado where they joined with the southern part of the Arctic Sea. The earliest Cretaceous sediments to be deposited were of the Trinity group. The only really significant member of this group on the Edwards Plateau is the Glen Rose formation (Fisher, 1974, 1981a).

Glen Rose sediments are generally accepted to be low-energy, shallow water deposits of supratidal, intertidal and subtidal facies (Loucks et al., 1978; Adkins, 1978). Nelson (1973) and Rose (1978) have indicated that these formed on a protected shelf in a backreef area. The reef was described as running in a NE to SW direction about 100 miles east of Austin and San Antonio, and being comprised mainly of rudists [elongate, conical pelecypods (clams) of several families] (Nelson, 1973). The Glen Rose is typically described as containing thin to medium bedded hard crystalline limestone alternating with shale, marl, or marly limestone (Adkins, 1978; Loucks et al., 1978). The terrigenous sediments are presumably derived from the Llano Uplift (Central Basin) which was at that time exposed and subject to erosion, but was later covered during mid-Fredericksburg deposition (Loucks et al., 1978; Adkins, 1978). These alternating beds of hard and soft

material have been responsible for the characteristic benched or stair-stepped topography of landscapes on this formation.

At the beginning of the Fredericksburg deposition, there was a rapid transgression (shoreward advance) of the sea northward across the Glen Rose sediments. Initial deposits were argillaceous sediments containing a variety of mollusk shells. These clays were subsequently covered by carbonate muds dominantly of miliolid foraminifera and shell fragments. These sediments occurred conformably over the Glen Rose (Rose, 1978). While the Walnut and Comanche Peak formations are commonly exposed in Central Texas and toward the Grand Prairie, they are of little importance in the Edwards Plateau. Only the Edwards formation is of significant areal extent. Adkins (1978) has suggested that the formations in the Fredericksburg group and the Washita (overlying) group may not represent true stratigraphic formations but may rather in fact only represent different facies. This should be kept in mind, although the following discussion will refer to them as formations. Rose (1978) has described the Edwards formation as a shallow marine deposit of intertidal and supratidal facies forming west of the Stuart City reef. Most commonly, the Edwards is considered to be a reef complex consisting of reef and inter-reef deposits which themselves transgressed northward across the Glen Rose. Both biohermal (mounds) and biostromal (shell beds) forms have been observed, largely dominated by rudists, other mollusks, and miliolid formaminifera (Nelson, 1973; Lozo et al., 1959; Adkins, 1978). Southward, the Edwards grades into the Devils River limestone which also contains abundant rudists, shell fragments, and miliolid formaminifera

(Rodda et al., 1966). Rudistid reefs are, however, less common in the Devils River Formation. Rose (1978) has reported that a rapid rise in sea level was responsible for bringing the Fredericksburg deposition to a close. Lozo et al. (1959), however, stated that a slight regional uplift was the cause. In either case, the Edwards is thought to have undergone lithification and some alteration (boring, recrystallization, or dolomitization) prior to Washita deposition (Lozo et al., 1959; Nelson, 1973).

During Washita sedimentation, reefs still provided protection for deposition in shallow water environments (Rose, 1978). These early Washita deposits also contained abundant rudists and formed the Georgetown formation. The Georgetown is more distinct in the northeastern part of the Edwards Plateau and in Central Texas but tends to grade indistinguishably into the Edwards and Devils River formations in the south (Rodda et al., 1966; Rose, 1978). A rise in sea level later in the Washita gave rise to an influx of terrigenous sediments resulting in the Del Rio Clay (called the Grayson Clay in the northern and eastern portion of the Edwards Plateau) (Rose, 1978; Adkins, 1978). Subsequent deposition of rudist and calcareous muds occurred until the end of the Washita. This resulted in the formation of the Buda limestone. A drop in sea level exposed the Washita to erosion and to subaerial alteration and brought the Washita to a close (McFarlan, 1977).

The Washita is the uppermost unit in the Comanchean series (lower Cretaceous). The Gulfian series marks the beginning of the upper Cretaceous units. The Boquillas formation (part of the Eagle Ford

group) which is dominated by flaggy, marly and clayey beds, and the Austin formation which is a white chalky limestone that becomes more crystalline toward the west, are both present and exposed on the Edwards Plateau, particularly in the southwest portion in Val Verde and Terrell Counties. For reasons to be discussed later, these formations were not included in the main portion of this study and therefore will not be discussed further.

In general, the Edwards Plateau has been subject to erosion and downcutting such that the surface geology in the eastern 20% (from Austin and New Braunfels to Kerrville, Fredericksburg, and Bandera) is dominated by the Glen Rose limestone. The primary exception to this is along the Balcones escarpment where faulting has preserved substantial areas of Fredericksburg and younger rocks. Depending on the stratigraphic model, most of the remainder of the Edwards Plateau is either Fredericksburg (mainly Edwards formation) or Fredericksburg and Washita. Fairly recently, the Edwards formation has been divided into a lower member (Ft. Terrett) and an upper member (Segovia) (Rodda et al., 1966; Jacka, 1977; Rose, 1978). In the central and western parts of the Edwards Plateau, the dissected landscapes primarily expose the Segovia member of the Edwards, except in more deeply cut valleys where the Ft. Terrett is exposed. Rose (1978) has included the upper Segovia in the Washita group as apparently has the American Association of Petroleum Geologists (1973). If the Segovia were kept in the Fredericksburg group, then Washita exposures would be limited to high broad divides where the Buda limestone is exposed in Crockett, Sutton, Schleicher Counties and further north and west (Fisher, 1981b). As

mentioned earlier, the Edwards limestone grades southward into the Devils River limestone in Val Verde and Edwards Counties.

Climate as a Soil Forming Factor

Climate has long been recognized as an important agent of pedogenesis and it was included by Jenny (1941b) as one of five factors responsible for soil formation. The two most significant components of climate are temperature and precipitation. Emphasis in this discussion will be given to precipitation and its effects on calcareous soils in subhumid, semiarid, and arid regions. For a more comprehensive discussion of the effects of climate in soil formation see Jenny (1941b). Temperature is included only indirectly as it is related to evaporation, which modifies the effectiveness of precipitation in certain pedogenic processes.

Simonson's (1959) model of pedogenesis includes four major processes: additions; losses; translocations; transformations. While precipitation does affect vegetative cover, organic matter additions, and organic and mineral transformations, the main effects under the previously described conditions are to cause translocations and losses of labile materials such as carbonates. While the general relationship between precipitation and carbonate leaching has been established, relatively little work has been done to quantitatively or statistically relate these conditions.

While attempting to hold other factors constant, Jenny and Leonard (1934) measured various soil properties across an area having a precipitation gradient. Strong relationships were observed between

rainfall and such properties as depth to carbonates, percent N, percent clay, pH, and cation exchange capacity (Jenny, 1941b). In a study in California, Arkley (1963) observed a positive correlation ($r=0.76$) between annual precipitation and depth to the carbonate horizon. A stronger relation ($r=0.95$) was observed between depth to the carbonate horizon and the calculated depth of leaching (leaching index). Arkley's leaching index included potential evapotranspiration and water holding capacity as well as precipitation. Jenny (1941b) and Arkley (1963) developed different mathematical functions relating precipitation and depth to carbonates. This was due to differences in seasonal patterns of rainfall; the predominantly winter rainfall of California was more effective in the leaching of carbonates. Specific details concerning the climate of the Edwards Plateau region including precipitation and evapotranspiration are included in the results and discussion section.

Pedogenesis of Carbonate-Enriched Horizons

Carbonates are commonly present in soils in arid and semi-arid regions where precipitation is insufficient for leaching and removal of carbonates. Horizons of carbonate enrichment are generally considered to be the result of the translocation of carbonates within a pedon. While some have suggested the translocation to be upward through capillary rise from a water table (Redmond and McClelland, 1959; Sobecki, 1980), the downward movement of water is generally held to be the primary mode of translocation (Jenny, 1941a). The zone of carbonate accumulation is generally thought to occur at the depth of

frequent wetting (Flach et al., 1969) or near the lower depth of water penetration (Harper, 1957). Stuart and Dixon (1973) have also reported the effect of abrupt textural discontinuities in restricting water movement through soils, resulting in carbonate accumulations at the textural interface.

There have been four main hypothesized and/or substantiated sources for the calcium bicarbonate in the soil solution. The most obvious source is the case where the soil parent material itself is calcareous, such as calcareous glacial till, limestone residuum, calcareous loess, or calcareous lacustrine deposits. A second source is carbonates carried as airborne dusts. Several workers have invoked this hypothesis as a carbonate source (Reeves, 1970; Gardiner, 1972; Brown, 1956). Gile and Grossman (1979) have collected particulate carbonates in dust traps in New Mexico. A third source is dissolved calcium in rainwater. Gardiner (1972) has estimated that one-fourth of the carbonate in a Nevada caliche has its origin in rainfall. Gile and Grossman (1979) estimate that 2 to 3 times as much calcium is entering New Mexican desert soils dissolved in rainwater as is being added as particulate dusts. Finally, calcium bicarbonate may also occur in soil solutions through the weathering of Ca-rich minerals (Flach et al., 1969).

Once calcium bicarbonate becomes dissolved in the soil solution and is translocated, precipitation can be induced in three ways. In dry areas, this is most commonly effected by dessication of the soil such that the solubility of calcite is exceeded (Jenny, 1941a; Gillam, 1937). A second mechanism for carbonate precipitation is the lowering

of the $p\text{CO}_2$ (Gillam, 1937; Hendy, 1971). Thirdly, it has been suggested that a higher pH in the vicinity of previously existing carbonates or in a sodium rich environment such as a natric horizon, may cause precipitation of carbonates (Gillam, 1937; Hassett et al., 1976).

Pedogenic carbonates have been observed in a great variety of macroscopic forms. These include: pebble coatings (Flach et al., 1969; Gile et al., 1966); pore linings and ped coatings (Flach et al., 1969; White, 1971); filaments along rootlets and former root channels (Gile, 1961; Sherman and Ikawa, 1958; Hawker, 1927); nodules (Flach et al., 1969; Gile, 1961; James, 1972; Sehgal and Stoops, 1972); concretions and pisolites (Gile, 1961; Hawker, 1927; Dunham, 1962; Thomas, 1965); cylindroids (Gile, 1961); laminar zones (Flach et al., 1969; Gile, 1961; James, 1972; Read, 1974); and massive zones (Gile, 1961; Read, 1974). Pedogenic carbonates can also occur in finely divided form in the soil matrix (Flach et al., 1969; Rostad and St. Arnaud, 1970).

Micromorphological examination of thin sections has also revealed a number of characteristic micro-forms of pedogenic carbonates. These include: discrete or diffuse nodules (Sehgal and Stoops, 1972) or micritic pelletoids (James, 1972); crystal chambers filled with coarse granular calcite (crystallaria) (Sehgal and Stoops, 1972); pisolites or laminated nodules (concretions) (Thomas, 1965; Dunham, 1962); flower spar (bladed habit) (James, 1972); microcrystalline inflorescences (micrite recrystallized to micro-spar) (Sehgal and Stoops, 1972); calcans (Sehgal and Stoops, 1972); random calcite needles

(James, 1972; Sehgal and Stoops, 1972); tangential calcite needles (James, 1972); and finely divided micrite (James, 1972).

The calcic horizon is briefly defined as "a horizon of accumulation of calcium carbonate or of calcium and magnesium carbonate." If carbonate accumulation continues in the calcic horizon such that it "becomes plugged with carbonates and cemented into a hard, massive, continuous layer," it is considered to be a petrocalcic horizon (Soil Survey Staff, 1975). Caliche has been defined as "a prominent zone of secondary carbonate accumulation in surficial materials of warm, sub-humid to arid areas formed by both geologic and pedologic processes. Cementation ranges from weak in non-indurated forms to very strong in types that are indurated" (Hawley and Parsons, 1980). While soil scientists have generally adopted the terms "calcic" and "petrocalcic" in lieu of "caliche," the latter is still in common usage, particularly in geologic circles. The terms are in fact nearly synonymous with the exception that materials formed through "geologic processes" would not be considered calcic or petrocalcic horizons. Hypothesized origins which would be considered to be geologic processes of caliche formation include sedimentary deposition (Price et al., 1946) and capillary rise from a deep groundwater table (Nikiforoff, 1937) and will not be discussed further. Hypotheses regarding petrocalcic or caliche formation through pedological, near-surface processes can be grouped into three main types: 1) downward translocation and accumulation; 2) continual carbonate and ground surface aggradation; 3) in situ alteration and carbonate enrichment of limestone.

Most reports of soil-formed caliche or petrocalcic material explain its occurrence through the translocation of carbonates from the upper to the lower horizons by water and consequent accumulation (Bretz and Horberg, 1949; Buol, 1964; Flach et al., 1969; Harper, 1957). Over 50 years ago, Hawker (1927) described the genesis of petrocalcic horizons in the Rio Grande Valley of Texas in a five-stage model beginning with a uniform soil carbonate distribution and culminating with a carbonate-free solum underlain by thick caliche with a hardened surface. Gile et al. (1966) have proposed a four-stage sequence in the formation of petrocalcic horizons in both gravelly and fine-textured soils. The basic scenario is similar to that of Hawker (1927). The final stage, however, has a distinctly laminated crust overlying a massive indurated petrocalcic zone, and may have a calcareous rather than a carbonate-free solum. In his discussion of calcrete formation at Shark Bay, Australia, Read (1974) describes a process similar to Gile et al. (1966) for a soil formed from an eolianite skeletal grainstone (unconsolidated sand-sized carbonate skeletal deposit) containing very little non-carbonate silt or clay. The complete profile has five distinct zones which, from the surface downward are: 1) unconsolidated soil containing pisolites (concretions); 2) laminar zone consisting of thinly laminated sheets; 3) massive, dense, structureless calcrete; 4) zone of calcrete mottles (small areas of pedogenic carbonates in a matrix of dominantly unaltered carbonate skeletal material); 5) unaltered eolian carbonate skeletal grainstone. Although the starting parent materials are somewhat different,

the petrocalcic zone in this profile is very similar to stage IV of Gile et al. (1966).

The second mode of pedogenic caliche formation is the continually aggrading ground surface through the gradual accumulation of eolian clastics and carbonates (Brown, 1956). While downward translocation of carbonates and cementation occur in this process (similar to the previous mode of formation) the distinguishing feature is the gradual accumulation of eolian dusts and desert loess (Reeves, 1970). Particle size and mineralogical discontinuities, total carbonate levels and horizonation have all been cited as evidence for this process (Gardiner, 1972).

Blank and Tynes (1965) have proposed a third mode for caliche formation in the near-surface soil environment. They describe the in situ alteration of limestone to caliche. As soil water enters a limestone and is detained or delayed in draining, the limestone undergoes dissolution and precipitation in place. Petrographic evidence has shown the transition from limestone to caliche as indicated by the absence of fossils and the change from a coarser crystalline to a micritic fabric. James (1972) has also described a similar process occurring in the formation of caliche in Barbados. He suggests that percolating vadose water (above the water table) causes both the alteration of micrite to microspar and the alteration of carbonate skeletal fragments to micrite, forming micritic pelletoids and a clotted micritic fabric. Read (1974) and Kahle (1977) have described "calcretization" and "sparmicitisation" respectively as diagenetic or dissolution-reprecipitation processes responsible for the alteration

of primary limestones to a pedogenic caliche in the soil or vadose zone. In addition to the in situ alteration of the limestone, James (1972) also describes several forms of pedogenic carbonate which precipitate in the caliche, presumably added by downward moving water. James (1972) is careful to cite such evidence as parallel occurrence of caliche with the topographic surface as evidence for the caliche being the product of near-surface pedogenic processes rather than being a geologic stratum.

Calcic and petrocalcic horizons or caliche have been described according to their degree of expression. Harper (1957) has categorized them as minimal, medial or maximal corresponding to an increase in plugging, density and hardness. The degree of expression is generally held to be related to the genetic stage of development. Stuart et al. (1961) observed caliche on older surfaces (presumably older caliche) to occur nearer the soil surface and to be more firm and strongly cemented. The four genetic stages of petrocalcic development of Gile et al. (1966) also represent an increasing degree of expression of the carbonate enrichment. The strongest expression of these horizons occurred on the oldest surfaces (Gile and Grossman, 1979). Hawker's (1927) five genetic stages in caliche development also culminate with the maximum expression of the petrocalcic.

Once petrocalcic horizons or caliche form, climatic or other changes may result in the alteration or degradation of these materials, or repeated changes in climate may cause the formation of multiple sequences of petrocalcic materials. Bretz and Horberg (1949) describe solution features and degraded caliche profiles which they

ascribe to changes in paleoclimates. Gile and Grossman (1979) describe a similar disintegration of stage IV horizons which they explain to be the result of increased leaching of water due to truncation of the soils and to biotic activity and mixing. They also describe instances of multiple sets of laminar horizons showing evidence of fracturing and recementation.

Dust Contributions and Characterization

Thick eolian deposits, such as loess, are commonly recognized in some parts of the world as the primary parent material for many soils. More gradual eolian or airborne additions have also been widely observed in soils and sediments. Gradual, continuous deposition has been observed by some workers at accumulation rates of between 0.1 and 1.0 mm per 1000 yrs (approximately 0.15 to 1.5 g per square meter per yr) (Windom, 1969; Delany et al., 1967). Collection rates in the desert of New Mexico, measured over an 11-year period, ranged between 10 and 60 g per square meter per year (Gile and Grossman, 1979). Episodic depositions such as that associated with dust storms have also been well documented (Choun, 1936; Robinson, 1936; Martin, 1936; Alexander, 1934; Warn and Cox, 1951; Winchell and Miller, 1918, 1924). As much as 9 g per square meter have been reported deposited in a single event (Winchell and Miller, 1922).

Several workers have collected and analyzed dust, either directly from outfall or as preserved in snowfields and glacial ice. While most have found dust to be primarily in the fine (2-5 μ m) and medium (5-20 μ m) silt-size range (Winchell and Miller, 1918, 1922; Robinson,

1936; Delany, 1967; Gile and Grossman, 1979), reports of coarser textured material have also been made (Winchell and Miller, 1924; Warn and Cox, 1951; Gile and Grossman, 1979). It appears that episodic depositions of dust tend to be coarser in texture than more gradual depositions.

Although exceptions exist, the silt mineralogy of the dust is reported by most to be dominated by quartz and feldspar (Winchell and Miller, 1918, 1922, 1924; Robinson, 1936). In addition, Windom (1969), Rex et al. (1969), and Robinson (1936) also report significant quantities of mica. In a few instances feldspar was either absent or present only in small amounts (Warn and Cox, 1951; Robinson, 1936; Yaalon and Ganor, 1973). Some have reported calcite to be prominent (Warn and Cox, 1951; Yaalon and Ganor, 1973) while Alexander (1934) reported a dominance of volcanic glass. The mineralogy is no doubt directly related to the source area.

The clay (<2 μ m) mineralogy of the dust is usually dominated by illite and kaolinite with lesser amounts of smectite and quartz (Delany, 1967; Yaalon and Ganor, 1973; Smith et al., 1970; Windom, 1969). The carbonate content in clay-size airborne dust is usually low.

Dust collected in North Central Texas between 1963 and 1965 showed mean monthly deposition rates of 21 to 24 kg per hectare (2.1 to 2.4 g per square meter), which is only one-half to one-quarter the deposition rate in Kansas, Nebraska, Missouri, and Montana (Smith et al., 1970). Texas dust samples had clay contents of 38 to 47 percent,

which were somewhat higher than the other locations. The clay mineralogy of the Texas dust was dominated by kaolinite and illite, with lesser amounts of smectite, quartz, feldspars, and chlorite, which was not appreciably different from that of the other plains states.

In instances where direct measurement and analysis of dust were not made, airborne materials have still been identified in soils and ocean sediments. The presence of primary minerals in soils, which are common in dust (such as quartz, feldspar, and mica) but absent from the soil parent material, has been cited as evidence of eolian additions to soils (Jackson et al., 1971, 1972; Rabenhorst et al., 1982). Comparisons of oxygen isotope ratios of quartz in soils, sediments, and dust have also been used to document additions of airborne materials (Syers et al., 1969; Mokma et al., 1972; Jackson et al., 1971, 1972; Rex et al., 1969).

METHODS AND MATERIALS

Site Selection

To establish a climo-sequence, attempts were made to span the climate (moisture) gradient across the study area while minimizing differences in other factors which affect soil development. Sites were therefore selected to maximize landscape stability by choosing such locations as high broad hilltops, divides, plateaus, or interfluves which would not be highly erosive nor subject to inwash from other landscape positions.

Sites were also selected to minimize parent material differences. Attention was focused on the hard Cretaceous limestones of the Washita and Fredericksburg groups while avoiding the upper portion of the Trinity group known to be dominated by interbedded hard and soft limestones of the Glen Rose formation (Adkins, 1978). Using maps and publications of the Bureau of Economic Geology as guides (Bur. Econ. Geol. 1979; Rose, 1978; Rodda et al., 1966), two preliminary trips were taken across the study area in the spring and summer of 1980 to collect limestone samples from potential sampling areas (Figure 1).

To evaluate the mineralogical composition of the limestones, X-ray diffraction (XRD) analyses of randomly oriented powder specimens were made. The percent CaCO_3 was determined gasometrically (Dreimanis, 1962) to estimate the amount of non-carbonate constituents in the limestone. Thin sections were prepared and examined to evaluate the fabric and texture of the rocks. Bulk density (Brasher et al., 1966) of the rocks was measured to estimate the percent total porosity.

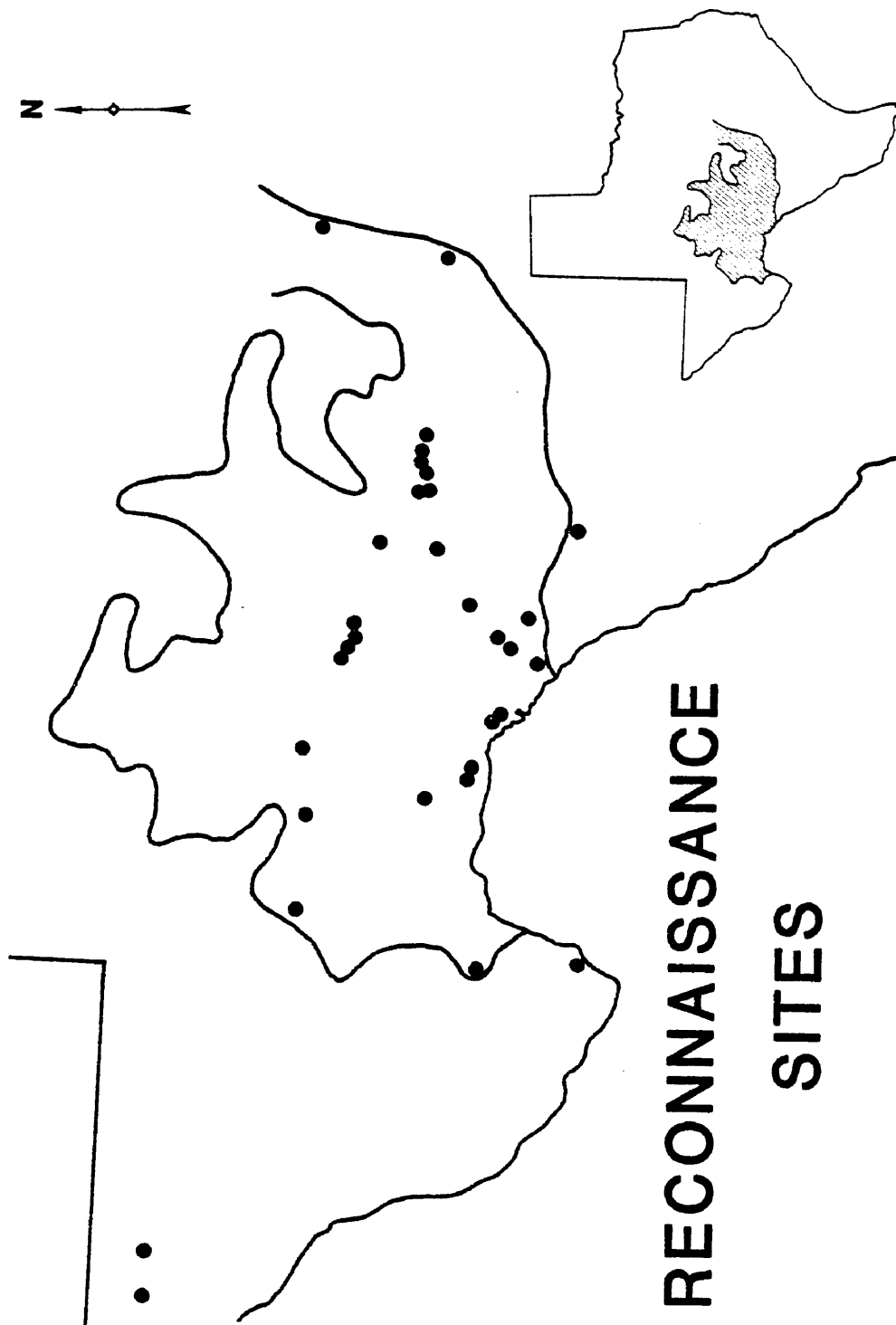


Fig. 1. Locations of reconnaissance sites sampled for limestone analyses during preliminary stages of the study.

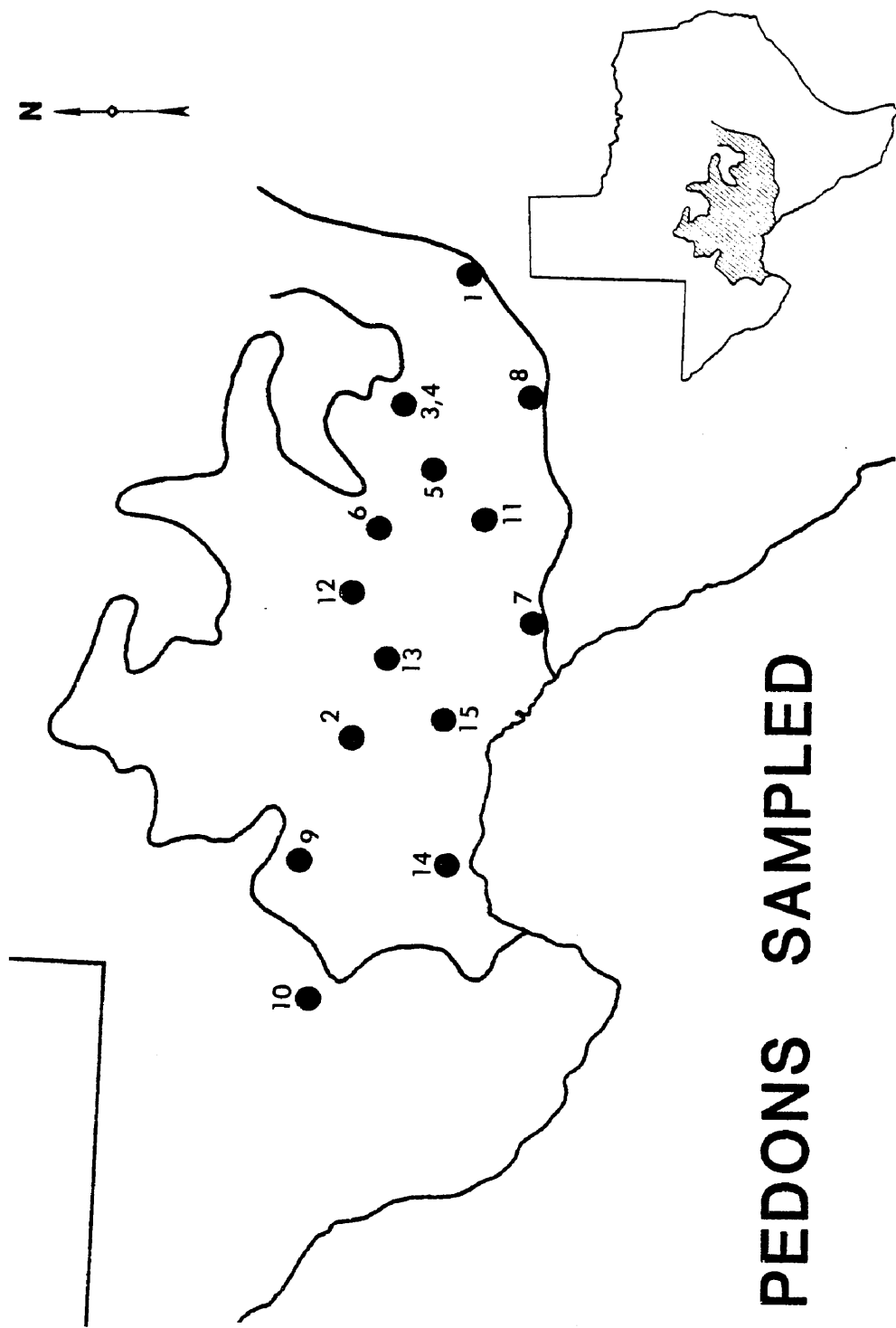
From field observations and laboratory analyses, certain geologic formations such as the Austin and Boquillas were deemed unacceptable for this study. The non-carbonate residue levels of the Austin Formation were too high (12-15%) and the Boquillas formation had common shaley and flaggy beds. Dolomitic rocks were much less prevalent than first thought and were therefore generally not included in the study (although two sites were inadvertently located over dolomitic limestone).

With aid from the Soil Conservation Service to gain access and approval from landowners, 15 pedons at 14 locations were finally selected for sampling and detailed analyses. As shown in Figure 2, these sites span the east west extent of the Edwards Plateau, taking full advantage of the moisture gradient across the area. Due to the difficulty in locating stable landscape positions in some areas (which was considered essential) less weight was given parent material homogeneity (hard limestone rock) during final site selection than originally proposed. See Table 1 for site numbers, county name and classification of soils (Soil Survey Staff, 1975).

Field Procedures

Pedon Sampling and Description

At each site, a pit of about 1 m² and 0.5 to 1 m deep was excavated for description and sampling. A 30-kg electric jackhammer powered by a 5-hp electric generator proved extremely helpful in opening the pit and collecting samples from carbonate indurated horizons and underlying limestone bedrock. Standard soil descriptions were



PEDONS SAMPLED

Fig. 2. Locations of sites selected for detailed sampling, analyses, and pedon descriptions. Site numbers were assigned alphabetically according to county name and then sequentially for counties with more than one pedon.

Table 1. Pedon number, county, and classification of the 15 pedons sampled for detailed analyses during this study.

Pedon #	SCS Pedon Nomenclature	County	Classification
1	S81TX-091-1	Comal	Udic Argiustoll; clayey-skeletal, mixed, thermic
2	S81TX-105-1	Crockett	Petrocalcic Calciustoll; fine-loamy, mixed, thermic, shallow
3	S81TX-171-1	Gillespie	Lithic Haplustoll; clayey-skeletal, montmorillonitic, thermic
4	S81TX-171-2	Gillespie	Lithic Haplustalf; clayey, mixed, thermic
5	S81TX-265-1	Kerr	Lithic Haplustoll; clayey, montmorillonitic, thermic
6	S81TX-267-1	Kimble	Petrocalcic Calciustoll; clayey, mixed, thermic, shallow
7	S81TX-271-1	Kinney	Petrocalcic Calciustoll; loamy-skeletal, mixed, thermic, shallow
8	S81TX-325-1	Medina	Lithic Argiustoll; clayey, montmorillonitic, thermic
9	S81TX-371-1	Pecos	Typic Paleorthid; loamy-skeletal, mixed, thermic, shallow
10	S81TX-371-2	Pecos	Petrocalcic Calciustoll; coarse-loamy, mixed, thermic, shallow
11	S81TX-385-1	Real	Udic Haplustalf; clayey-skeletal, montmorillonitic, thermic
12	S81TX-435-1	Sutton	Petrocalcic Calciustoll; loamy-skeletal, mixed, thermic, shallow
13	S81TX-435-2	Sutton	Petrocalcic Calciustoll; clayey-skeletal, montmorillonitic, thermic, shallow
14	S81TX-443-1	Terrell	Ustollic Paleorthid; loamy-skeletal, carbonatic, thermic, shallow
15	S81TX-465-1	Val Verde	Lithic Calciustoll; loamy-skeletal, mixed, thermic

made for each pedon sampled (Appendix A). Bulk samples were collected from each horizon or sub-horizon, including the limestone bedrock, for physical, chemical and mineralogical analyses in the following manner. The horizons were sequentially removed (A11 then A12, etc.) from a 0.2-0.5 m² area adjacent to the pit excavated for the pedon description until the petrocalcic horizon or limestone was encountered. The upper surface of the Ccam or R horizon was brushed clean of extraneous material before the jackhammer was used to dig through and break apart the indurated carbonate. These horizons were also sampled sequentially (C1cam then C2cam, etc.) over the same 0.2-0.5 m² area. Care was taken to remove extraneous material from the upper surface of each horizon prior to sample collection. Samples were collected to a depth beyond which it was impractical to dig using the jackhammer or digging iron (usually 0.5-1 m). Oriented clods were also collected from each horizon for impregnation and thin section preparation. As soil conditions permitted, clods from A and B horizons were collected for bulk density measurements.

Dust Collection

To estimate the contributions of eolian materials to soils in the study area, dust collection traps were installed at seven locations and monitored at four month intervals. The locations were selected to span the study area while also being in proximity to towns where local SCS personnel would be available to assist in monitoring the traps. The approximate locations are as follows: 1) Austin; 2) Kerrville; 3) Del Rio; 4) Sanderson; 5) Ft. Stockton; 6) Ozona; 7) Junction. See

Appendix B for details concerning site selection criteria and physical arrangement of the dust traps.

Laboratory Procedures

Sample Preparation

Bulk samples were dried in a drying oven at 35°C, hand ground with a wooden mallet and rolling pin to pass a 2 mm sieve and weighed. The >2 mm fraction was weighed, washed to remove adhering soil particles, dried and re-weighed; the difference between the weighings was added to the weight of the <2 mm portion.

Limestone Dissolution

One-kg samples of limestone and petrocalcic horizons which were ground to pass an 8 mm sieve were dissolved in pH 4.5 NaOAc buffer solution. The dissolution took approximately two weeks. See Appendix C for detailed methodology and justification. Three samples containing dolomite (R horizons from Gillespie Co. pedons 3 & 4) would not dissolve in the NaOAc solution, and thus 1N HCl was used to dissolve these samples which took approximately one day. One sample (R horizon from Comal Co. pedon #1) which contained quartz-occluded dolomite, resisted dissolution of gravel size material even in 1N HCl.

Analysis of Limestone and Petrocalcic Residues

Following dissolution, residues were transferred to 2-liter bottles and were washed several times with 0.5N pH 5 NaOAc to reduce levels of dissolved Ca prior to organic matter oxidation with H₂O₂ to

prevent formation of Ca oxalates. Approximately 100 ml of 30% H₂O₂ was added to each bottle containing approximately 500 ml of NaOAc suspension. The suspension was permitted to remain at room temperature for approximately one month. During this time the color of the residues became generally lighter indicating oxidation of organic matter.

Sands were removed from each sample by sieving and were weighed. An aliquot of the <50 μm material (the size of which depended on the total quantity of residue in the sample) was washed free of salts, placed into a 400 ml shaker bottle, and taken to the TAES Soil Characterization Laboratory for particle size analysis by the pipette method. An aliquot was pipetted from the sample while being stirred in order to calculate the total quantity of <50 μm in the bottle, from which was calculated (together with the weighed sand fraction) the total quantity of residue in the sample.

"Whole Soil" Mineralogy

In order to obtain a quick screening of the minerals present, samples of the A and B horizons (if present) and limestone residue from each pedon, were analyzed for <20 μm mineralogy. Suspended sediments representative of the <20 μm material from a single decantation were Mg or K saturated, washed free of salts, and washed once with a 20% glycerol solution. After draining as much of the glycerol solution as possible, the soil was stirred with a small spatula and the glycerated sample smeared evenly and smoothly onto a glass slide for XRD analysis. Samples were scanned from 2-36° 2θ at 2°/min using a Cu-target X-ray tube.

Particle Size Fractionation

After consideration of field characteristics and examination of the $<20\ \mu\text{m}$ mineralogy, four representative pedons were selected for detailed examination [S81TX 271-1 Kinney Co. (pedon #7), S81TX 371-1 Pecos Co. (pedon #9), S81TX 385-1, Real Co. (pedon #11), S81TX 465-1 Val Verde Co. (pedon #15)]. For A and B horizons, 50-g samples were treated with pH 5.0 NaOAc buffer to remove carbonates and residues were subsequently treated with H_2O_2 for organic matter oxidation as described by Jackson (1974). The $<50\ \mu\text{m}$ material was transferred to 2-liter bottles for sedimentation fractionation after removal of the sands by sieving. Limestone or petrocalcic residues were also placed into 2-liter bottles after particle size analysis had been completed. Samples were fractionated into clay ($<2\ \mu\text{m}$) and fine (2-5 μm), medium (5-20 μm), and coarse (20-50 μm) silt fractions by sedimentation and siphoning. The clay fraction was further split into the fine ($<0.2\ \mu\text{m}$) and coarse (0.2-2 μm) fractions by centrifugation.

Mineralogy

For the four pedons selected for detailed analyses, parallel oriented specimens of the coarse and fine clay fractions were plated onto ceramic tiles by suction and analyzed by XRD after Mg or K saturation. They were scanned from 2 to $38^\circ 2\theta$. The following treatments were run for each sample: Mg saturation and ethylene glycol solvation; Mg saturation, air dry (25°C); K saturation, air dry (25°C); K saturation, heated to 350°C for 2 hours; K saturation, heated to 550°C for 2 hours. Randomly oriented specimens of medium (5-20 μm) and coarse

(20-50 μm) silt fractions were prepared in box mounts and were scanned from 4 to 50° 2 θ . Randomly oriented box mounted specimens of ground limestone and petrocalcic materials were scanned from 24 to 32° 2 θ to identify the carbonate minerals present. All X-ray diffraction analyses were performed using a scan speed of 2° 2 θ /min on a Philips X-ray diffractometer equipped with a curved crystal monochromator and a theta compensating slit. Copper K α radiation was used. Permanent grain mounts of the medium and coarse silts were prepared for optical examination.

Elemental Analysis of Silts

Pellets were prepared for X-ray spectroscopic analysis from the coarse and medium silt fractions of each horizon fractionated. Two parts silt were mixed with one part (by weight) boric acid as a binding agent and ground for two minutes in a disc mill before being pressed into metal cups at 3000 kg/cm². Analyses were made for Ti, Fe, Ca, K, and Zr with a Philips X-ray spectrograph and Cr radiation using a fixed counting technique. For residue and soil samples of insufficient size to prepare a pellet, the silts were placed into polypropylene X-ray cells and covered with 1/4 mil mylar film. The cells were inverted and analyzed in the spectrograph like the pellets. Standards from the NBS were similarly prepared and analyzed. The medium silt fractions of dust samples collected were also analyzed using polypropylene X-ray cells.

Analyses of Dusts

Dust collection buckets which were mailed to the university were treated to remove organic materials and then filtered and fractionated. Clay ($<2 \mu\text{m}$) and medium silt (5-20 μm) fractions were analyzed by XRD techniques and selected silt fractions were examined using scanning electron microscopy (SEM). Cations in the filtrates were analyzed by atomic absorption or flame emission spectroscopy. See Appendix B for details concerning processing and analyses.

Scanning Electron Microscopy

Selected silt fractions of residues, soils and dusts were examined using scanning electron microscopy. Samples were generally mounted on copper tape which had been attached to 10 mm aluminum stubs and then coated with approximately 200 \AA of Au-Pd. Specimens were then examined using a JEOL JSM-25 II scanning microscope. Selected samples were mounted on carbon stubs and were carbon coated prior to electron microprobe semi-quantitative chemical analysis of individual grains. A JEOL JSM-35U scanning microscope equipped with both energy dispersive and wavelength dispersive systems and interfaced with a Tracor minicomputer was used for the analyses.

Micromorphology

Air-dried oriented clods were impregnated under vacuum using a polyester resin:acetone 3:1 solution by volume. One and one-half drops of accelerator (methyl ethyl ketone peroxide) per 100 ml of

solution were used which caused jelling of the liquid in about one week. After the impregnating liquid had jelled, samples were placed in a 45°C oven for several days after which the temperature was raised to 65°C to complete the hardening process. Slabs were then cut, polished and mounted on frosted glass slides with epoxy resin after which thin sections were cut and ground to an appropriate thickness.

Stable Carbon Isotopes

Samples from selected pedons were analyzed for stable carbon isotopes. Samples were run by the Chemical Oceanography Laboratory, TAMU. Carbonate carbon was analyzed following acidification with concentrated phosphoric acid. Organic carbon was analyzed after oxidation at 800°C following removal of carbonate carbon with acid. Analyses were made on a Nuclide 60° sector isotope ratio mass spectrometer.

Light-Heavy Mineral Separations

Light and heavy minerals from selected silt fractions were separated by centrifugation using tetrabromoethane (TBE) (SG 2.95) and a mixture of TBE and ethanol (SG of mixture 2.31). The heavy fraction was retained in the centrifuge tube by freezing with liquid nitrogen.

Characterization Analyses

Particle size distribution. Particle size analyses were run by the pipette method after a modification of Kilmer and Alexander (1949) and Steele and Bradfield (1934). Ten grams of soil were dispersed in a 400 ml bottle which was placed in a constant temperature water

bath. Five-ml aliquots collected at a 5 cm depth were removed for weighing.

Bulk density. Bulk density measurements were made on saran coated clods as described by Brasher et al. (1966).

Total carbon. Total carbon was determined by dry combustion and gravimetric determination of adsorbed CO₂ as described in analysis 6A2 in USDA, SCS (1972).

Carbonate carbon. Percent calcite, dolomite and calcium carbonate equivalent were determined gasometrically as described by Dreimanis (1962).

Organic carbon. The percent organic carbon was calculated as the difference between total C and carbonate C using the analyses described above.

Soil reaction. Hydrogen ion activity was determined on a 1:1 soil:water mixture using a glass electrode.

Extractable bases. Ammonium acetate extractable Mg, Ca, Na, and K were determined using a method similar to 5A6 (USDA, SCS, 1972) as adapted for use with a mechanical extractor described by Holmgren et al. (1977). Cations were measured using atomic absorption or flame emission spectrometry.

Cation exchange capacity. Cation exchange capacity was determined by Na saturation and subsequent displacement by NH₄ using a method similar to 5A2 (USDA, SCS, 1972) as adapted for use with a mechanical extractor.

Soluble salts. Electrical conductivity and soluble cations and anions were determined on saturated paste extracts prepared as

described by U. S. Salinity Laboratory Staff (1954). Cations were measured by atomic absorption or flame emission spectrometry. Anions were determined as described in USDA, SCS (1972).

Free iron oxides. Free iron oxides were extracted with a sodium dithionite and sodium citrate solution as described in method 6C2 (USDA, SCS, 1972). Iron in solution was then measured using atomic absorption spectrometry.

RESULTS AND DISCUSSION

Effect of Climate on Soil Properties

Climate of the Study Area

The climate of the Edwards Plateau region includes dry subhumid semi-arid, and arid areas, according to Thornthwaite's (1948) classification. The average annual rainfall decreases steadily from 800 mm in the eastern portion to about 300 mm in the western part as shown in Fig. 3. Figure 4 shows a marked steady increase in class A pan evaporation (estimate of potential evapotranspiration) in an east to west transect across the area. Together these provide for increasing dryness or decreasing water available for weathering and soil forming processes as one moves westward across the study area. Thornthwaite (1948) has combined monthly precipitation and potential evapotranspiration (based on monthly temperatures adjusted for latitude) in a moisture index called the P-E index. As would be expected from precipitation and pan evaporation data, the P-E index decreases (becomes dryer) in an east to west direction as illustrated in Fig. 5.

The present dry climatic conditions in the region may not reflect the long term conditions which have existed. There is substantial evidence that one or more pluvial and/or cooler periods occurred in the Southwest U.S. during the Pleistocene. Evidence includes geologic features such as lakebed deposits (Snyder and Langbein, 1962), biological features such as fossil snail occurrences (Metcalf, 1967) and pedologic features such as argillic horizons in soils which are presently plugged with carbonates (Gile and Grossman, 1979). This

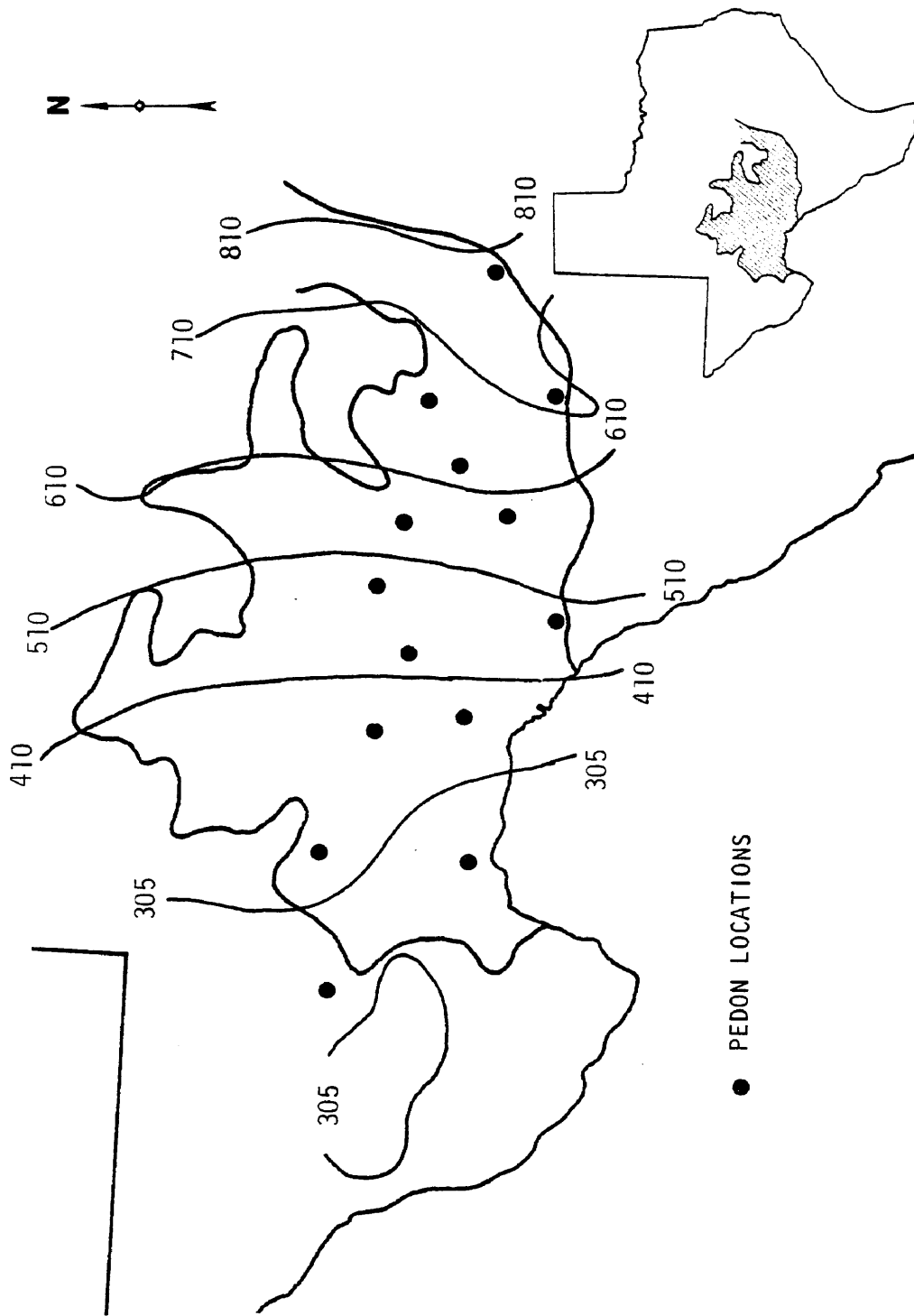


Fig. 3. Annual rainfall (mm) across the Edwards Plateau region. Note the steady decrease from east to west (modified from Texas State Climatologist, 1974).

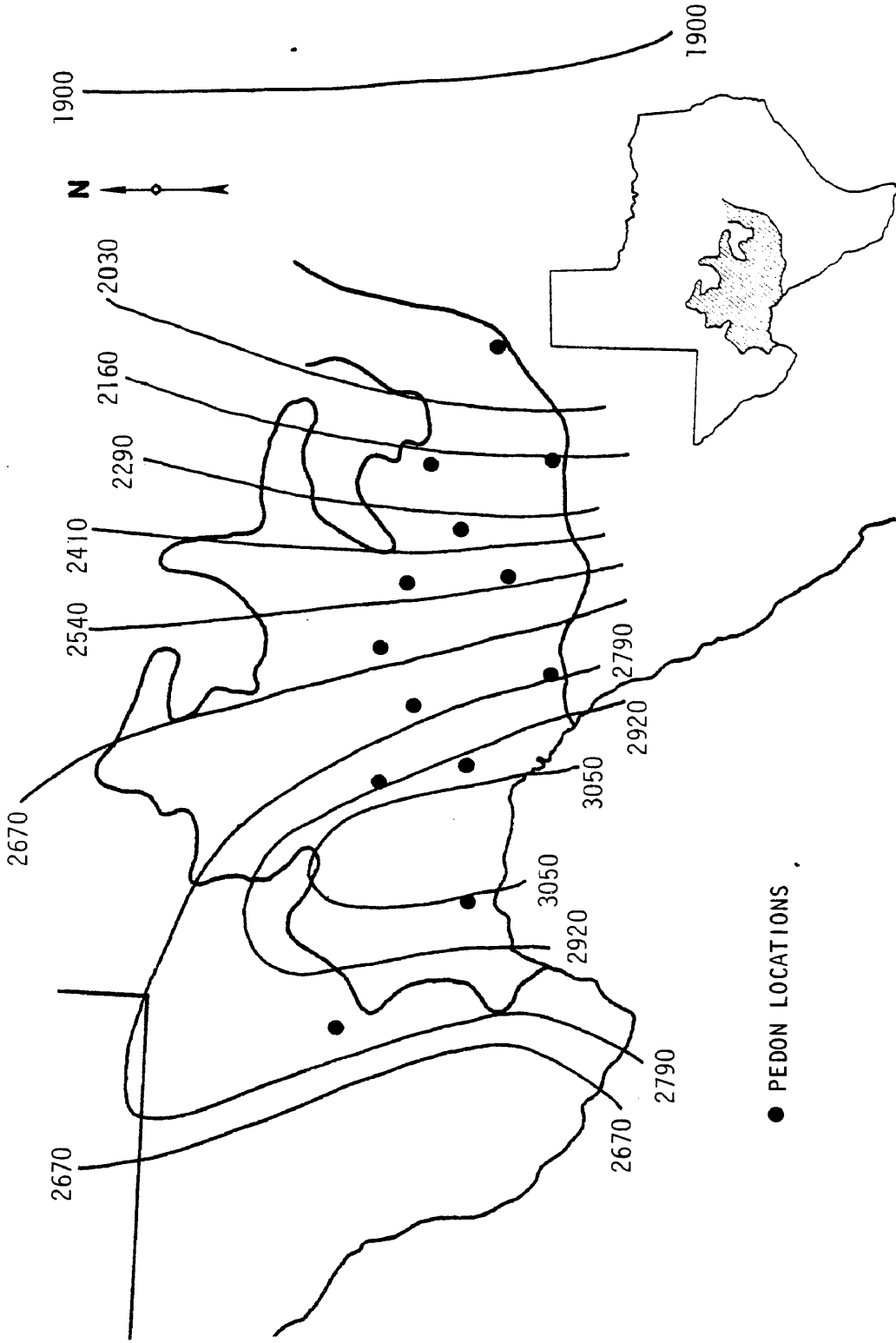


Fig. 4. Annual class-A pan evaporation (mm) across the Edwards Plateau region. Note the strong east-west gradient (modified from U.S. Dept. Commerce, 1968).

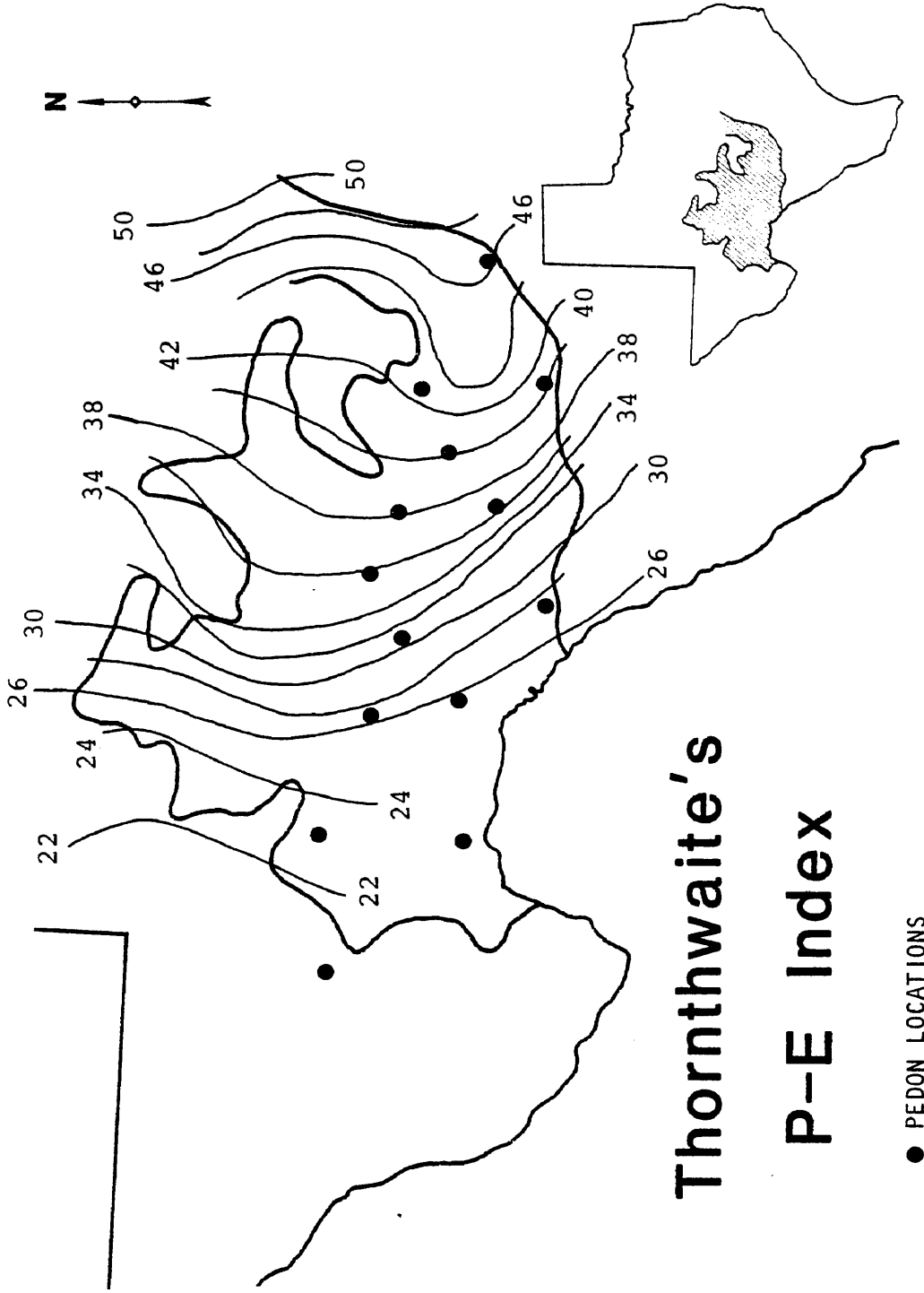


Fig. 5. Values of Thornthwaite's P-E index across the Edwards Plateau region (modified from USDA, 1957).

suggests that during the Pliestocene, greater amounts of water were effectively available for soil formation than at present.

Soil Properties

Free carbonates. Soils in the eastern part of the study area were non-calcareous in the solum. Figure 6 shows the carbonate levels in A horizons of the pedons sampled. Those soils west of Leaky (Real Co.) contained varying amounts of free carbonates in the solum. The dividing line roughly corresponds to a P-E index of about 38 or an annual precipitation of 600 mm. A significant (99% level) negative relationship exists between carbonate levels in the solum and the P-E index based on the present climatic conditions. There is also a statistically significant trend toward decreased solum thickness with lower P-E indices. This relationship is statistically significant at the 95% level (Fig. 7). Limestone weathering and soil formation are fairly slow processes so that the depth to limestone or petrocalcic material is generally a function of long-term climatic factors as well as parent material characteristics. This may in part explain the lack of significant correlation with the present P-E index.

Petrocalcic horizons. Most of the calcareous soils also showed some evidence of pedogenic carbonate accumulation and many had indurated carbonate-rich zones identified as petrocalcic horizons. Although field evidence alone is often not sufficient for identification of petrocalcic horizons (see section entitled Differentiation of Pedogenic and Lithogenic Carbonates), Fig. 8 shows the distribution of pedons containing petrocalcic horizons as identified in the field.

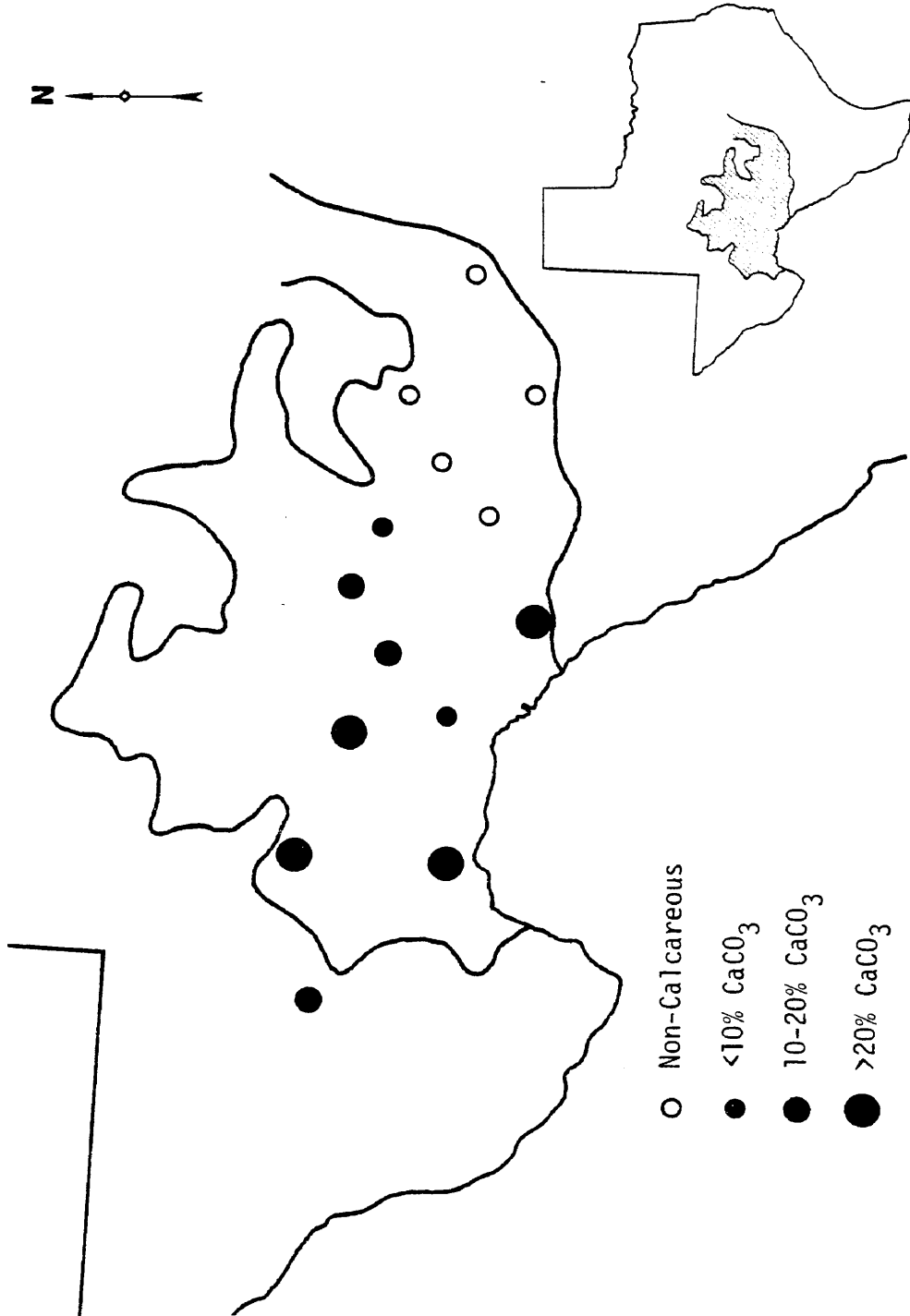


Fig. 6. Levels of CaCO₃ occurring in the <2 mm fraction of A horizons of pedons sampled in this study. Note the general though variable trend of increasing levels in an east to west direction.

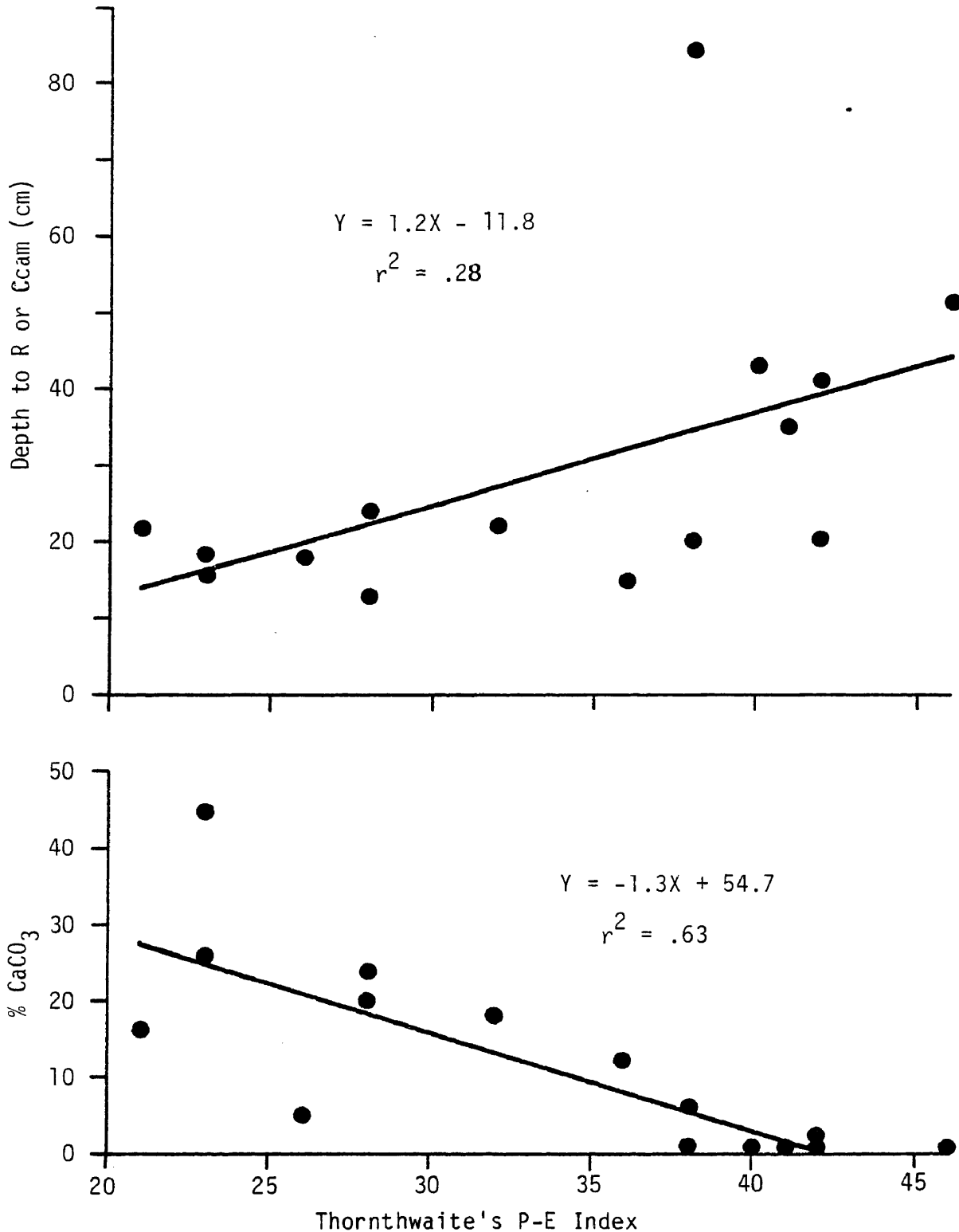


Fig. 7. Graphs showing Thornthwaite's P-E index versus depth to indurated carbonate and versus percent CaCO₃ in the A horizons of the 15 pedons sampled.

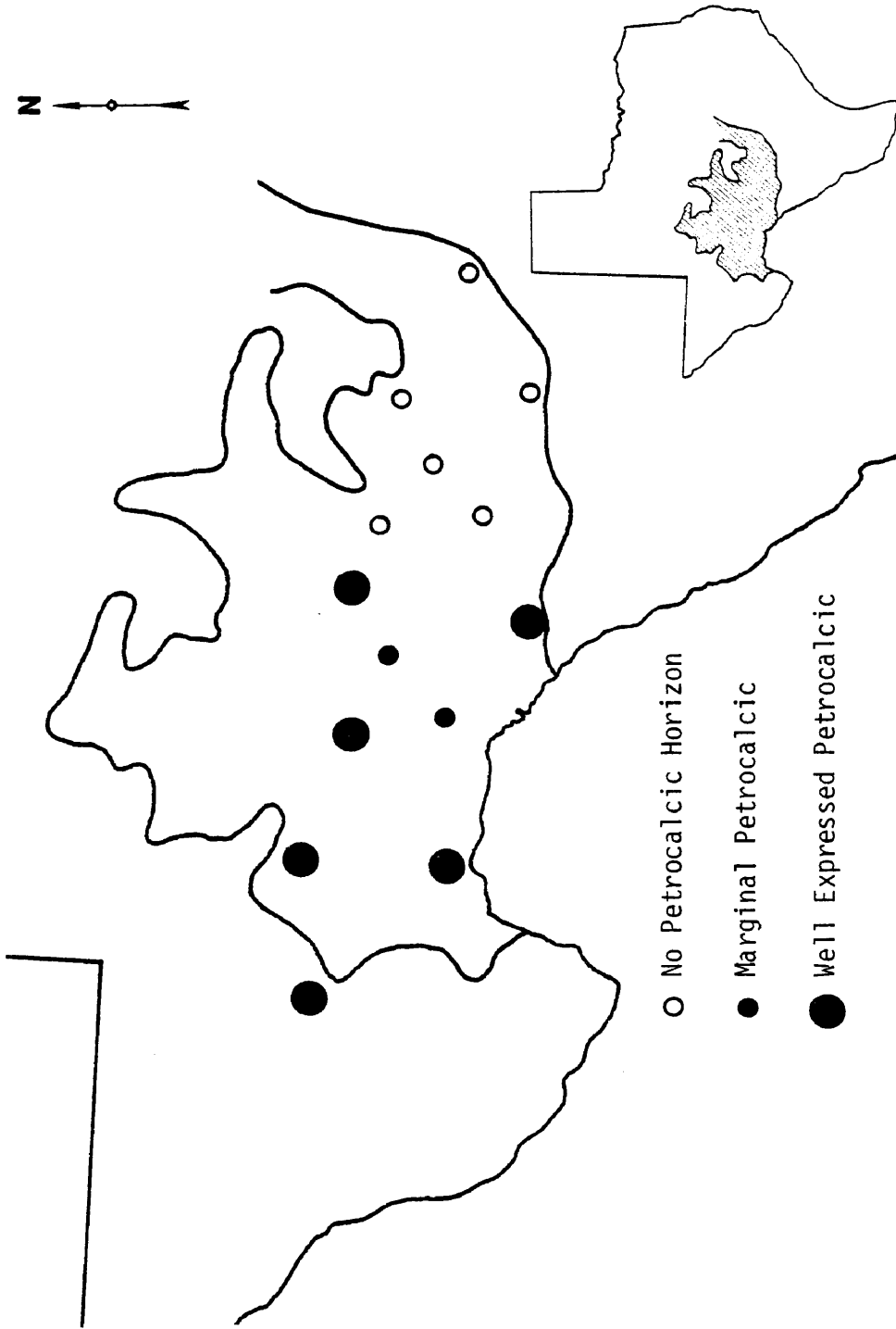


Fig. 8. Occurrence of petrocalcic horizons in pedons sampled during this study based on field identification.

These are restricted to the dryer western part of the Edwards Plateau where moisture is sufficient only for movement and accumulation of carbonates within the soil but not for leaching and removal of carbonates.

A number of the petrocalcic horizons observed in the field showed evidence of multiple layering and cracking in the upper portion of the petrocalcic. Laminar coatings were observed both on upper surfaces and along the walls of cracks in the upper part. Bretz and Horberg (1949) have attributed similar degradational features to paleoclimatic changes.

Argillic horizons. In the eastern part of the study area, where carbonates had been leached from the solum, 4 of the pedons sampled had argillic horizons as shown in Fig. 9. Field identification was made on the basis of increased clay content and the presence of oriented clay films on peds. The argillic horizons themselves were quite high in clay (45-57% <2 μ m) and some showed evidence of shrink-swell pressure faces which made identification of illuvial clay films difficult.

Moderating Factors on Soil Properties

The effect of the moisture gradient can be clearly seen through general trends in the soil properties just discussed. It is also evident, however, that climatic factors alone are insufficient to explain some of the geographical variations observed. For example, the deepest solum (80 cm) and most strongly expressed argillic horizon were observed in Real County where the P-E index is 38. Due north in

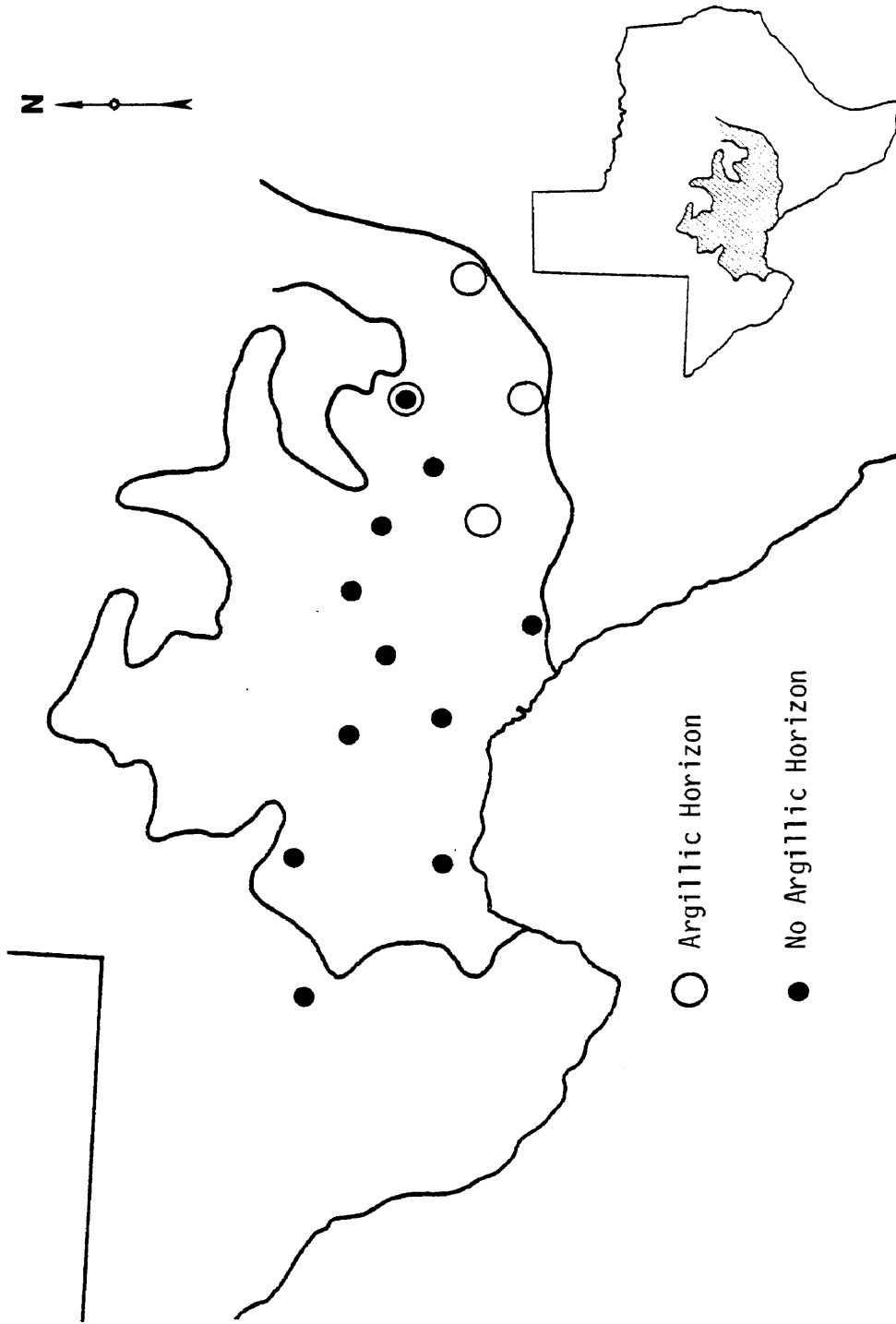


Fig. 9. Occurrence of argillic horizons in pedons sampled during this study.

Kimble County, where the P-E index is also 38, a shallow (20 cm) calcareous soil was observed. Similarly, two pedons were sampled in Gillespie County within 100 meters of each other. One was 41 cm to rock and contained an argillic horizon while the other lacked an argillic and had a solum thickness of only 20 cm.

It appears that factors other than climate may have strongly moderating effects at any given location. Although attempts were made to minimize differences in parent materials and landscape stability, some variation no doubt did exist. Two of the four soils with argillic horizons also had large quantities of chert fragments in the solum suggesting that cherty limestones may be more subject to weathering and clay illuviation. More subtle parent material differences not easily observed such as total porosity, interconnected porosity or size and frequency of fractures, may also affect pedogenic development. Since the genesis of a given volume of soil from limestone residuum usually requires the weathering and dissolution of between 10 and 100 times that same volume of rock, there remains the possibility that the rock from which the soil formed is different from the underlying rock. Soil variation may therefore be partially attributed to variations that existed in stratigraphically overlying rock.

Parent Material Identification and Uniformity

The soils occurring on stable upland positions in the Edwards Plateau area have generally been considered to be formed from limestone residuum. Researchers have also been aware, however, that airborne dust additions from desert regions to the south and west have occurred. Work tangential to this study has been done to collect and analyze dusts blown into this region (see Appendix B). There are therefore several hypotheses for source or origin of the soil parent materials. These include:

1. Weathering of limestone bedrock.
 - a. The limestone from which the soil formed is similar to the presently underlying bedrock.
 - b. The limestone from which the soil formed is unlike the presently underlying bedrock.
2. Accumulation of eolian dusts.
 - a. The dusts forming the parent materials are similar to the present dust contributions.
 - b. The dusts forming the parent materials are unlike the present dust contributions.
3. Some combination of the above hypotheses including both processes of limestone weathering and dust accumulation.

Field observations indicate that soil formation in this region is substantially linked to limestone weathering. The abundance of coarse fragments (both limestone and chert) in most of these soils indicates that airborne dusts are not the primary parent material. Therefore,

hypothesis #1 will first be addressed to determine whether or not the residual portion of the soil has formed from rock like the underlying rock. Secondly, the impact of airborne dusts on the soils will be evaluated.

Four pedons were selected for detailed analysis including mineralogy, elemental analysis, and SEM examination. These were chosen to 1) represent the range in morphological characteristics observed, and 2) to reflect the range in mineralogical relationships between the soil and the underlying rock. The pedons selected were S81TX 271-1 (Kinney Co., Pedon #7), S81TX 371-1 (Pecos Co., Pedon #9), S81TX 385-1 (Real Co., Pedon #11), and S81TX 465-1 (Val Verde Co., Pedon #15). These were classified as Petrocalcic Calciustoll, Typic Paleorthid, Udic Haplustalf, and Lithic Calciustoll respectively. Based on preliminary "whole soil" XRD analysis of soils and limestone residues, each of the last three pedons showed increasing disparity between mineralogy of the soil and that of the residue from the underlying limestone. The Kinney Co. pedon had similar soil and carbonate residue mineralogy. This soil was suspected of having formed from softer limestone material, and was chosen as representative of that type. Each of these pedons were evaluated for parent material uniformity by PSD, mineralogy, elemental analysis, and SEM.

Kinney Co. Pedon

Carbonate-free and clay-free particle size distribution (PSD), the medium silt (5-20 μm):coarse silt (20-50 μm) ratio, and the coarse sand (.25-2 mm):fine sand (.05-.25 mm) ratio for the Kinney Co. pedon

are shown in Fig. 10. From a cursory examination of the particle size data, the abundance of fine and coarse clay in the C4cam horizon, and the relative lack of fine clay in the A1 horizon indicate variation in parent materials.

The purpose of using clay-free and carbonate-free particle size data is to remove the effects of mobile constituents which may change the PSD of a given horizon over time. Use of particle size information for parent material analysis in this pedon is complicated by the accumulation of secondary silica in the petrocalcic zone. Optical examination of silt and sand fractions in petrocalcic horizons showed an abundance of secondary silica. Estimates indicated that the sand fractions ranged between 40 and 85% secondary silica (Table 2), which may explain the variations in sand percentages. The value for secondary silica in the C1cam horizon is, however, insufficient alone to explain the large increase in sand content in the C1cam relative to the A1 horizon.

Medium silts were generally higher in secondary silica than coarse silts ranging between 10-60% and 5-40% respectively. The greatest difference in the quantity of secondary silica between the medium and coarse silts was in the C2cam horizon where they were 40% and 15% respectively. This explains the medium:coarse silt ratio maximum in this horizon. It appears that substantial variations in the PSD of this pedon are due to accumulations of secondary silica. Parent material non-uniformity within the carbonate-cemented zone cannot, therefore, be established on this basis.

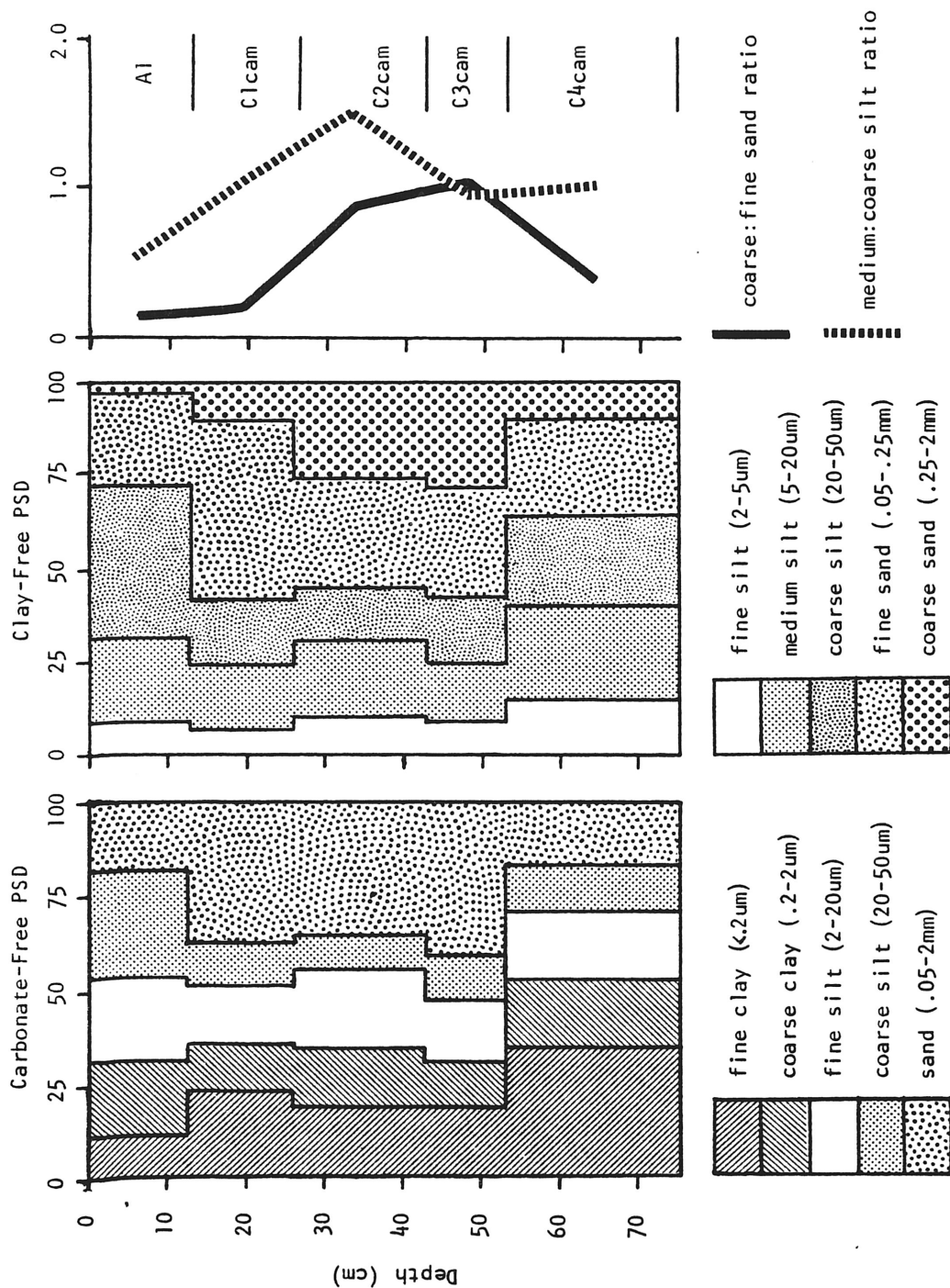


Fig. 10. Carbonate-free and carbonate-free, clay-free PSD and sand and silt ratios shown with depth for the Kinney Co. pedon (#7).

Table 2. Estimates of secondary silica content in selected fractions and horizons of the Kinney Co. pedon (#7) based on optical examination.

Lab #	Horizon	Sand .05-2 mm	C. Silt 20-50 μ m	Med. Silt 5-20 μ m
1214	C1cam	35-45	<5	<10
1215	C2cam	55-65	10-20	30-50
1216	C3cam	80-90	35-45	50-60
1217	C4cam	75-85	5-15	30-40

Elemental analyses of medium and coarse silt fractions from the Kinney Co. pedon are illustrated in Fig. 11. Within the carbonate cemented zone (13-75 cm), variations in elemental content can be largely explained on the basis of enrichment of the silt fractions with secondary silica. Maximum silica enrichment in the C3cam horizon, for example, corresponds to Zr, Ti, Fe, and K minima in that same horizon. There do, however, appear to be differences in the A1 horizon that cannot be accounted for by silica enrichment. Higher K and Ca values in the A1 horizon are too large to be explained by the 5 to 10% enrichment in silica which has occurred. Values for Zr and Ti actually show a decrease in the A1 relative to the C1. This trend is opposite that expected by silica enrichment in the C1, and suggests that the A1 horizon has been influenced by material richer in K and Ca, and lower in Zr and Ti than the C horizons.

Interpretations of XRD analyses of clays and silts are presented in Table 3. Mineralogical variations through the pedon are relatively

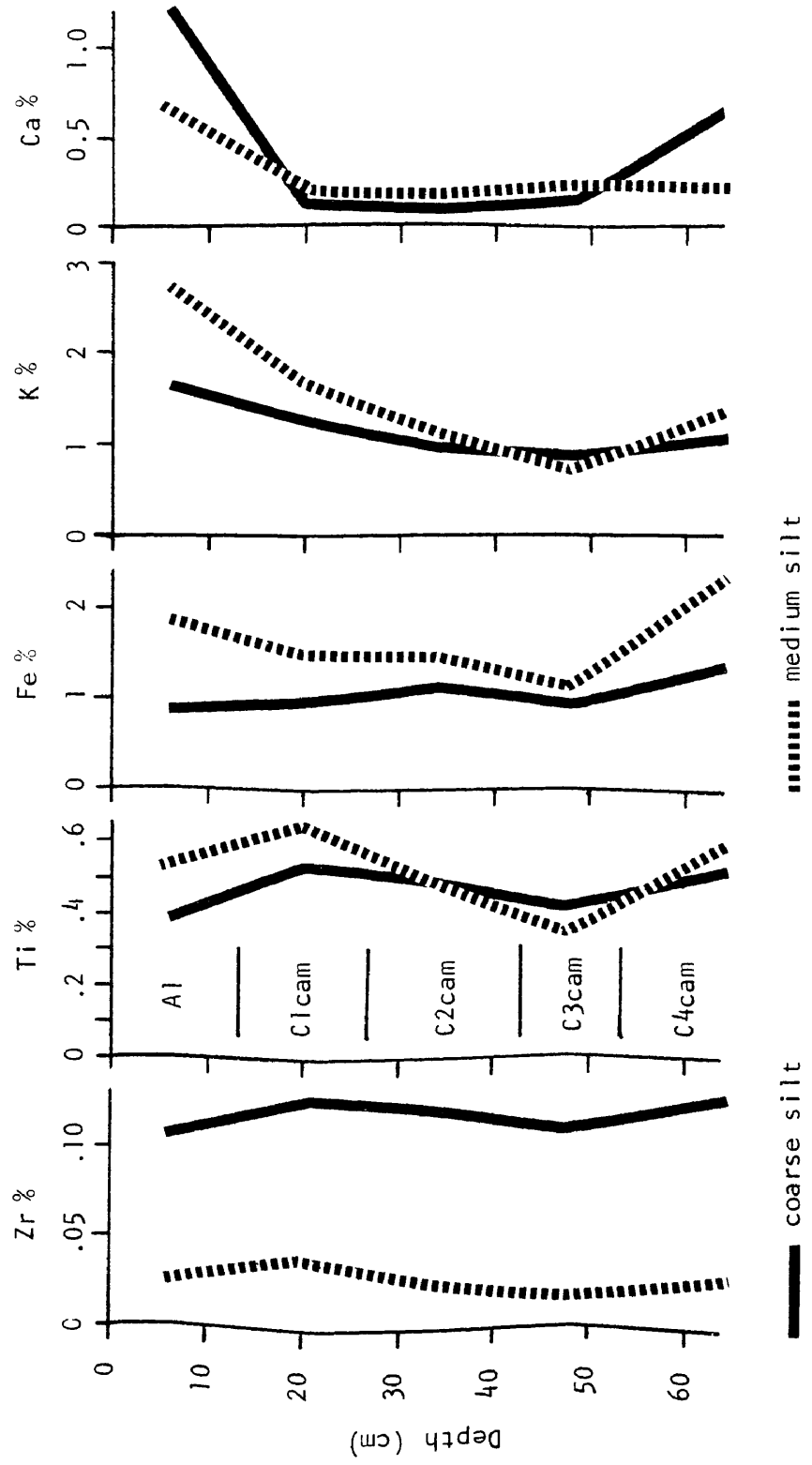


Fig. 11. Elemental analyses of carbonate-free silt fractions from soil and residue of the Kinney Co. pedon (#7).

Table 3. Semi-quantitative[†] interpretations of XRD analyses of the Kinney Co. pedon.

Horizon	Fraction (μm)	Qtz	Kaol	Mica	Sm	K Spar	Plag	Fe oxide	Anatase
A1	<.2	--	XX	XX	XXXX	--	--	--	
C1cam		--	X	XX	XXXX	--	--	--	
C2cam		--	X	XX	XXXX	--	--	--	
C3cam		--	X	XX	XXXX	--	--	--	
C4cam		--	X	XX	XXXX	--	--	--	
A1	.2-2	XX	XX	X	XXX	Tr	--	--	X
C1cam		XX	XXX	Tr	XXX	X	--	--	X
C2cam		XX	XXX	Tr	XX	X	--	--	X
C3cam		XX	XXX	Tr	XX	X	--	--	X
C4cam		XX	XXX	Tr	XX	X	--	--	X
A1	5-20	XXXX	--	Tr	--	XX	XX	X	
C1cam		XXXX	--	--	--	X	X	X	
C2cam		XXXX	X	--	--	X	X	X	
C3cam		XXXX	X	--	--	X	X	X	
C4cam		XXXX	X	--	--	X	X	X	
A1	20-50	XXXX	--	--	--	X	X	--	
C1cam		XXXX	--	--	--	X	X	Tr	
C2cam		XXXX	--	--	--	X	X	Tr	
C3cam		XXXX	--	--	--	X	X	Tr	
C4cam		XXXX	--	--	--	X	X	Tr	

† Tr - trace
 X - low <10%
 XX - moderate 10-30%
 XXX - high 30-70%
 XXXX - dominant >70%

Qtz - Quartz
 Kaol - Kaolinite
 Sm - Smectite
 Plag - Plagioclase
 K Spar - K Feldspar

minor. Slightly higher quantities of feldspars and mica in the medium silt and slightly lower levels of kaolinite in the coarse clay and medium silt of the A1 horizon may substantiate previous inferences that the A1 horizon has been formed from a somewhat different parent material. Mineralogical evidence alone, however, would be insufficient for such a conclusion.

Pecos County Pedon

Particle size data for the Pecos Co. pedon are presented in Fig. 12. This pedon shows considerable similarity to the Kinney Co. soil in that it shows 1) a lower amount of fine clay in the A1 horizon and 2) a strong increase in the sand content in the petrocalcic zone. Secondary silica also comprises a substantial portion of the sand and silt fractions as presented in Table 4. The increase in sand content with depth in the petrocalcic horizon can largely be accounted for by the enrichment with secondary silica. Consideration of silica enrichment, however, does not account for the low medium:coarse silt ratio in the A1 horizon. Neither does it account for the low amount of fine clay; rather, it increases the disparity in fine clay content between the A1 horizons and the petrocalcic horizons. This suggests that the

Table 4. Approximate estimates of secondary silica content in selected fractions and horizons of the Pecos Co. pedon (#9). Estimates based on optical examination and/or specific gravity separations.

Lab #	Horizon	Sand	C. Silt	Med. Silt
		.05-2 mm	20-50 μ m	5-20 μ m
		-----%		
1236	A12	0	<10	5-15
1237	C1cam	10-20	<10	10-20
1238	C2cam upper	40-50	15-25	40-50
1239	C2cam lower	60-70	20-35	70-80
1240	R	15-25	5-20	5-15

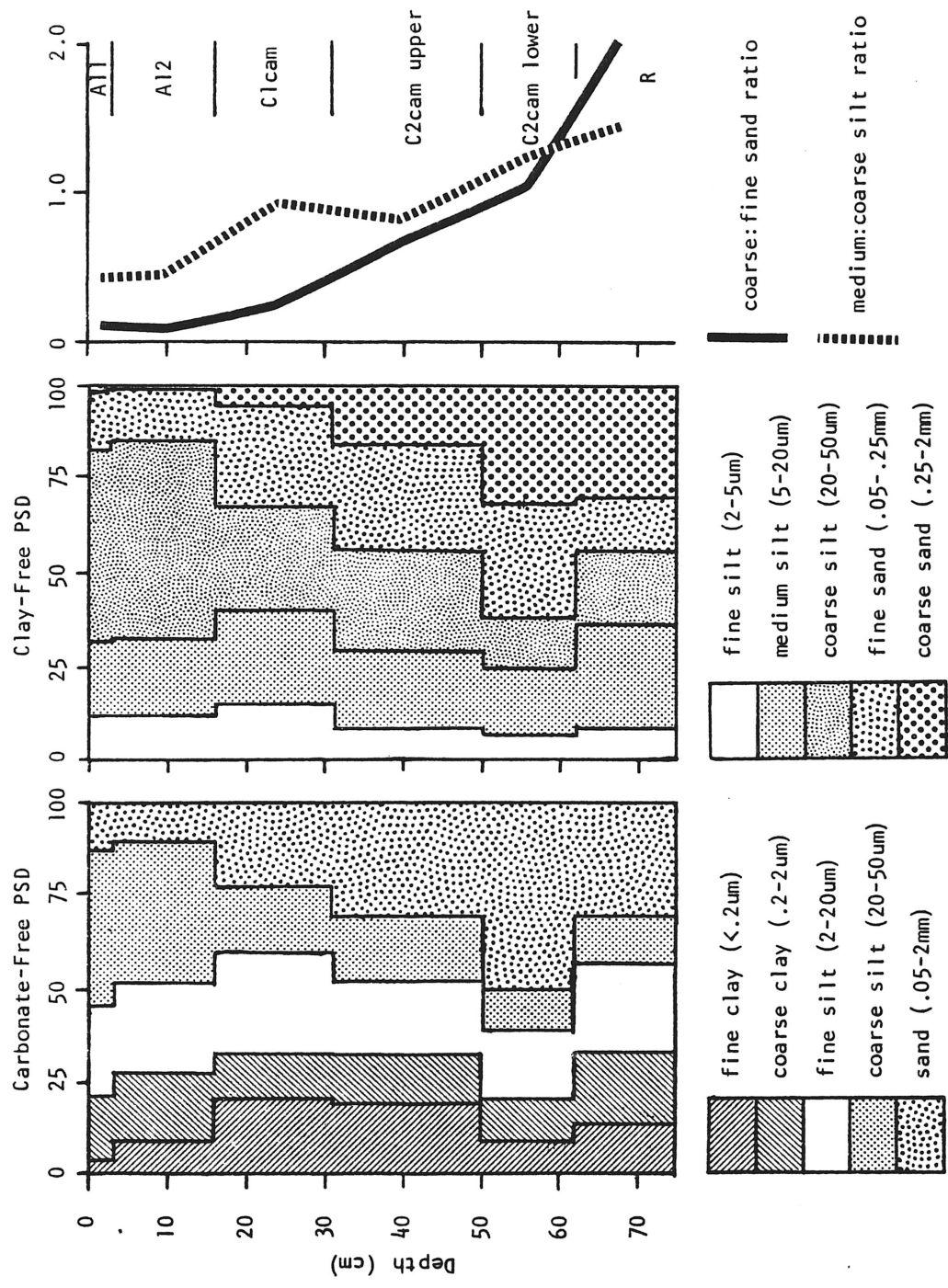


Fig. 12. Carbonate-free and carbonate-free, clay-free PSD and sand and silt ratios shown with depth for the Pecos Co. pedon (#9).

Al material in this pedon, like the one in Kinney Co., has been formed from, or admixed with, a different parent material.

Elemental analyses of silt fractions and mineralogy of clays and silts are presented in Fig. 13 and Table 5, respectively. Elemental concentrations in the Al horizon are similar to those in the upper petrocalcic horizons. The general decrease in Zr, Ti, Fe, and K toward minima in the lower C2cam horizon can be substantially explained by the enrichment in secondary silica in the silt fractions. Increasing Ca levels with depth are the result of the presence of fluorite (CaF_2) in the petrocalcic and R horizons. The continued decrease in K and Zr into the R horizon, while secondary silica levels have decreased, does, however, suggest that the limestone from which the petrocalcic horizons formed was richer in Zr and K. Mineralogical evidence also supports the inference that the R horizon is not identical to the limestone precursor to the petrocalcic zone. Lower silt-sized feldspar levels in the R horizon as well as higher kaolinite levels illustrate this. The gradual change in mineralogy from the R to the upper petrocalcic horizon, as well as the presence of fluorite in both R and Ccam horizons, indicates, however, that the compositional differences between the R horizon and the limestone precursor to the petrocalcic horizon may not in fact be great.

Examination of the silt fractions of the R horizon residue by SEM revealed an abundance of euhedral, prismatic quartz as shown in Fig. 14. Since such structures would not easily survive transport and deposition, these grains are most likely authigenic crystals formed in voids in the limestone. The euhedral quartz prisms were also observed

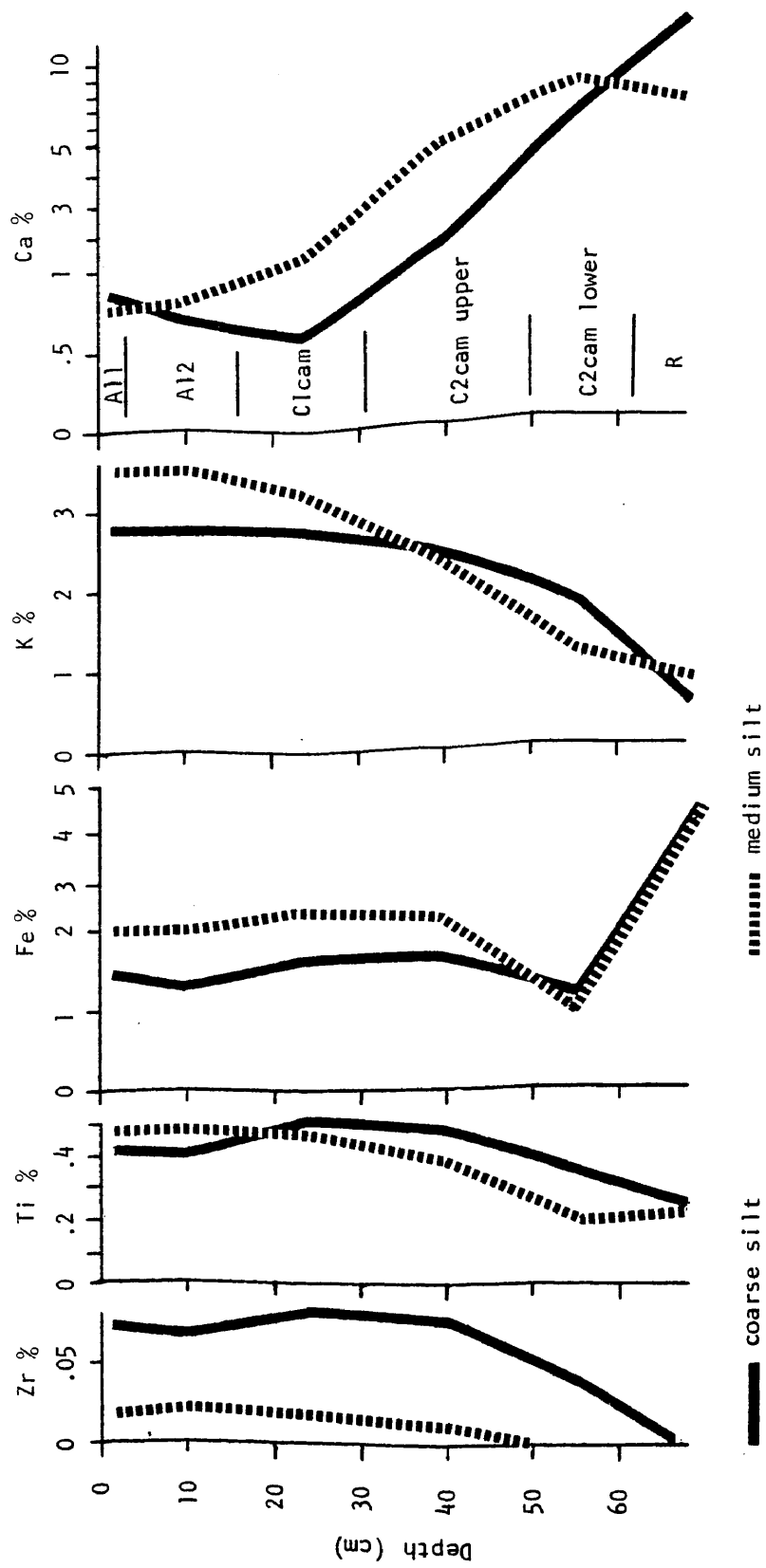


Fig. 13. Elemental analyses of carbonate-free silt fractions from soil and residue of the Pecos Co. pedon (#9).

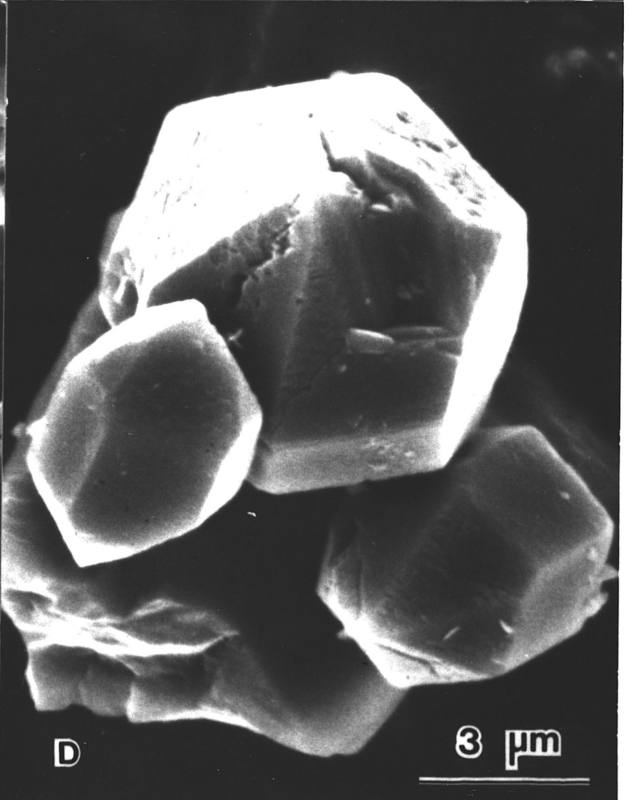
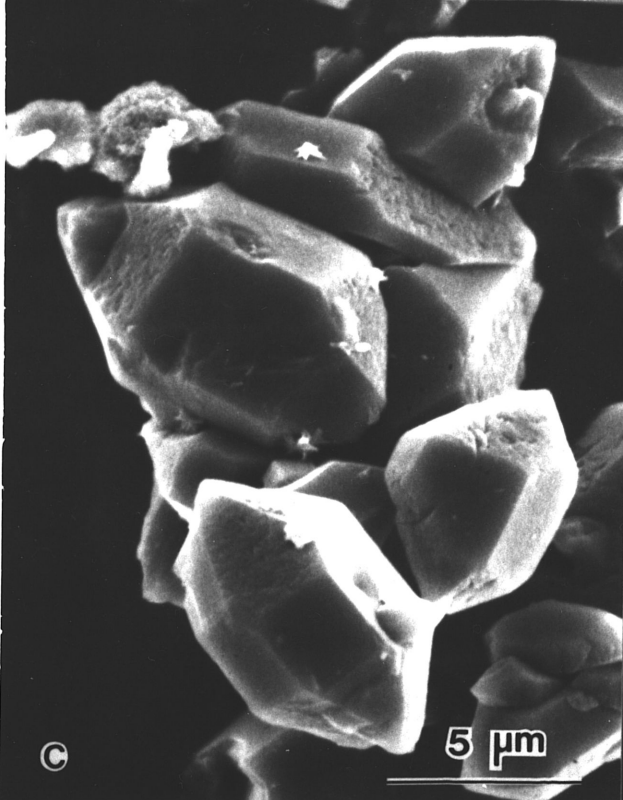
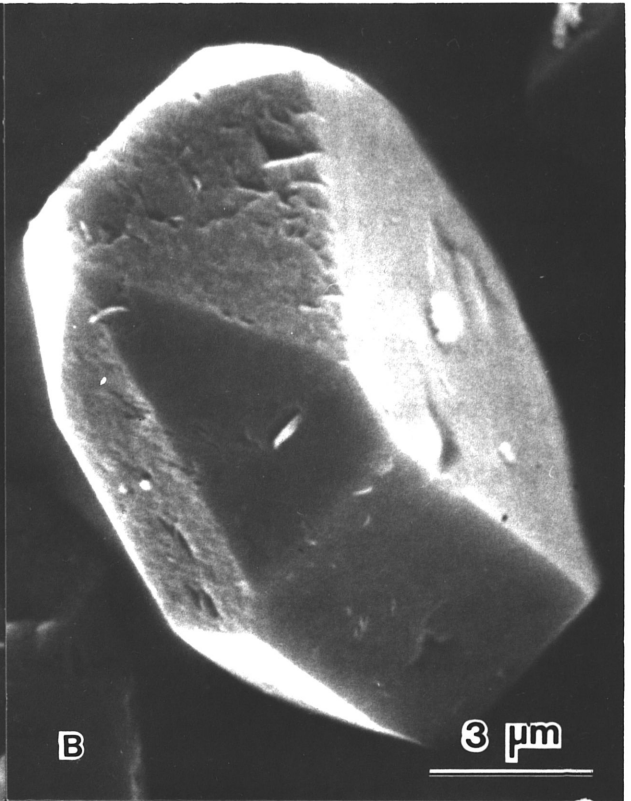
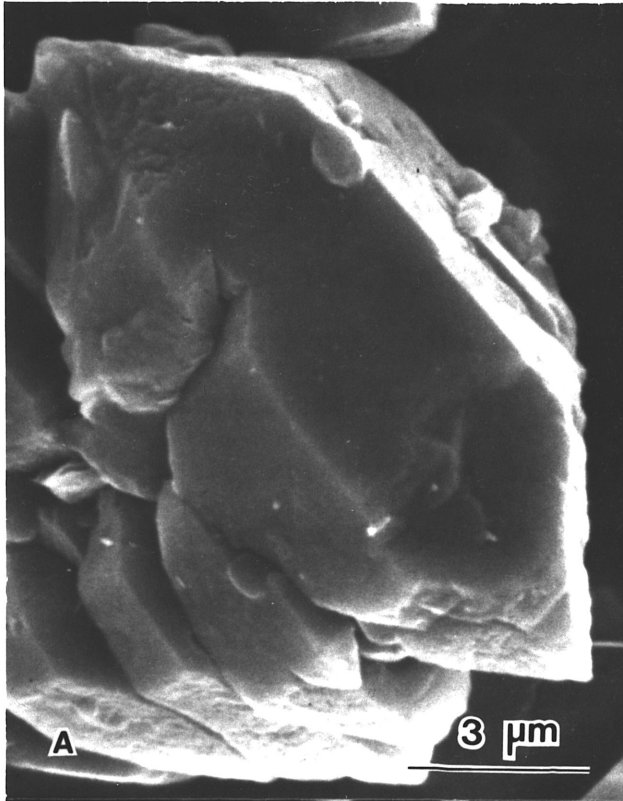
Table 5. Semi-quantitative[†] interpretations of XRD analyses of the Pecos Co. pedon.

Horizon	Fraction (μm)	Qtz	Kaol	Mica	Sm	K Spar	Plag	Fe Oxide	Fluorite	Comments
A11	<.2	--	X	XX	XXXX	--	--	--	--	Goethite; High Charge Sm
A12		--	X	XX	XXXX	--	--	--	--	
C1cam		--	X	XX	XXXX	--	--	Tr	--	
C2cam		--	X	XX	XXXX	--	--	X	--	
C2cam		--	X	XX	XXXX	--	--	Tr	--	
R		--	Tr	XXX	XXX	--	--	XX	--	
A11	.2-2	XX	XX	XX	XX	X	--	--	--	
A12		XX	XX	XX	XX	X	--	--	--	
C1cam		XX	XX	XX	XX	X	--	Tr	Tr	
C2cam		XXX	XX	XX	XX	X	--	X	XX	
C2cam		XXX	XX	X	XX	--	--	Tr	XXX	
R		XXX	XXX	X	X	X	--	XX	Tr	
A12	2-5	XXXX	Tr	Tr	X	XX	X	Tr	--	XBarite TrBarite
C1cam		XXXX	Tr	--	X	XX	X	Tr	X	
C2cam		XXXX	Tr	--	X	X	X	Tr	XX	
C2cam		XXXX	Tr	--	Tr	--	--	--	XXX	
R		XXXX	XX	--	--	--	--	X	X	
A11	5-20	XXXX	--	Tr	--	XX	XX	--	--	XBarite TrBarite
A12		XXXX	X	X	--	XX	XX	--	--	
C1cam		XXXX	--	--	--	XX	XX	X	X	
C2cam		XXXX	--	--	--	XX	XX	X	XX	
C2cam		XXXX	--	--	--	X	X	--	XXX	
R		XXXX	Tr	--	--	Tr	Tr	--	XXX	
A11	20-50	XXXX	--	X	--	XX	X	--	--	
A12		XXXX	--	--	--	XX	X	--	--	
C1cam		XXXX	--	--	--	XX	X	--	--	
C2cam		XXXX	--	--	--	XX	X	--	X	
C2cam		XXXX	--	--	--	XX	X	--	XX	
R		XXXX	--	--	--	X	--	--	XXX	

† Tr - trace
 X - low <10%
 XX - moderate 10-30%
 XXX - high 30-70%
 XXXX - dominant >70%

Qtz - Quartz
 Kaol - Kaolinite
 Sm - Smectite
 Plag - Plagioclase
 K Spar - K Feldspar

Fig. 14. Euhedral prismatic quartz from the medium silt (5-20 μ m) fraction of the non-carbonate residue of the limestone underlying the Pecos Co. pedon (#9).



in the petrocalcic horizons. Figure 15 shows a prism from the upper C2cam horizon, partially coated with secondary silica. While common in the petrocalcic horizons, euhedral prisms were not the dominant form of quartz, in contrast to the R horizon. Figure 16 shows representative SEM fields of medium silt grains of the R and petrocalcic horizons. The occurrence of prismatic quartz in both the R and petrocalcic horizons suggests some degree of commonality, although the abundance of non-prismatic quartz in the petrocalcic horizons indicates a precursor different from the R horizon.

Examination of silts from the A1 horizons revealed almost a complete absence of euhedral quartz prisms. Typical grains showing rounded edges and rough pitted surfaces are shown in Fig. 17. Diligent searching did, however, yield a few rare prisms in the A1 horizons which are shown in Fig. 18. The relative lack of weathering features such as rounding and pitting on these grains indicates that the soil environment is not harsh with respect to quartz. The absence of prisms in the A1 horizons must therefore be attributed to soil formation from a different parent material rather than to weathering and alteration of the quartz in the soil.

Val Verde County Pedon

This pedon is a Lithic Calciustoll and lacks a petrocalcic horizon. It does, however, have a laminar cap of pedogenic carbonate 2-4 cm thick directly overlying the limestone bedrock. Particle size data for this pedon are presented in Fig. 19. Both carbonate-free and

Fig. 15. Prismatic quartz from the carbonate-free residue of the C2cam horizon of the Pecos Co. pedon (#9). Note the partial coating of secondary silica on the lower portion of the grain (arrows).

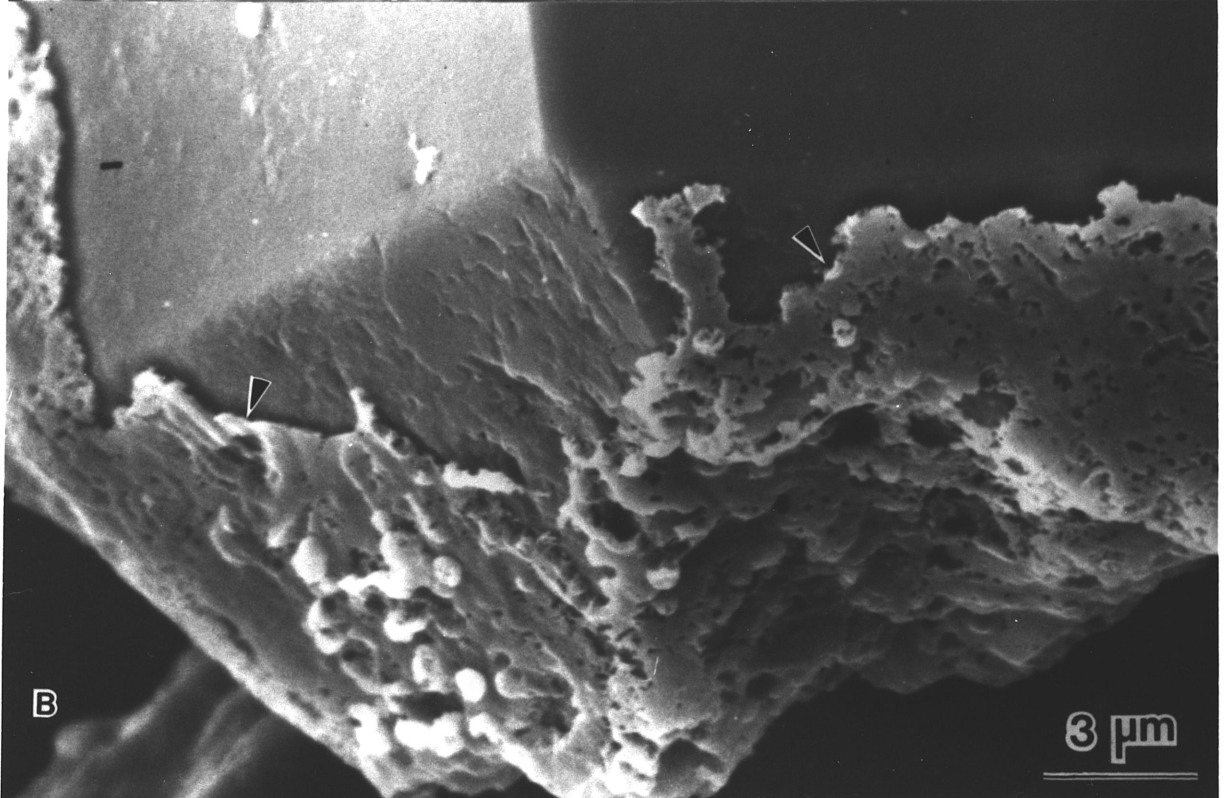
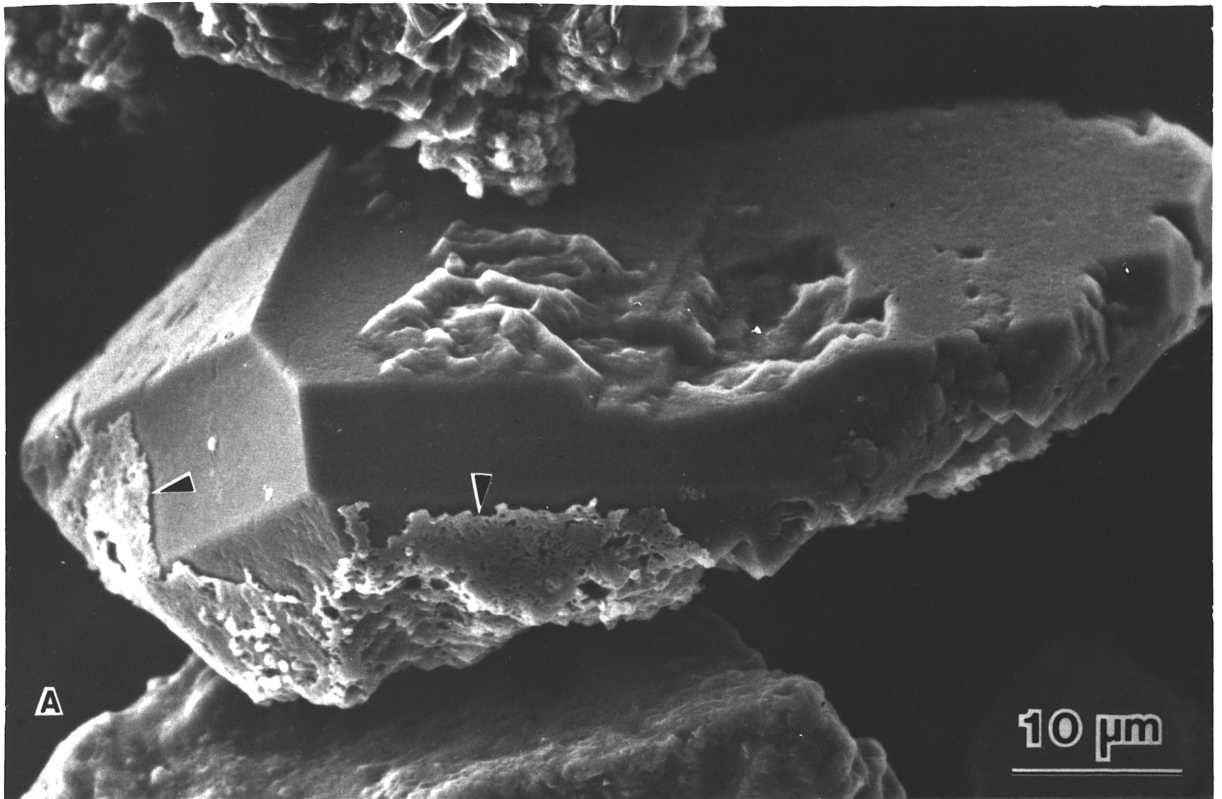


Fig. 16. General SEM fields showing representative grains from carbonate-free residues of the C1cam (A), C2cam upper (B), C2cam lower (C), and R (D) horizons of the Pecos Co. pedon (#9). Note quartz prisms present in all horizons but especially abundant in the R horizon. Note also the abundance of spongy opaline materials (o) in the lower C2cam field (C). Line scale is 20 μ m.

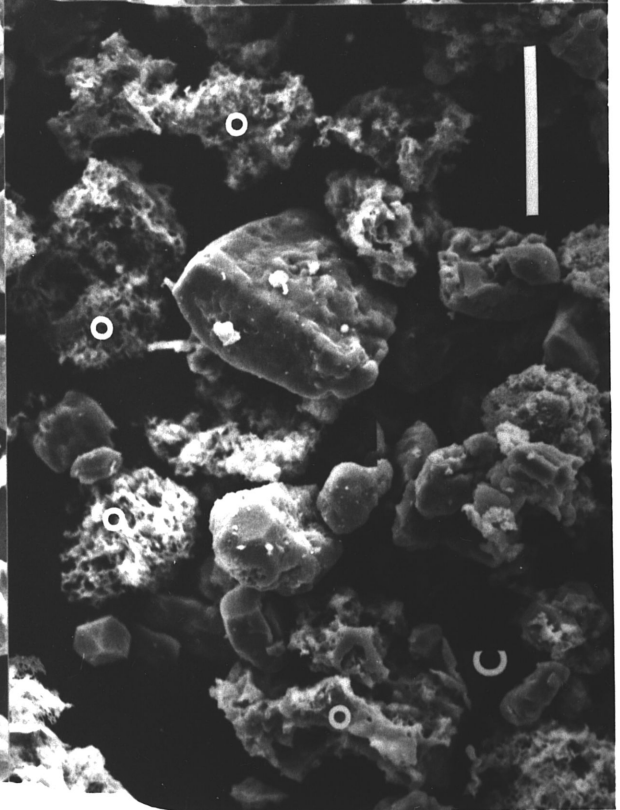
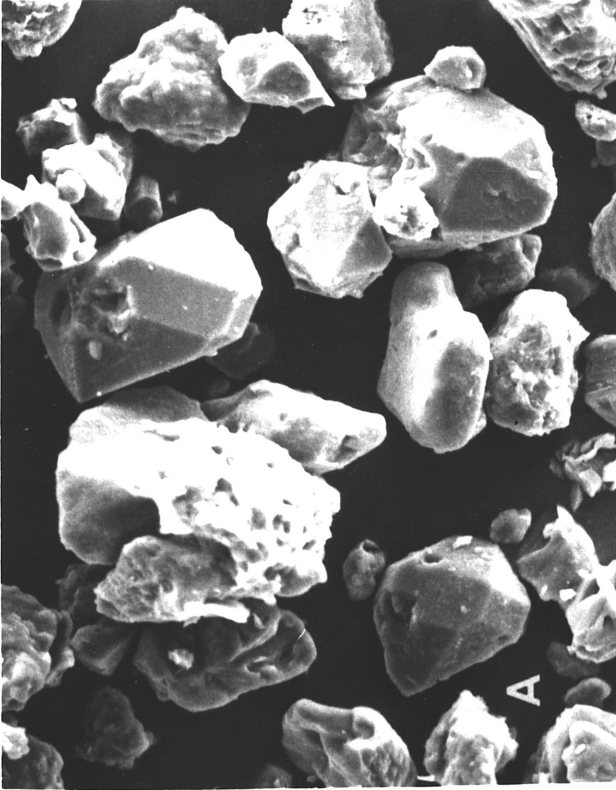
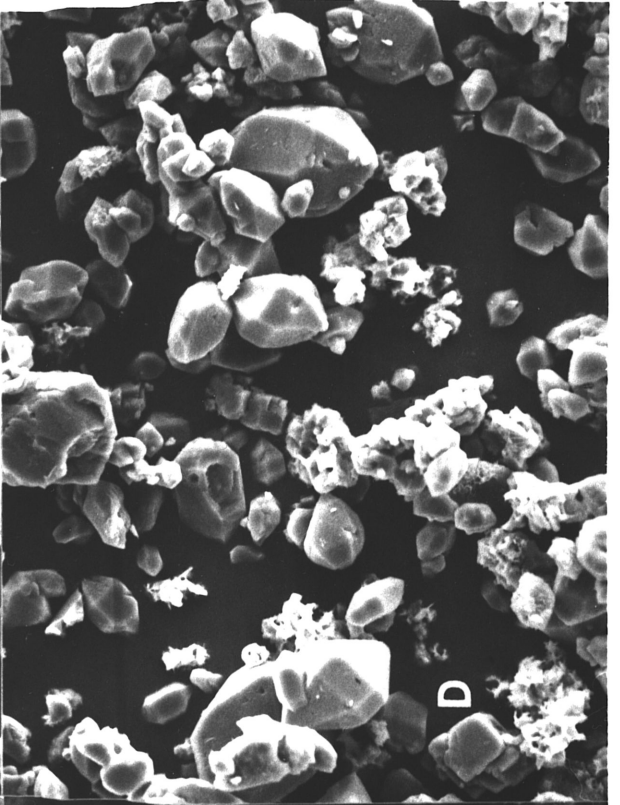
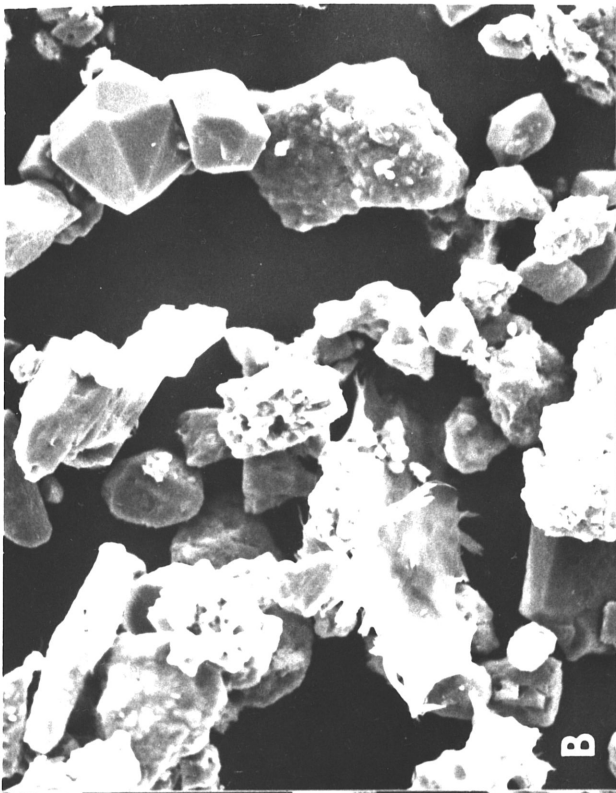


Fig. 17. Representative quartz grains from the silt fractions of the A11 (C and D) and the A12 (A and B) horizons of the Pecos Co. pedon (#9). Note the rounded edges and rough pitted surfaces.

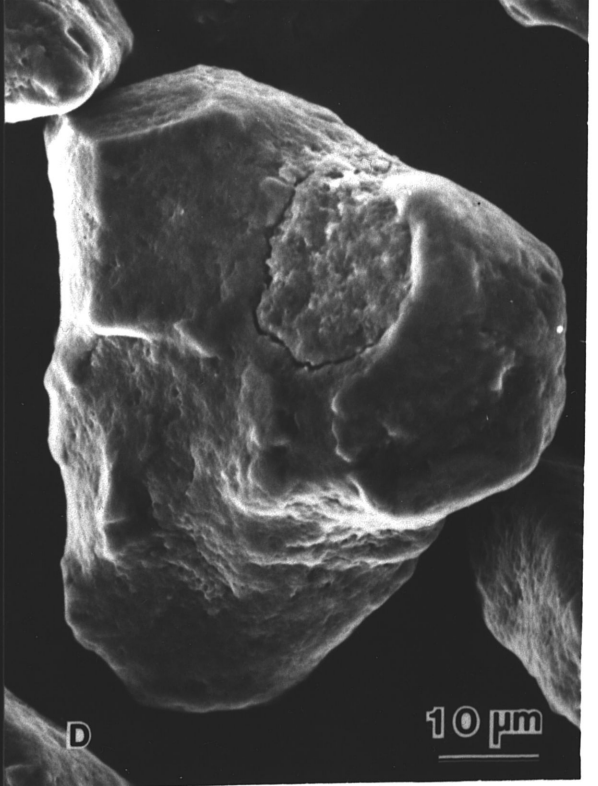
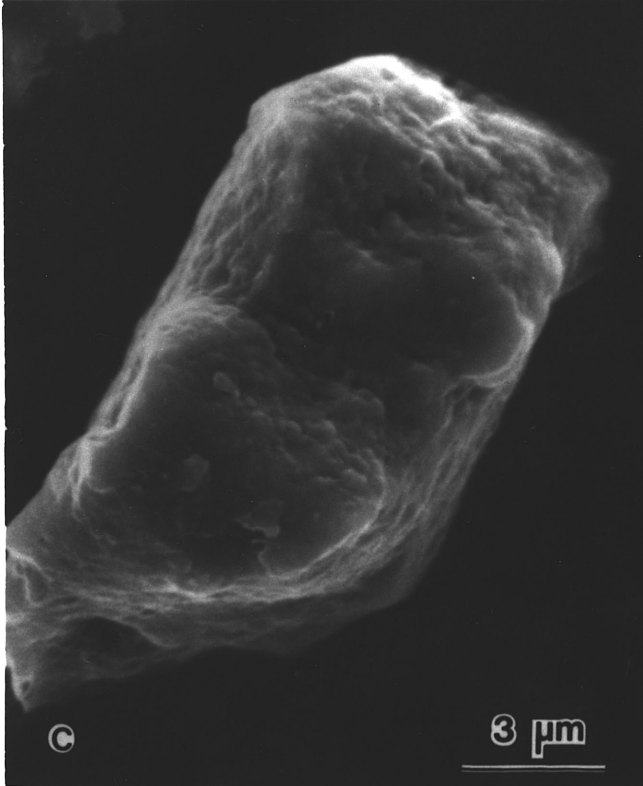
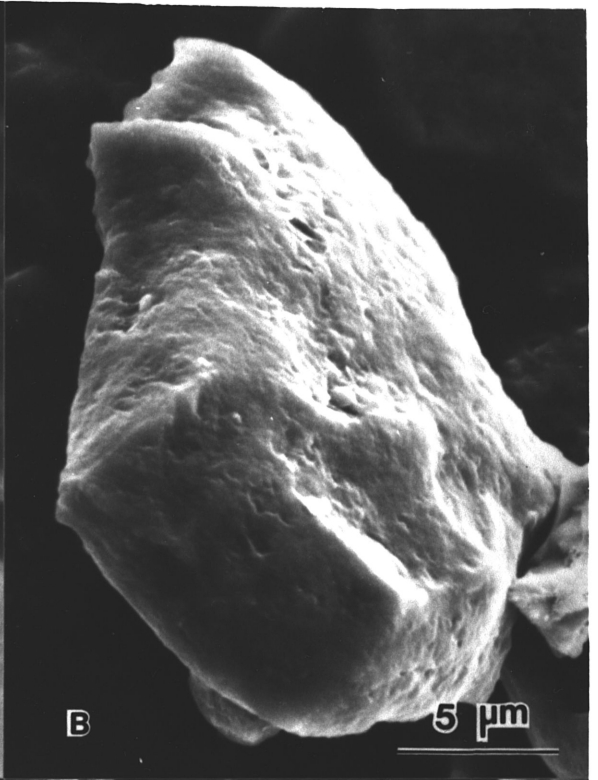
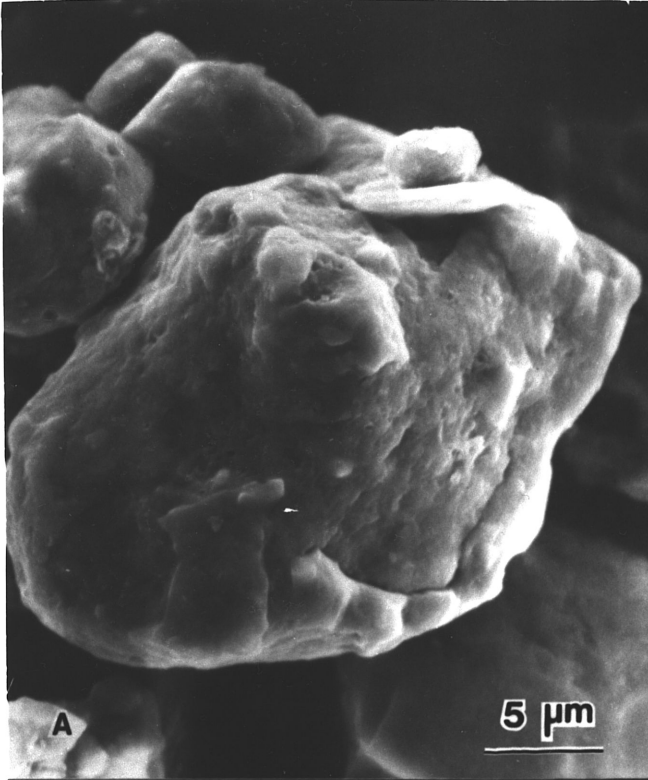
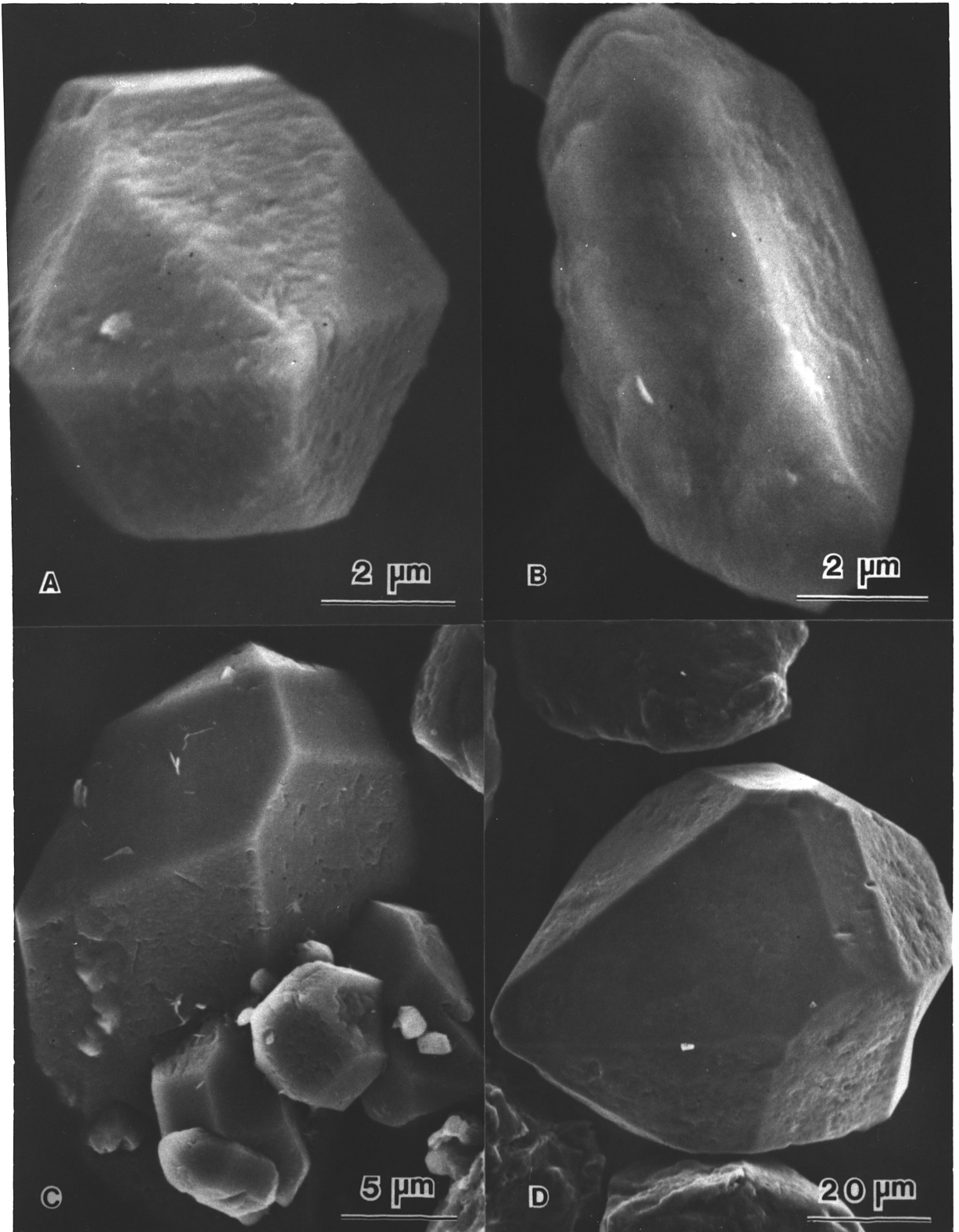


Fig. 18. Rare prismatic quartz grains from the A horizons of the Pecos Co. pedon (#9). Note the well preserved euhedral morphology.



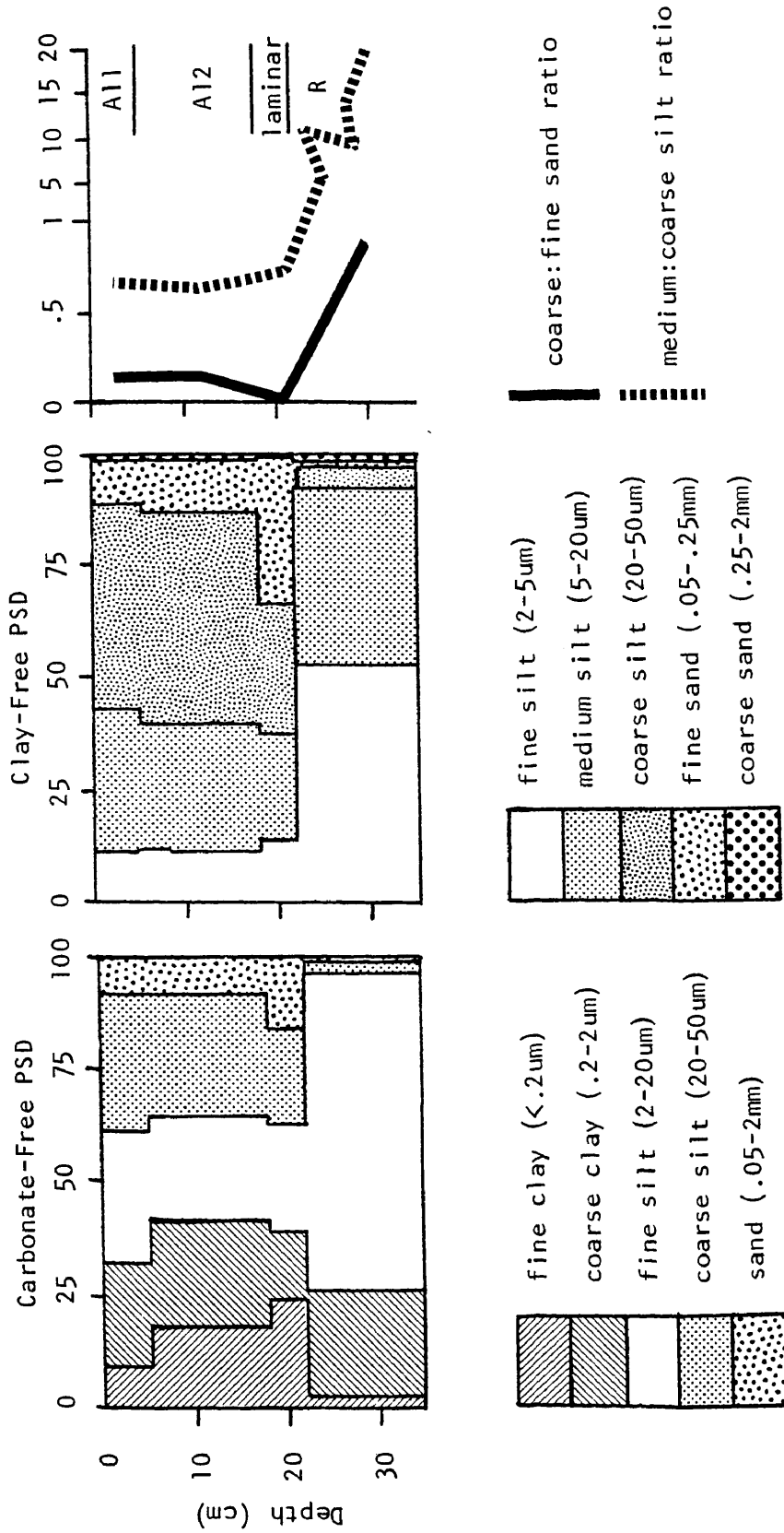


Fig. 19. Carbonate-free and carbonate-free, clay-free PSD and sand and silt ratios shown with depth for the Val Verde Co. pedon (#15).

clay-free data show a high degree of similarity between the A1 horizons and the laminar cap residue. The fine sand levels are, however, greater in the laminar cap at the expense of coarse silt. A drastic change in PSD is encountered in the R horizon residue. Fine and medium silts dominate with very little coarse silt or sand. Elemental analyses for silt fractions in this pedon (Fig. 20) also show similarity among the A1 horizons and the laminar cap but a striking difference with the subjacent R material, which has much lower Zr, Ti, K, and Ca values than the overlying horizons. This indicates that the parent material from which the A1 horizons formed was much different in composition than the R horizon.

This inference is further substantiated by mineralogical evidence. Clay and silt mineralogy is presented in Table 6. Again, a strong similarity exists amongst the A1 horizons and the laminar cap residue while differences with the R horizon residue are plain. Differences are more striking in the coarser fractions where for example the medium silt (5-20 μm) contains moderate amounts of feldspar and some mica but only small amounts of kaolinite. This fraction of the limestone residue, in contrast, contains no mica or feldspar but has high levels of kaolinite. Mineralogical differences between these horizons are also evident in both the coarse and fine clay fractions.

Examination of silts by SEM confirms the previous assessment of parent material differences. Figure 21 shows representative SEM fields of medium silt grains from the A12 horizon, laminar cap residue, and limestone residue. The limestone residue is primarily euhedral quartz prisms and euhedral kaolinite plates which are presumably

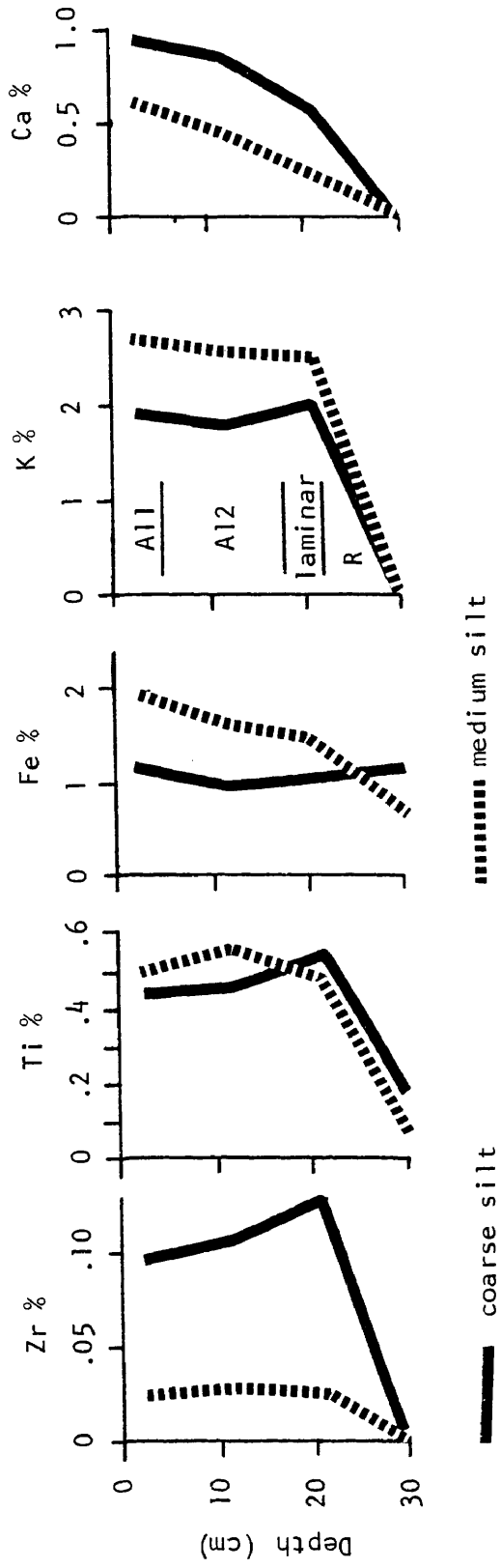


Fig. 20. Elemental analyses of carbonate-free silt fractions from soil and residue of the Val Verde Co. pedon (#15).

Table 6. Semi-quantitative[†] interpretations of XRD analyses of the Val Verde Co. pedon.

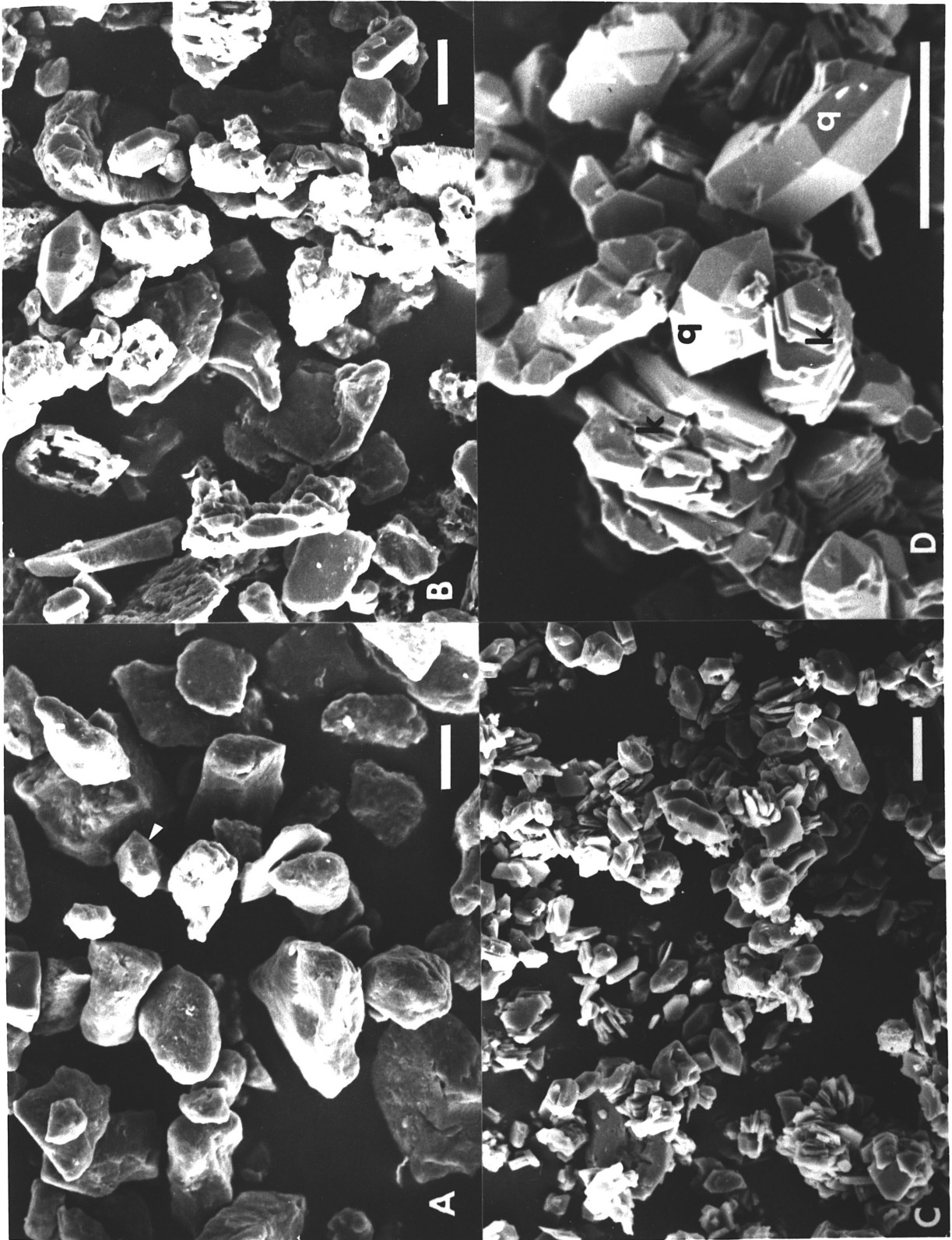
Horizon	Fraction (μm)	Qtz	Kaol	Mica	Sm	K Spar	Plag	Fe Oxide	Ana-tase	Comments
A11	<.2	--	X	XX	XXXX	--	--	--		low charge Sm.
A12		--	X	XX	XXXX	--	--	--		"
Laminar		--	XX	XX	XXXX	--	--	Tr		"
R		--	XX	XXX	XXX	--	--	XX	X	Goethite; Higher charge Sm
A11	.2-2	XX	XXX	X	XXX	Tr	--	X		
A12		XX	XXX	X	XXX	X	--	X		
Laminar		XX	XXX	X	XX	X	--	X		
R		XX	XXXX	--	--	--	--	X		
A11	5-20	XXXX	X	X	--	XX	XX	X		
A12		XXXX	X	X	--	XX	XX	X		
Laminar		XXXX	X	--	--	XX	XX	X		
R		XXX	XXX	--	--	--	--	--		
A11	20-50	XXXX	--	--	--	XX	XX	Tr		
A12		XXXX	--	--	--	XX	XX	Tr		
Laminar		XXXX	--	--	--	XX	XX	Tr		
R		XXX	XXX	--	--	--	--	--		

† Tr - trace
 X - low <10%
 XX - moderate 10-30%
 XXX - high 30-70%
 XXXX - dominant >70%

Qtz - Quartz
 Kaol - Kaolinite
 Sm - Smectite
 Plag - Plagioclase
 K Spar - K Feldspar

authigenic. Keller (1976) has shown similar kaolinite crystals formed authigenically in limestones and other rocks. Prismatic quartz occurred in the laminar cap residue but most grains were rounded and anhedral. Grains in the A1 horizon were also dominantly rounded and anhedral with only a very few quartz prisms observed. This very shallow soil (25 cm to rock), therefore, appears to have substantially

Fig. 21. General SEM fields showing representative grains of carbonate-free silts from the A horizon (A) and residue of the laminar cap (B) and underlying limestone bedrock (C and D). Note scarcity of quartz prisms in the A1 horizon (arrow), common occurrence in the laminar cap, and prominence (with kaolinite) in the bedrock. Both euhedral quartz prisms (q) and euhedral hexagonal kaolinite plates (k) are considered to be authigenic. Line scales are 10 μ m.



formed from a parent material of different particle size, mineralogy and grain morphology than the subjacent limestone.

Real County Pedon

Carbonate-free and clay-free PSD data are shown in Fig. 22. Clay distribution within the solum reflects processes of eluviation and illuviation. Both fine and total clay contents of the limestone residue are, however, substantially lower than the mean clay content of the soil. Minerals which could potentially be weathered to form clays are virtually absent from the silt fractions of the residue, eliminating this as a possible clay source. Pronounced changes with depth in the coarse:fine sand ratio and the medium:coarse silt ratio in the residue also indicate parent material variation. The silt ratios otherwise indicate a high degree of uniformity within the solum. The bulge in the coarse:fine sand ratio in the B horizon is due to the increase in coarse sand size chert fragments in this horizon which has abundant chert coarse fragments.

Elemental analyses of silt fractions are generally uniform throughout the solum. As illustrated in Fig. 23, Zr, Ti, and Ca distributions show only minor fluctuations within the solum. The Fe bulge in the B horizon corresponds to micromorphological observation of silt and sand size Fe nodules in this zone which have presumably formed by Fe movement and segregation. The gradual increase in K toward the soil surface corresponds to observations of XRD patterns indicating a definite, though subtle, increase in K-feldspar levels in

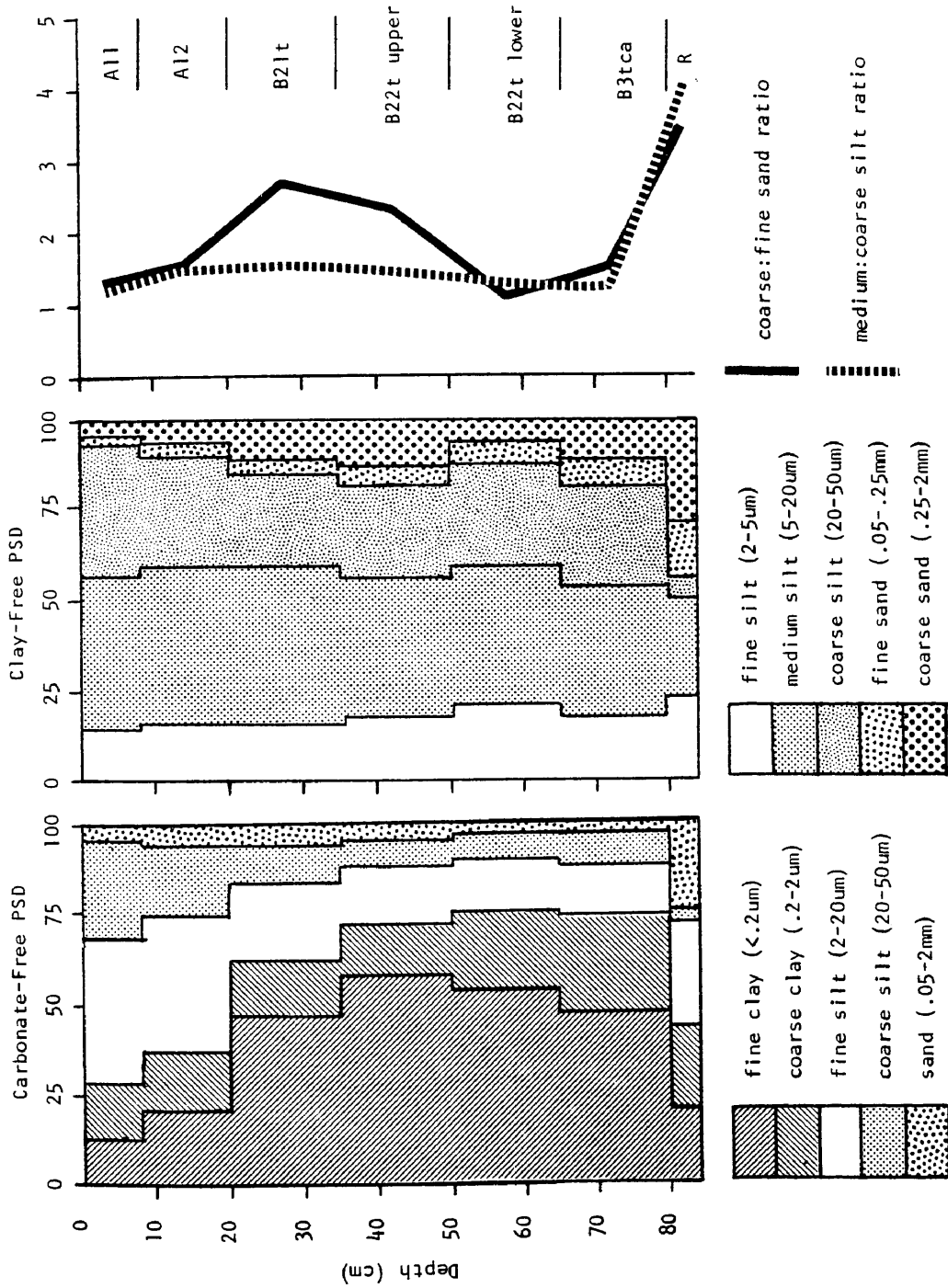


Fig. 22. Carbonate-free and clay-free PSD and sand and silt ratios shown with depth for the Real Co. pedon (#11).

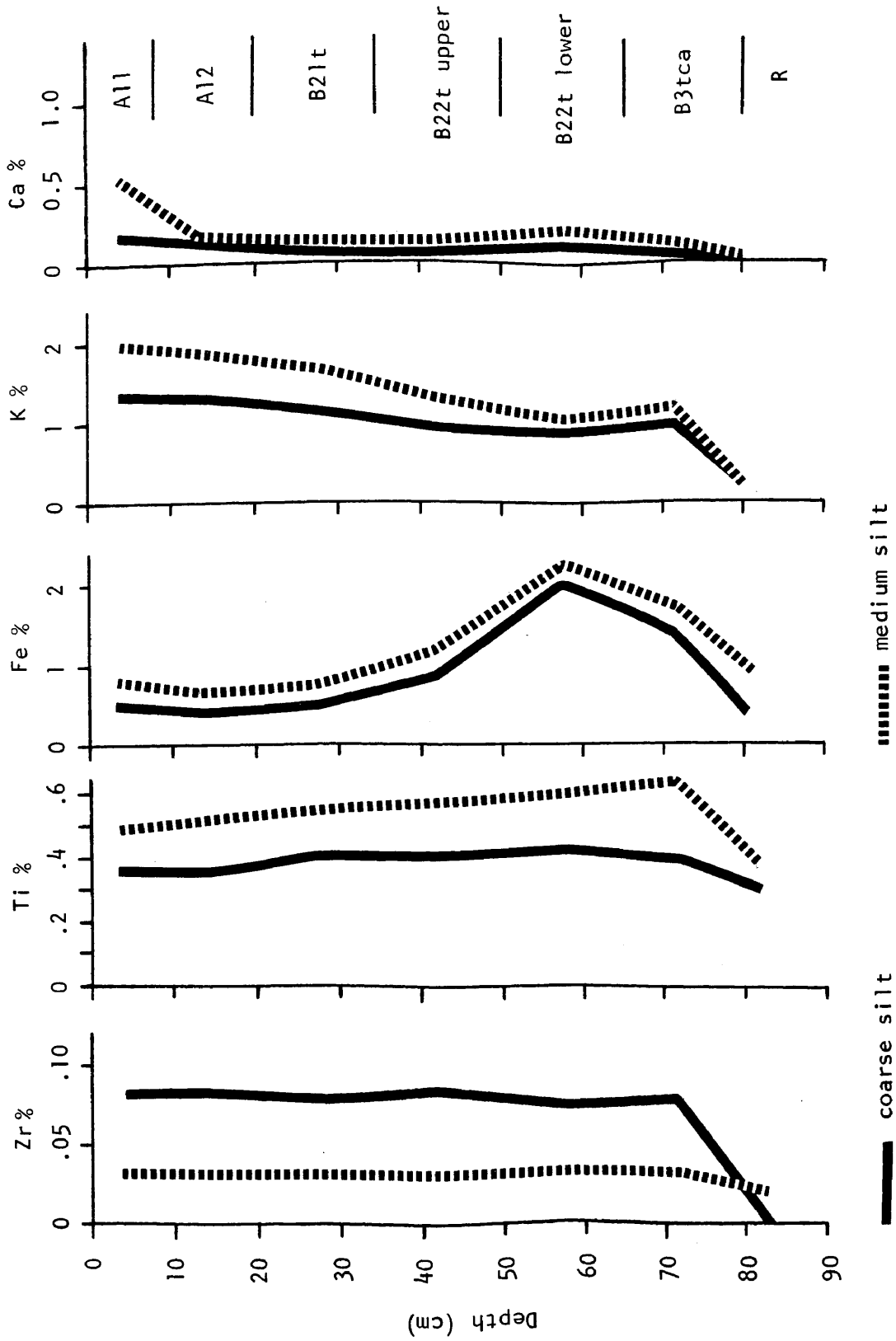


Fig. 23. Elemental analyses of carbonate-free silt fractions from soil and residue of the Real Co. pedon (#11).

the silt fractions. This is not considered to be a residual concentration due to weathering since the elements of stable minerals (Zr and Ti) show no corresponding increase toward the surface. Distinct decreases of all elements measured were observed in the limestone residue. This supports the postulated parent material difference for the formation of the solum.

Mineralogical evidence supports the previous discussion. As presented in Table 7, the mineralogy throughout the A and B horizons is quite uniform. The absence, or only trace amounts, of feldspar in the silts and the low levels of smectite in the coarse clay of the limestone residue, is generally in accord with the previous observations regarding parent material uniformity.

Medium silt fractions of the limestone residue, the B3tca horizon (0-15 cm above bedrock), and the B22t horizon (30-45 cm above bedrock) were examined by SEM. Micrographs of representative fields are shown in Fig. 24. Quartz in the limestone residue was primarily euhedral prisms although some rounded anhedral grains were present. In the B3tca horizon immediately overlying the bedrock, however, quartz prisms were very rare. None were observed in the B22t horizon.

In summary, the A or A and B horizons of all four pedons appear to have formed from parent materials that differ in PSD mineralogy and/or silt grain morphology from the subjacent carbonate material (either bedrock or petrocalcic horizon). In the two pedons without petrocalcic horizons, there was very little incorporation of residues from the presently underlying bedrock into the solum as evidenced by a

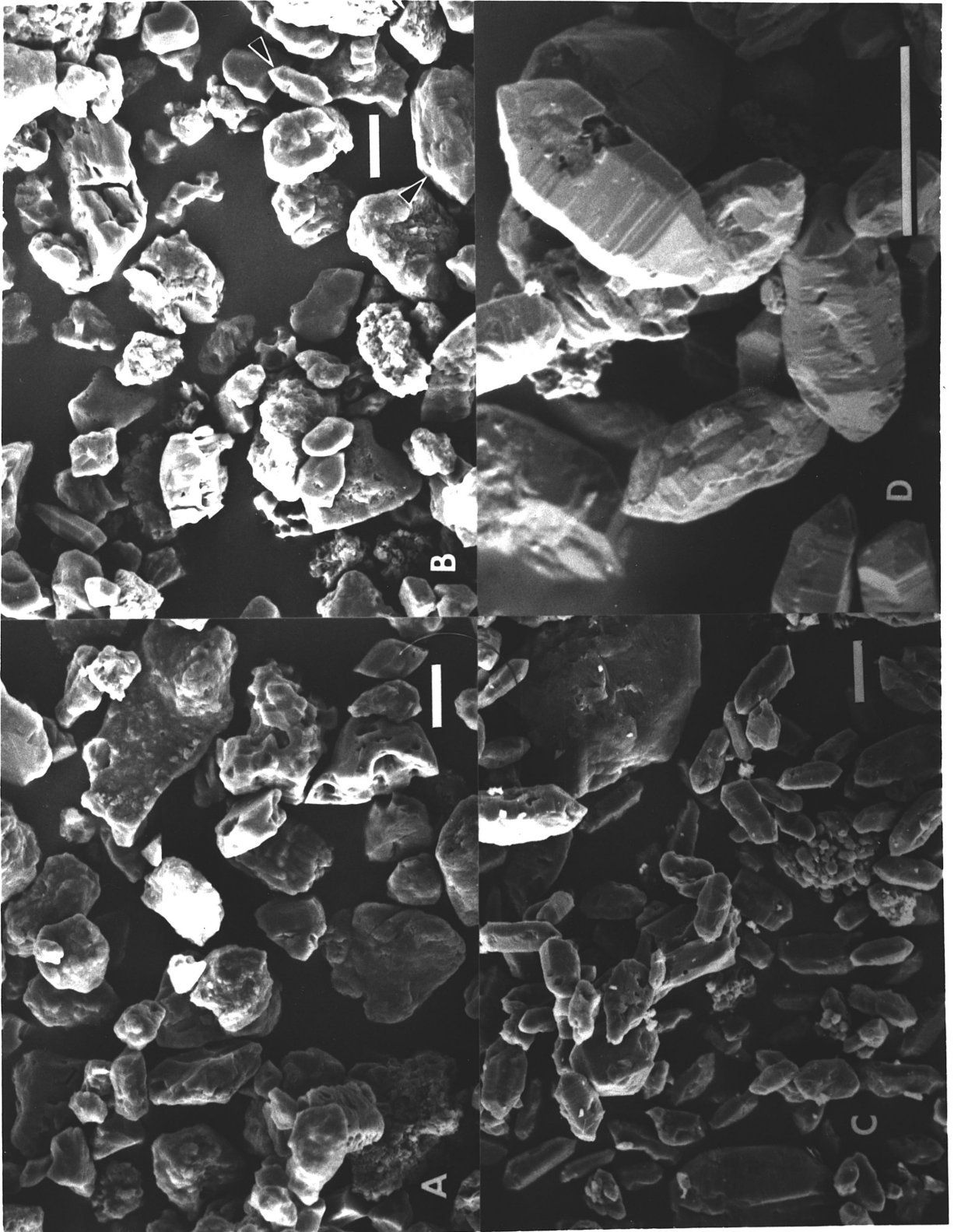
Table 7. Semi-quantitative[†] interpretations of XRD analyses of the Real Co. pedon.

Horizon	Fraction (μm)	Qtz	Kaol	Mica	Sm	K Spar	Plag	Fe Oxide	Other	Comments
A11	<.2	--	XX	XX	XXXX	--	--	--		Goethite
A12		--	XX	XX	XXXX	--	--	--		
B21t		--	XX	XX	XXXX	--	--	--		
B22t		--	XX	X	XXXX	--	--	--		
B22t		--	XX	X	XXXX	--	--	--		
B3tca		--	XX	X	XXXX	--	--	--		
R		--	XX	XX	XXXX	--	--	XX		
A11	.2-2	XXX	XX	XX	XX	X	--	--		
A12		XXX	XX	XX	XX	X	--	X		
B21t		XXX	XX	XX	XXX	X	--	X		
B22t		XX	XXX	X	XXX	Tr	--	X		
B22t		XX	XXX	X	XXX	Tr	--	X		
B3tca		XX	XXX	X	XXX	Tr	--	Tr		
R		XXX	XXX	X	X	Tr	--	Tr		
A11	5-20	XXXX	--	--	--	X	--	Tr	Feldspar content generally increases toward surface	
A12		XXXX	--	--	--	X	--	Tr		
B21t		XXXX	--	--	--	X	--	Tr		
B22t		XXXX	--	--	--	X	--	Tr		
B22t		XXXX	--	--	--	X	--	Tr		
B3tca		XXXX	--	--	--	X	--	Tr		
R		XXXX	Tr	--	--	Tr	--	--		
A11	20-50	XXXX	--	--	--	X	--	--		
A12		XXXX	--	--	--	X	--	--		
B21t		XXXX	--	--	--	X	--	--		
B22t		XXXX	--	--	--	X	--	--		
B22t		XXXX	--	--	--	X	--	--		
B3tca		XXXX	--	--	--	X	--	--		
R		XXXX	--	--	--	--	--	--		

† Tr - trace
X - low <10%
XX - moderate 10-30%
XXX - high 30-70%
XXXX - dominant >70%

Qtz - Quartz
Kaol - Kaolinite
Sm - Smectite
Plag - Plagioclase
K Spar - K Feldspar

Fig. 24. General SEM fields showing representative silt grains from the B22t horizon (A), B3tca horizon (B), and the limestone residue (C and D). Note the abundance of quartz prisms marked by prominent striations in the limestone residue. Prismatic quartz crystals are rare in the B3tca (arrows) and absent from the B22t. Line scale is 10 μ m.



lack of euhedral quartz prisms. It is postulated that the stratigraphically overlying rock contained more detrital quartz and was perhaps less indurated than the presently underlying rock. A softer limestone having a higher porosity and being more subject to changes in pore fluid composition, would be less likely to provide the micro-environment necessary for the crystallization of prismatic quartz. Furthermore, the softer, higher porosity limestone would be more subject to weathering, loss of carbonates, and the residual accumulation of soil materials. The interface between the more indurated and the softer limestones would provide a natural barrier or restraint to further residuum accumulation.

In the cases where the soils did have petrocalcic horizons, the limestone precursor to the petrocalcic was in one case similar to, and in the other case different from, the underlying limestone. The lowest horizon sampled in the Kinney Co. pedon was a Crca/C4cam horizon. Micromorphological examination indicates that the material is a soft limestone with substantial enrichment in pedogenic carbonates. This material is similar in PSD and mineralogy to the precursor of the petrocalcic horizon. In the Pecos Co. pedon where the petrocalcic horizon overlies hard limestone, the petrocalcic precursor shared some similarities with, but also differed from the underlying limestone bedrock.

Impact of Dusts on Soil Parent Material

Having concluded that much of the A and B horizons in the soils studied has formed from a limestone residuum different from

immediately subjacent limestone, there still remains the need to estimate the degree of accumulation of airborne dusts in the soils. In order to make this evaluation, dusts were collected and characterized regarding PSD, mineralogy, silt grain morphology and elemental analysis. A complete description of the procedure and analyses is given in Appendix B. The dusts collected across the study area were quite uniform in the parameters measured. The quantity of dust collected in the dust traps may not reflect the long term rates of accumulation due to 1) differences in efficiency of collection due to trap design, 2) long term fluctuations in quantities of dust added due to climatic changes, and 3) removal of soil material through processes of geologic erosion. The qualitative nature of the dust could theoretically, however, be compared to the soil and the parent material and thereby used to estimate the long term impact. The average particle size distribution for the 7 sites and 4 collection periods is given in Table 8.

Table 8. Average particle size distribution for dusts (Seven sites and 4 collection periods).

<2 μm	2-5 μm	5-20 μm	>20 μm
----- % -----			
58	7	26	9

Mineralogical interpretations of XRD analysis for the clay and medium silt fractions (the two dominant fractions) over all locations and collection periods have been summarized in Table 9. Summary data for elemental analyses of the medium silt (5-20 μm) fraction of dusts

collected from the 7 locations during 4 collection periods are presented in Table 10.

Table 9. Semi-quantitative[†] interpretations of XRD analyses of dusts; Summary (Seven sites and 3 collection periods).

Fraction	Sm	Kaol	Mica	Qtz	K Spar	Na Spar
<2 μm	X	X	XXX	XXX	X	--
5-20 μm	--	--	Tr	XXXX	XX	X

[†] Tr - trace
 X - low <10%
 XX - moderate 10-30%
 XXX - high 30-70%
 XXXX - dominant >70%

Qtz - Quartz
 Kaol - Kaolinite
 Sm - Smectite
 Na Spar - Na Feldspar
 K Spar - K Feldspar

Table 10. Average elemental analysis of the 5-20 μm fraction of dusts collected.

	K	Ca	Ti
	----- % -----		
	1.04 \pm .43 [†]	.42 \pm .13	.28 \pm .05

[†] Mean value \pm std. dev. of 28 measurements (7 sites; 4 periods).

The PSD of the dust shows the clay (58%) and medium silt (26%) fractions to be dominant. The surface horizons of the 15 pedons sampled have clay contents which generally range between 15 and 40%, while sands (>50 μm) range between 5 and 25%. This supports earlier statements that the dusts are not the primary soil parent material. The soils could, however, admix significant quantities of dust with

relatively small and undetectable changes in the PSD. Particle size is therefore not a sensitive indicator of dust additions. The minerals contained in the dusts are also present throughout most of the soils examined. Mineralogy cannot therefore be used to estimate dust inputs.

No carbonate minerals were observed in the dusts. This may reflect dissolution of carbonates during processing of the dust or simply a lack of carbonates in the airborne material. Water soluble Ca levels in filtrates collected during dust processing were only 15-30% of calcite saturation. Any particulate carbonates would therefore be dissolved. Calcium values were, however, approximately equal to infall expected from rainfall (Junge and Werby, 1958; Lodge et al., 1968). The lack of a significant correlation between water soluble Ca and total dust infall further suggests that much if not most of the Ca is entering as dissolved Ca in rainfall and not as particulate carbonate dusts (See Appendix B). Since most of the surface soils, especially in the western part of the study area are calcareous, this further supports the idea that the dusts are not locally derived.

In order for the elemental analyses of dusts to be useful criteria for estimating additions, the levels in the dust must be substantially greater than those of the soil parent material. If the mid to lower part of the solum is considered to best reflect the elemental concentrations of the parent material, the Ti levels in the dusts are in all cases lower than the values for the same fraction in the soils analyzed (see Figs. 11, 13, 20 and 23). Values for Ca and K in the

dusts are also similar to or lower than carbonate-free values in the soil, with the exception of Ca in the Real Co. pedon. Calcium levels beneath the A11 horizon are approximately 0.1%, while it is 0.54% in the A11. It is unlikely that the higher Ca levels in the A11 are due solely to dust additions in that the levels are actually higher than those in the dust. Thus, even if the A11 horizon were comprised of 100% dust (which is not the case), the Ca level would only be approximately 60% of the measured level. It appears therefore that elemental analyses are not useful in estimating dust accumulation in these soils.

Examination of the 5-20 μm dust fractions by SEM revealed grains with two primary grain morphologies and a third less common form. Less than half of the grains had smooth surfaces, sharp edges and some conchoidal fracture. The other major group had rough, weathered, and sometimes pitted surfaces with rounded edges. The third less common group showed distinct linear or right angle weathering traces, presumably along cleavage planes or zones of weakness (see Appendix B for micrographs illustrating the 3 morphological types). Chemical analyses of individual grains using the electron microprobe showed the last group to be entirely feldspars (primarily K-feldspars). Prior to microprobe analysis, the smooth, conchoidally fractured grains were presumed to be quartz. During analysis, however, both quartz and feldspars were found with smooth, conchoidally fractured surfaces and with rough, pitted surfaces. Most of the smooth surfaced grains analyzed were in fact K-feldspars.

Examination of the 5-20 μ m fractions of limestone residues and lower soil horizons indicated that rough rounded grains were common but that conchoidally fractured grains with smooth surfaces were very rare. The smooth-surface dust grains could therefore be used to trace dust accumulations in soils. Analyses of silt fractions from surface horizons of the pedons studied revealed a stark absence of conchoidally fractured smooth-surfaced grains. Representative soil grains showing rounded edges and rough surfaces are shown in Fig. 17. There are two possible explanations for the absence of the characteristic conchoidally fractured grains from the soil. One possibility is that the weathering environment in the soils is harsh enough to cause rounding and pitting of the grains. The near neutral soil pH and slight to moderate leaching in these soils is not a particularly harsh environment as regards quartz or feldspars although during previous more pluvial conditions, the grains may have been more subject to alteration. During the previous discussion concerning the tracing of euhedral quartz prisms from the limestone into the soil, a few well preserved prisms were observed in the surface horizons (Fig. 18). This confirms that quartz is relatively stable in this environment. We cannot state conclusively that the K-feldspar grains are not subject to alteration in these soils, but we can state that conchoidally fractured quartz dust with smooth surfaces should maintain that grain surface morphology within the soil environment.

We must, therefore, move to the other possible explanation for the lack of these characteristic grains in the soil, which is that dusts must not be substantially accumulating in the soils. The

quantity of dust collected in the traps indicates that they are being presently added at the rate of approximately 1 mm/100 yrs. Erosional processes by water and/or wind must be equal to or greater than these rates to account for the lack of dust accumulation.

Differentiation of Pedogenic and Lithogenic Carbonates

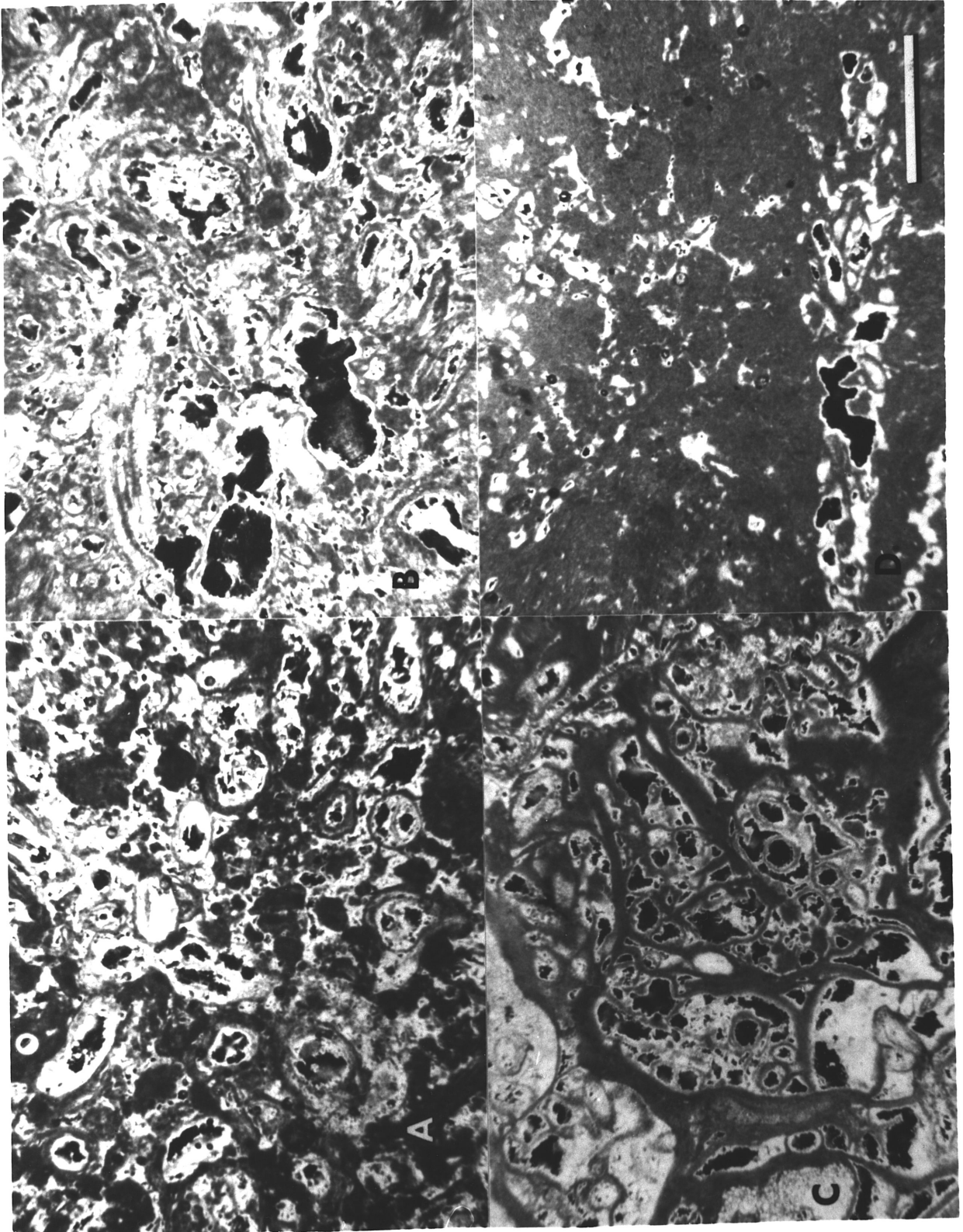
Horizons in several pedons were identified by field criteria as petrocalcic horizons. There was some doubt however whether these materials were in fact petrocalcic horizons of pedogenic origin or whether they were primarily limestone materials inherited from the parent lithology (lithogenic carbonates). It was felt that laboratory analysis was necessary to confirm or reject the field determinations. Differentiation of pedogenic from lithogenic carbonate forms was pursued through micromorphology and carbon isotope analysis.

Micromorphological Evidence for Pedogenic Carbonates

Observed fabrics. Examination of thin sections of questionable petrocalcic materials revealed a great variety of microfabrics. There was also often great heterogeneity within a given horizon or even within a given thin section, such that a single horizon may show several distinctly different fabrics. Fabrics were classified into four major groupings, although gradations and mixtures occur with all of them.

One type was a highly porous form with a convoluted micritic network. This is illustrated in Fig. 25 and will hereafter be referred to as the "convoluted" fabric. Figure 25D is an example where the

Fig. 25. Examples of convoluted microfabrics in petrocalcic horizons: C1cam horizon (A and D) and the R1ca/C2cam horizon (C) from pedon #12; A13 & Ccam horizon (B) of pedon #13. Both pedons are in Sutton Co. The line scale is 1 mm. Cross-polarized light.



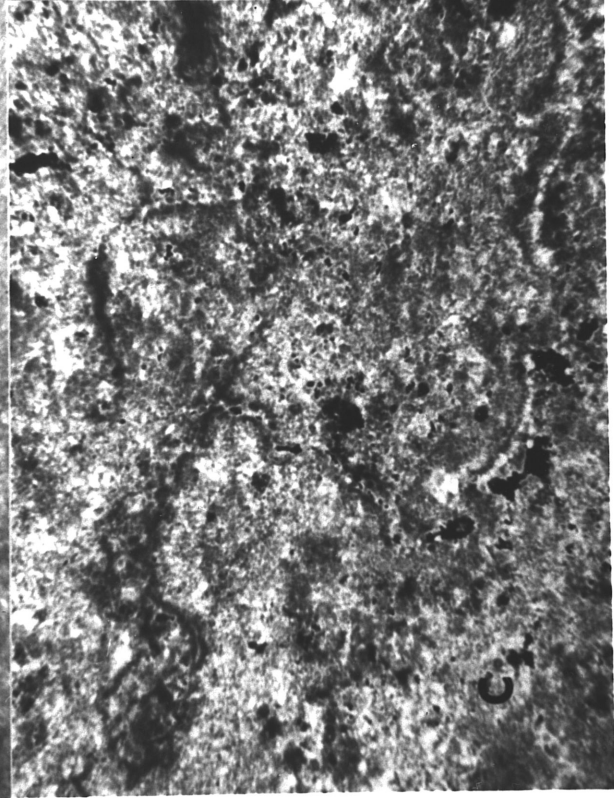
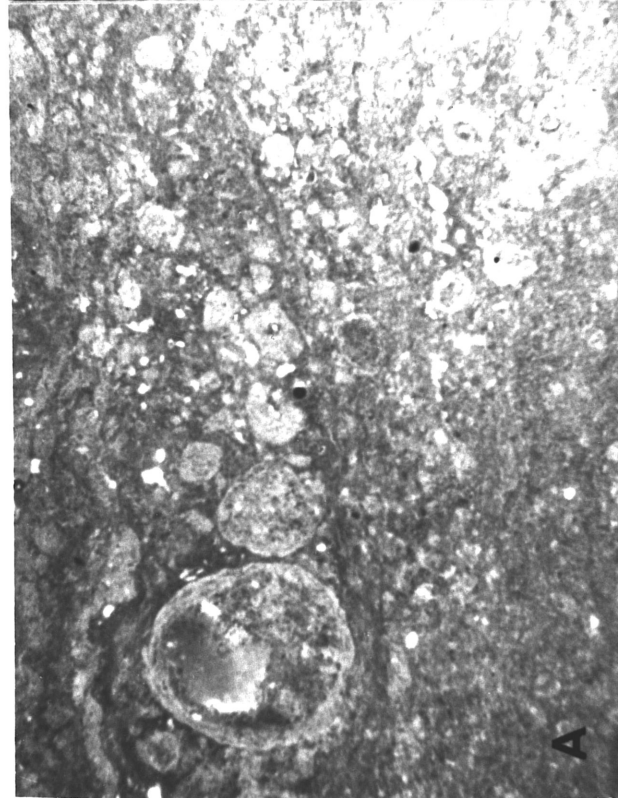
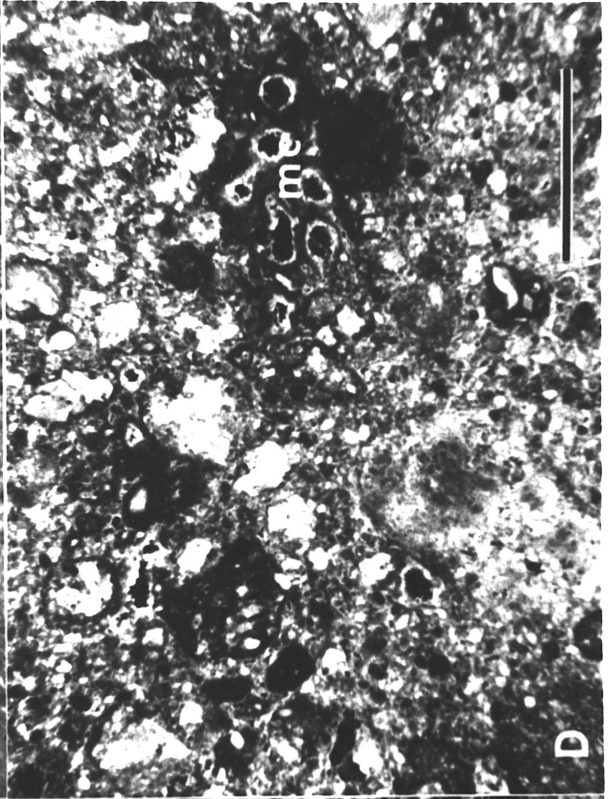
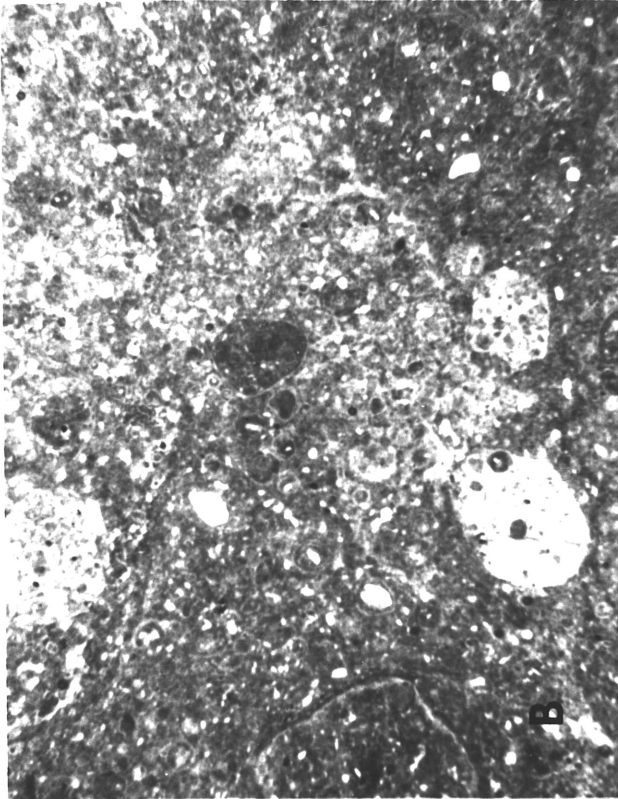
fabric is less porous and the convoluted network is less prominent, but the fabric is still more similar to this group than to the others and has therefore been grouped with the convoluted fabrics. Read (1974) and James (1972) have both reported highly micritized zones in petrocalcic (caliche) materials.

The second type of fabric is dominated by micritic nodules occasionally containing nuclei of larger calcite crystals. This fabric is illustrated in Fig. 26, and will be referred to as the "nodular" fabric. These appear similar to what some have referred to as soil or calcrete ooids (Read, 1974) or micritic pelletoids (James, 1972) which have a characteristic clotted fabric. The final two petrocalcic fabrics are shown in Fig. 27. One has been termed "pisolitic," in reference to the presence of larger (.25 mm to >1 mm) spherical bodies showing in some cases a concentric layering. The outer layer (and often other concentric layers) are yellowish in color, suggestive of the presence of silicate clay. Although smaller in size than what is usually termed "pisolites," they show a strong morphologic similarity (Dunham, 1962; Thomas, 1965). The remaining fabric type is dominated by neomorphic microspar with crystals in the range of 5-30 μm . This material has apparently recrystallized leaving no evidence of primary limestone features and thus has been called the "recrystallized" fabric. Sehgal and Stoops (1972) have reported similar zones of coarse granular calcite which has formed through the recrystallization of micrite and was interpreted to be a pedogenic product. James

Fig. 26. Examples of nodular microfabrics in petrocalcic horizons: C1cam (A) and C2cam (B) horizons of Pecos Co. pedon #9; Ccam horizon (C) of the Crockett Co. pedon (#2); Rca/Ccam horizon (D) of the Kerr Co. pedon (#5). Line scale is 1 mm. Cross-polarized light.



Fig. 27. Examples of pisolitic (A and B) and recrystallized (C and D) microfabrics in petrocalcic horizons: Ccam&A1 horizon (A) of the Crockett Co. pedon (#2); C1cam horizon (B) from Pecos Co. pedon #10; C2cam (C) and C1cam (D) horizons from Pecos Co. pedon #9. D shows a few zones of micritic convolutions (mc). Line scale is 1 mm. A and B under plane light. C and D under cross-polarized light.



(1972) has also illustrated the recrystallization of micrite to microspar in caliche which he explains as a result of the presence of vadose pore fluids.

Identifiable pedogenic carbonate forms. Certain carbonate forms can be identified on field evidence alone to be of pedogenic origin. These include laminar caps, pendants, and concretions. It was thought that micromorphological examination of known pedogenic forms may provide useful information in determining the origin of questionable "petrocalcic" fabrics.

Examination of thin sections of numerous laminar caps revealed several characteristic features. These can be seen in representative micrographs in Fig. 2 of Appendix D. As would be expected, they show a horizontal, though wavy, lineation parallel to the laminar surface. Virtually all of the caps examined also showed sand and silt sized quartz skeleton grains and Fe and Mn glaebules. The porosity of these materials was generally low, with the exception of the upper few tenths of a mm which in a few cases was more porous.

The pendants examined showed two distinctly different fabric types. These are illustrated in Fig. 3 of Appendix D. In one case the microfabric is highly reminiscent of the laminar cap material showing laminar foliations, incorporation of quartz grains, and manganese staining. The other type of pendants observed had a micritic fabric which was more porous, lacked quartz skeleton grains, and showed no manganese staining. The fabric itself is quite similar to the convoluted fabrics identified in some of the questionable massive petrocalcic materials and supports the designation of such materials as pedogenic in origin.

Carbonate concretions were observed only at one location. While the concretions have nucleated around various materials, the primary fabric of the concretions was characteristic. Like the first type of pendant, the concretions share characteristics with the laminar material. Representative micrographs can be seen in Fig. 4 of Appendix D. The concentric zoning in the concretions is similar to the horizontal laminations in the caps. The concretions also show distinct Fe and Mn stains and quartz skeleton grains. In addition to microfabric features held in common by the laminar caps, pendants, and concretions, stable carbon isotope data indicate a similar environment of formation for these forms (Appendix D). The micromorphological similarities are therefore perhaps indicative of the genetic similarities.

Evidence for fabric genesis. While the microfabrics observed in the questionable petrocalcic materials did not show features typical of lithogenic carbonates, this negative evidence was not considered sufficient for confident designation as pedogenic carbonates. Careful examination did, however, uncover evidence to support the pedogenic origin of the convoluted and nodular fabrics. Figure 28 shows a sequence of micrographs demonstrating the gradual alteration of a hard crystalline lithogenic fabric into a highly porous, micritic convoluted fabric. Initial alteration of sparry crystalline calcite to fine grained micrite through dissolution and reprecipitation at the solution-mineral interface (micritization) occurs around pores and fissures in the limestone. Continued micritization, presumably instigated by pore water, causes eventual coalescing of the micritic

Fig. 28. Progressive stages in the formation of micritic convoluted fabric through the weathering of limestone. Well crystallized limestone (A) shows slight micritic zones around some pores (arrows). B and C show further development of micritic zones around growing pores which begin to coalesce. D shows nearly complete development of convoluted fabric. R horizon from Gillespie Co. pedon #4. Line scale is 0.5 mm. Cross-polarized light.



network. Similar processes have been reported by James (1972) and Read (1974).

Sehgal and Stoops (1972) have reported the presence of randomly oriented calcite needles in pores of petrocalcic materials. Similar observations were made in a number of petrocalcic horizons in this study. A second mode for the formation of the convoluted fabric is illustrated in Fig. 29. Acicular calcite crystals growing in pores begin to form masses with preferential rather than random orientation. As calcite needles continue to grow, a network is developed demonstrating the characteristic convoluted fabric. James (1972) has also observed calcite needles arranged tangentially to particles or walls of microfractures occurring in bundles up to 50 μm thick and in some cases forming self supporting structures in voids. Aging and/or crystal growth pressures cause alteration of the needles to micrite in the more dense portions of the network.

Thin-section examination also revealed two possible modes of formation of nodular fabrics. Figure 30A shows the transition of a crystalline fossiliferous limestone to a very fine nodular fabric where the nodule size increases away from the limestone interface. This is also further illustrated in Fig. 30B wherein the alteration of limestone to a nodular material, a fragment of the lithogenic material has become engulfed in the fine, nodular, micritized matrix. James (1972) and Read (1974) have reported the pedogenic alteration of carbonate skeletal grains to micritic nodules which they have termed micritic pelletoids and calcrete ooids respectively. Figure 30C shows the agglomeroplasmic related distribution in the A1 horizon from the

Fig. 29. Formation of convoluted fabric through the growth of calcite needles. The higher magnification of A and B reveals growth and coalescing of needles to form a network. C and D show the network at a more advanced stage of formation with a distinctly convoluted appearance. Note in D the presence of fossils (f) still remaining in the yet unaltered soft limestone material. A, B, and C are from the Cr2 horizon and D from the Cr3 horizon of a soil in the Real series in Hays Co. (not from this study). Line scale is 0.5 mm. Cross-polarized light.

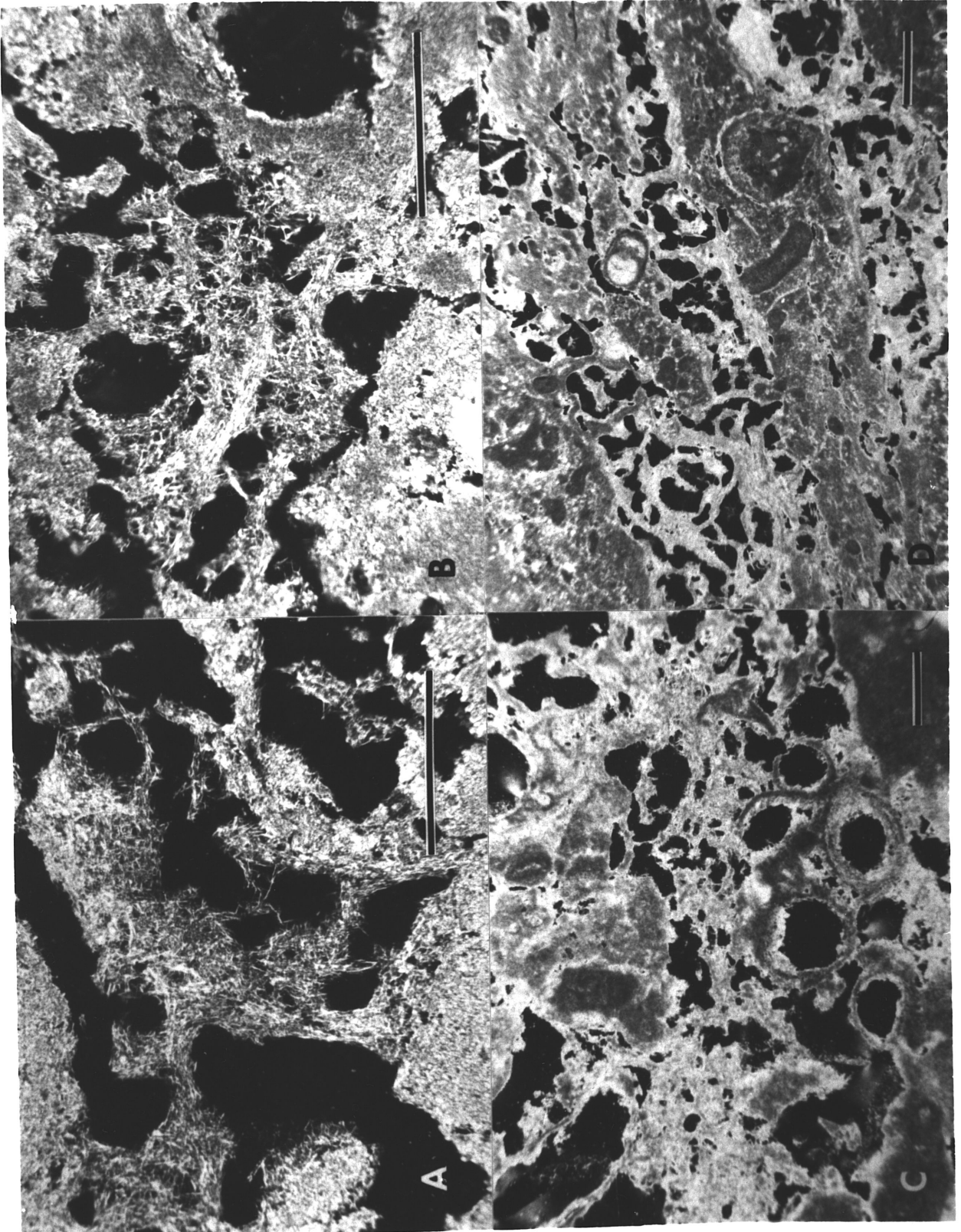
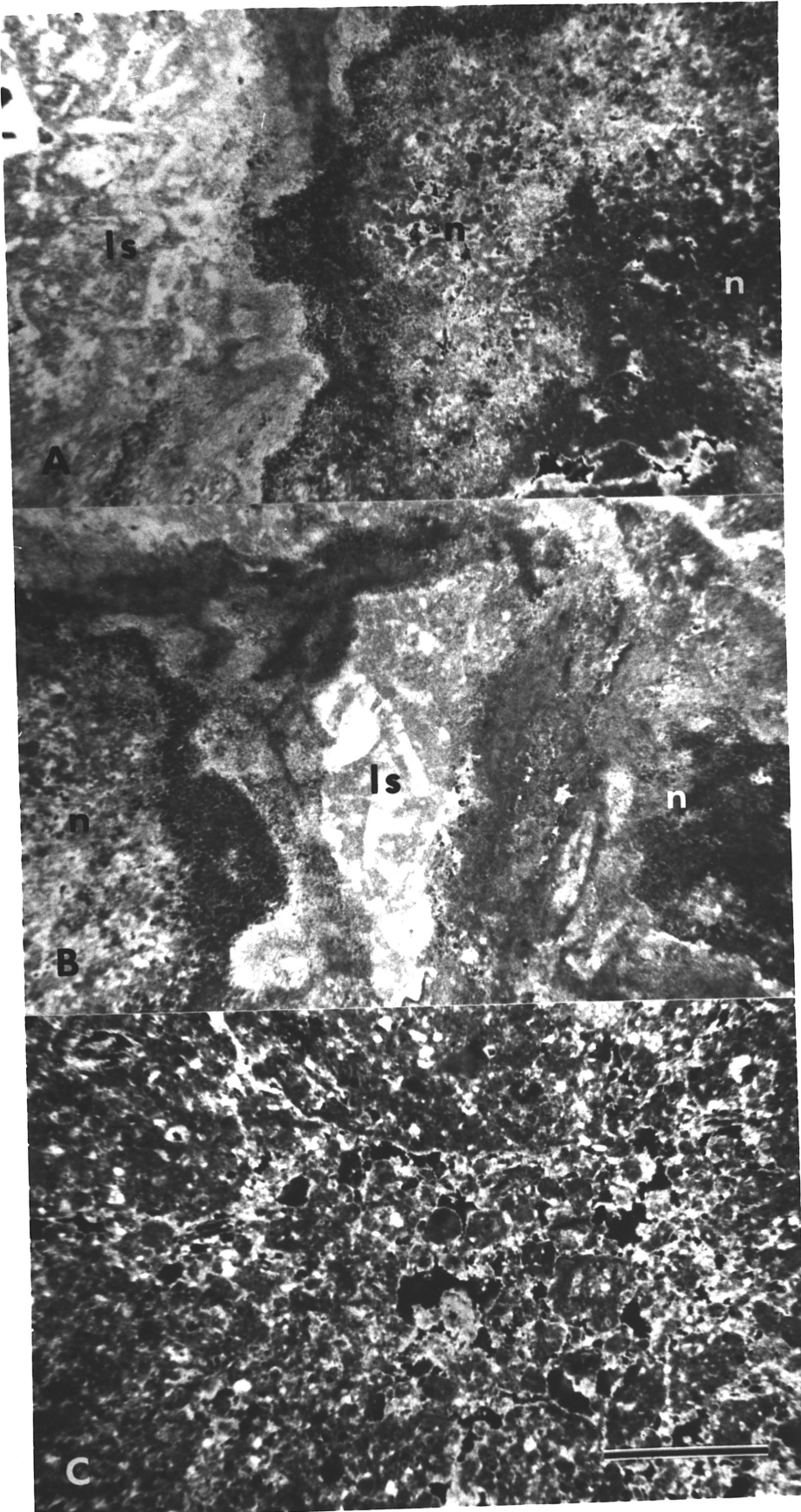


Fig. 30. Formation of nodular microfacbric. A and B show alteration of crystalline limestone (ls) (R horizon of Medina Co. pedon #8) to a nodular material (n). Note how in B a limestone remnant has been engulfed by the encroaching nodular matrix. C shows the highly calcareous (44% CaCO₃) A1 horizon from the Terrell Co. pedon (#14). It has a similar appearance to some nodular fabrics and might be considered a "proto-nodular" or "neo-nodular" fabric. Line scale is 1 mm. Cross-polarized light.



Terrell Co. pedon. This horizon contains 44% CaCO_3 and has a crystic plasmic fabric. While quartz skeleton grains are common (which may or may not occur in nodular fabrics) the soil material appears to be incompletely aggregated into roughly spherical bodies as a "neo-nodular" fabric (weakly expressed newly developing nodular fabric). This fabric was not observed in other soils lower in carbonates and it is postulated that the high carbonate levels may affect the development of the nodular or clotted fabric.

Although complete genetic mechanisms are not provided in the preceding discussion, the morphologic similarities and adjacent occurrence of features suggest that the convoluted and nodular fabrics have formed in near surface, pedogenic environments.

Carbon Isotope Evidence for Pedogenic Carbonates

In nature, both thermodynamic and kinetic factors have caused fractionation of carbon isotopes. While marine (lithogenic) carbonates usually have $\delta^{13}\text{C}$ values near zero, the processes of pedogenic carbonate formation result in considerably lower values which are dependent primarily on the $\delta^{13}\text{C}$ of the soil CO_2 gas. Therefore, a simple proportionality may be employed to quantitatively estimate pedogenic carbonates in the soil. See Appendix D for a complete discussion of the theory behind this method.

Several pedons were selected for isotopic analysis and data for the horizons having the questionable microfabrics are presented in Table 11. The five samples with convoluted fabrics had pedogenic carbonate values in the range of 58-100%. Samples with nodular and

Table 11. Percent calculated pedogenic carbonates in questionable petrocalcic materials based on carbon isotope analysis.

Fabric Type	Pedon	County	Horizon	Range in Calculated
				Pedogenic Carbonate
				%
Convoluted	Stop 9 [†]	Kimble	Ccam	58- 68
	Stop 30 [†]	Pecos	Ccam	66- 75
	S81TX 435-1	Sutton	C2cam	84-100
			C3cam	100
	Stop 32 [†]	Crockett	Ccam	91-100
Nodular	S81TX 371-1	Pecos	C1cam	77- 88
	Stop 30 [†]	Pecos	Ccam	66- 75
Recrystallized	S81TX 371-1	Pecos	C2cam	75- 87
	S81TX 435-1	Sutton	C3cam	100

† Samples collected at reconnaissance locations

recrystallized fabrics had values in the range of 66-88% and 75-100%, respectively. Although according to calculations not all of these materials are 100% pedogenic carbonate, within the range of error and assumptions of the procedure we may confidently state that these samples are primarily pedogenic carbonates.

Concluding from micromorphic and isotopic evidence, it appears that carbonate materials exhibiting the convoluted, nodular, or recrystallized fabrics have most likely formed as a result of pedogenic processes and would be correctly designated as petrocalcic horizons (Ccam) rather than as lithogenic materials (Cr or R).

Pedogenesis of Petrocalcic Horizons

Gile et al. (1966) and Read (1974) have proposed models for the formation of carbonate enriched soil horizons. These models have as their starting point, unconsolidated soil materials that may be gravelly or non-gravelly, calcareous or carbonate-free. Downward moving waters carry dissolved carbonate material to a zone of accumulation where precipitation occurs. In this way, the pedogenic carbonates fill and plug the soil pores and engulf the surrounding soil material as the petrocalcic horizon develops. For this reason, the non-carbonate residues of the petrocalcic horizons are similar to the overlying soil materials.

As discussed previously under "Parent Material Identification and Uniformity," A horizons overlying petrocalcic materials in this study often show parent material discontinuity. Furthermore, these petrocalcic horizons often have non-carbonate residue percentages of 5% or less. Grain displacement by growing calcite crystals would certainly not be an adequate explanation for these low residue percentages. Gile and Grossman (1979) report carbonate-free residue percentages for plugged, indurated petrocalcic horizons ranging from 25 to 54 percent, much greater than the values observed in this study. Therefore, Gile's model depicting plugging of soil horizons as the mode of petrocalcic formation is inadequate to describe the genesis of these horizons over limestone bedrock on the Edwards Plateau.

An alternative explanation is proposed below. Meteoric waters moving through the solum become charged with CO_2 and some dissolved

organic components. This solution proceeds into the pores in the underlying limestone causing some enlargement of the pores through carbonate dissolution. The crystalline calcite around the pores begins to be altered to micrite through a process analogous if not similar to the "sparmicritisation" reported by Kahle (1977) and Tompkins (1980). In marine environments this process is believed to be related to the presence of dissolved organic compounds in pore waters formed during the metabolism of fungi and bacteria. Water percolating through the solum might similarly become charged with organic compounds from the microbial decomposition of soil organic matter. Numerous limestones were examined, nearly all showing micritic linings around pores or in exterior weathering rinds. As this process proceeds, the overall porosity of the limestone increases and micritic linings begin to coalesce forming a convoluted type of fabric in a dominantly micritic matrix.

During this process, dissolved carbonates may not be flushed entirely from this system, but may be locally redistributed forming crystallaria within pores of the convoluted network. Many of the samples examined showed calcite in a variety of crystal habits growing as rim cements (pore linings) within the protected convoluted pores. Needles, blades, prisms, and equant blocks have all been observed growing within the pores.

Through continued Ca influx by atmospheric additions (primarily dissolved in rainwater) with insufficient rainfall for leaching, rim cements may continue to grow until the pores become largely plugged. Alternatively, changes in the magnitude of precipitation during long

term climatic changes may cause changes in carbonate movement within this neo-petrocalcic zone such that crystal growth within pores causes plugging of the zone. At this point, the horizon is similar to Gile's Stage III. Its mode of formation is however, distinctly different from that proposed by Gile et al. (1966). A similar explanation for caliche formation has been discussed by Blank and Tynes (1965) and James (1972).

If plugging has occurred to the extent that the percolation of water is restricted, laminar caps may form as carbonate charged waters stand or through gravity move laterally over the plugged horizon. Laminar caps ranging from a few millimeters to a few centimeters in thickness were commonly observed on the upper surfaces of these petrocalcic horizons.

In addition to the micromorphological observations and carbon isotope data presented earlier in support of this model, the presence of the mineral fluorite (CaF_2) in pedon #9 (Pecos Co.) has proved useful as an indicator of the processes occurring during petrocalcic formation. Fluorite is a fairly labile mineral having roughly the same solubility as calcite in distilled water (making it somewhat less soluble than calcite in CO_2 charged meteoric waters. This pedon has already been discussed regarding parent material uniformity. Elemental analyses, PSD of residues, and the distribution of euhedral quartz prisms have indicated a parent material discontinuity between the A horizons and the petrocalcic zone. Although some differences exist, there is considerable parent material similarity between the

petrocalcic zone and the underlying rock. The petrocalcic horizons themselves appear to be formed from the same parent material.

Fluorite quantities were estimated from a combination of XRD, elemental analyses and PSD of carbonate-free residues. Figure 31 shows the total fluorite distribution and the PSD of the fluorite within the pedon including the limestone bedrock. Of first notice is the absence of fluorite from the A horizon. This may be due simply to the parent material discontinuity at this point. If fluorite were present in the parent limestone however, the small amount present would certainly have been dissolved while dissolving carbonates during the accumulation of the non-carbonate residuum. Conversely, the presence of fluorite in the petrocalcic horizon is further evidence that this carbonate zone did not form through carbonate enrichment of a previously leached, carbonate-free soil.

The steady decrease in total fluorite from the lower to the upper portion of the petrocalcic zone suggests that there has been dissolution and removal of this mineral from the upper part. The fluorite "bulge" in the lowermost petrocalcic horizon may indicate an actual translocation and accumulation of reconstituted fluorite, although the quantities of this mineral may not actually be significantly greater than the underlying bedrock. The abundance of fluorite in the clay ($<2\ \mu\text{m}$) and fine silt ($2-5\ \mu\text{m}$) of the petrocalcic zone while being virtually absent from these fractions in the underlying bedrock indicates that there has been reduction in particle size during the formation of the petrocalcic horizons. The formation of clay size fluorite has probably been the result of dissolution and reprecipitation.

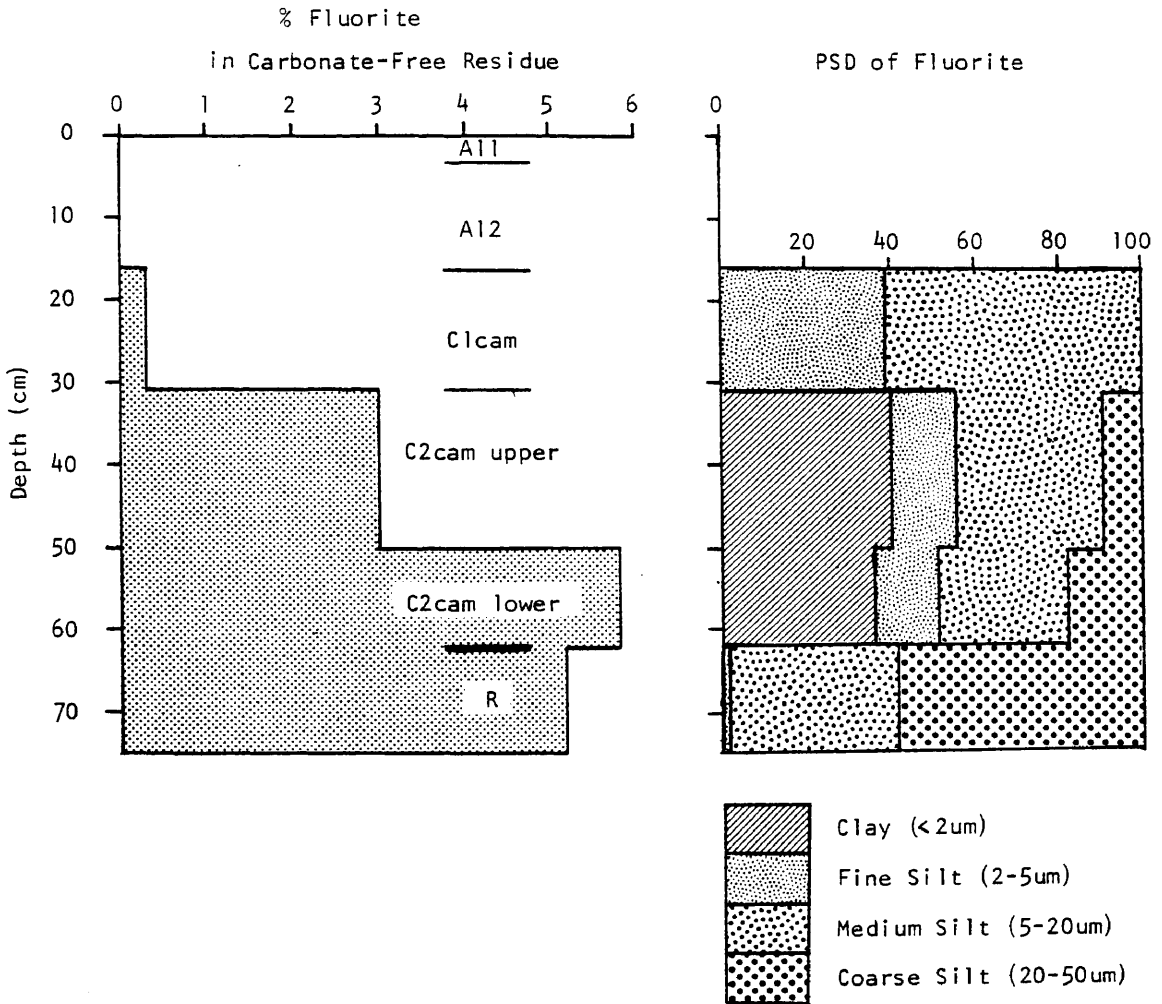


Fig. 31. Fluorite percentages in the carbonate-free residues and fluorite PSD for Pecos Co. pedon #9.

In summary, the evidence presented concerning fluorite distributions indicates the following:

- 1) The petrocalcic horizon has formed through the reconstitution of a limestone material without previous dissolution and removal of carbonates, rather than from carbonate plugging of a soil profile previously leached of carbonates.
- 2) Percolating waters have moved downward through the petrocalcic material.
- 3) The moisture regimes in the petrocalcic horizon have been such that in situ dissolution and reprecipitation (of a mineral of similar solubility to calcite) has occurred.

Further evidence that water has percolated through the petrocalcic zone during pedogenesis is the translocation and accumulation of secondary silica in the pedon. Data for approximate values of secondary silica were based on PSD, specific gravity separations, and/or optical examination and are presented in Table 12. The secondary

Table 12. Approximate levels of secondary silica in major horizons of the Pecos Co. pedon (#9) based on optical examination and/or specific gravity separations.

Horizon	Approximate Secondary Silica Values	
	Carbonate-free Residue	Total Sample
	----- % -----	
A1	4	2.6
C1cam	7	0.4
C2cam upper	24	1.0
C2cam lower	46	3.5
R	9	0.1

silica content increases steadily with depth through the petrocalcic horizon to a maximum just above bedrock. This distribution is strikingly similar to that of fluorite. In the A horizons, this material is mainly in the form of plant opal. Within the petrocalcic horizon it is mainly of a spongy isotropic form assumed to be opal. Some grains show a partial alteration and recrystallization as quartz. The initial source of Si may have been glassy volcanic ash deposited on the soil surface and subsequently dissolved and translocated to within the petrocalcic zone. Although the secondary silica comprises substantial proportions of the carbonate-free residues, they constitute only a very minor part of the petrocalcic horizon as a whole.

As just discussed, opaline or secondary silica was observed in many of the petrocalcic horizons. In some cases, it constituted a large portion of the non-carbonate residue, although it may have only been a minor component in the horizon overall (see Table 12). It was identified in the residues by its isotropic character under cross-polarized light and by its low specific gravity (<2.3). It is the opinion of the author that this silica is of pedogenic origin rather than being a lithogenic feature inherited from the limestone parent material.

The evidence for a pedogenic origin is two-fold. First, SEM examination shows the dominant form to be a highly porous spongy network that could have developed by the plugging of interconnected pores in a porous yet indurated carbonate material (Fig. 16, p. 59). Furthermore, authigenic quartz prisms (formed in and inherited from the

limestone parent material) have been observed with coatings of secondary silica (Fig. 15, p. 57). Since it is unlikely that two strongly contrasting Si forms (quartz prisms and opaline coatings) would be co-precipitated, this is strongly suggestive that there has been silica movement within the petrocalcic horizon. Secondly, optical examination of silts and sands shows the silica in the petrocalcic horizons to be mainly opaline (isotropic) although small zones within the spongy grains show evidence of alteration to quartz (anisotropy). Only a small portion of the grains showed a more complete alteration to quartz. In contrast, silica in the underlying bedrock having the morphology of secondary silica was nearly all altered to quartz. The zone of maximum silica concentration in the Pecos Co. pedon (#9) (lower C2cam) is also the zone of maximum isotropic silica with minimum alteration to quartz. Assuming the alteration from opal to quartz to be a time dependent process, this suggests that the silica has been translocated and precipitated in a pedogenic (geologically recent) environment. Since silica (especially quartz) solubilities are low in the present soil environment, it is postulated that volcanic ash (in small quantities) has been the Si source. Amorphous silica glass is considerably more soluble than either quartz or opal and could therefore provide a better source for mobile silica (Wilding et al., 1977).

Identification and Genesis of Argillic Horizons

In the humid, eastern part of the Edwards Plateau where greater rainfall has leached carbonates from the solum, argillic horizons were recognized in four pedons. Field evidence for argillic horizons

included finer textures in the B horizons and the presence of clay coatings or shiny surfaces on peds. The identification of clay films was somewhat complicated by the presence of pressure faces in several of the pedons, which can be difficult to distinguish from illuvial clay on ped surfaces. Shrink-swell activity may also tend to obliterate any evidence of illuvial clay by disruption or destruction of clay films. Since there were some questions surrounding the identification of clay films, and since clay increases in the B horizon do not in themselves constitute argillic horizons, laboratory confirmation was sought.

Particle Size Evidence

Clay distributions for the four pedons are illustrated in Fig. 32. All pedons show marked increases in total clay content from the A to the B horizons. The increase in total clay is primarily the effect of large increases in fine clay resulting in much higher fine:coarse clay ratios in the B horizons. The greater ease of downward translocation of fine clay than coarse clay makes higher fine:coarse clay ratios a characteristic of argillic horizons (Soil Survey Staff, 1975).

Since argillic horizons are formed through the enrichment and accumulation of translocated clay from overlying horizons, they are also generally expected to have a greater clay content than underlying horizons. This criterion is useful in the identification of an argillic horizon since coarser textures in surface horizons can occur through processes other than eluviation. Pedon 11 (Real Co.), which

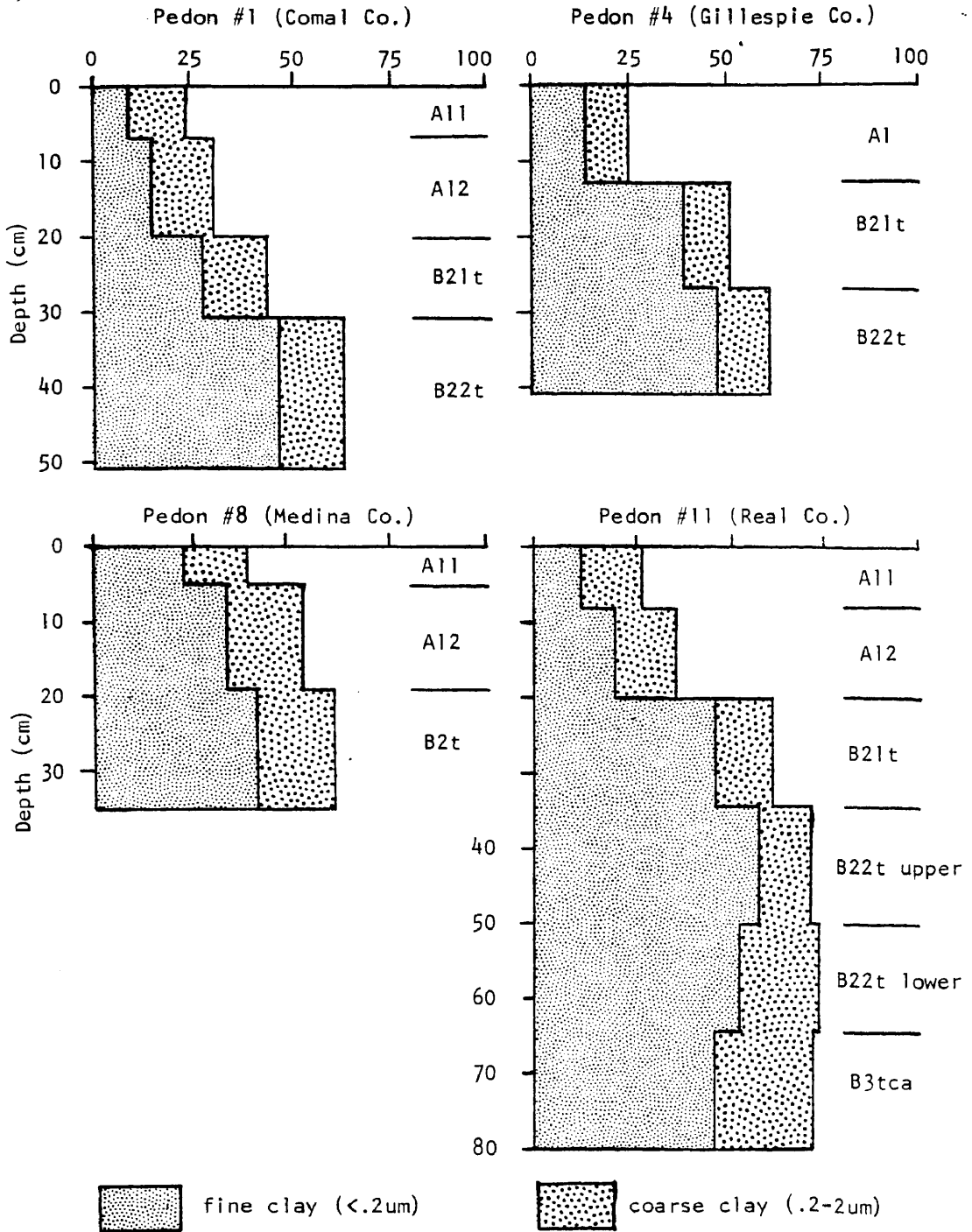


Fig. 32. Clay distribution depth functions for the 4 pedons containing argillic horizons. The B3tca horizon (65-80cm) of pedon #11 was reported on a carbonate-free basis. All other horizons were non-calcareous.

was the deepest soil encountered (80 cm), does show a slight decrease in both fine clay and total clay in the B3 horizon relative to the B2. The other pedons, owing to their shallow nature (35-50 cm), all have clay maxima in the horizon immediately above the bedrock. Comparisons with carbonate-free residue from the parent materials of these soils should (if these lowest horizons are argillic) have clay contents and fine: coarse clay ratios which are lower than in the argillic horizons. Analyses have shown however, that in the Edwards Plateau region, sola occurring over hard limestones often have formed from limestone residuum of contrasting character to the rock immediately subjacent to the soil (see section on Parent Material Identification and Uniformity). Therefore, comparisons of soils with residue from the underlying rock should not be used to substantiate or invalidate argillic horizon identification unless parent material continuity can be established.

Micromorphological Evidence

Thin-sections were examined for the soils thought to have argillic horizons. Micromorphic fabrics and major features are reported with COLE values in Table 13. Argillans were common in the B horizons of all four pedons. They were for the most part however, striated and showed some evidence of stress orientation. It was, thus not immediately clear whether or not the argillans were illuvial features.

Stress features caused by shrink-swell activity were common in the soils as evidenced by masepic and skelsepic plasmic fabrics. COLE values, which are a linear measure of shrink-swell potential,

Table 13. Plasmic fabrics† and major micromorphic features of four pedons containing argillic horizons.

Pedon	Horizon	Depth	COLE	Related Distribution	Plasmic Fabric (125X)	Comments and Features
1	A11	0-7	.06	Porphyroskelic	Argillasepic to Undulic	Some argillans in rhombahedral chert pores. Many irregular ortho voids.
	A12	7-20	.07	Porphyroskelic	Argillasepic to Undulic	Argillans present in rhombahedral chert pores. Many irregular ortho voids.
	B21t	20-31	.09	Porphyroskelic	Weak Skel-masepic	Argillans present in rhombahedral chert pores. Many irregular ortho voids.
	B22t	31-51	ND	Agglomeroplasmic	Moderate Ma-skelsepic	Argillans present in rhombahedral chert pores. Moderate striated argillans around skeleton grains and some voids. Many irregular ortho voids.
4	A11	0-13	.08	Porphyroskelic	Argillasepic to Weak Skelsepic	Strong argillans in rhombahedral chert pores. Many irregular ortho voids.

Table 13. (Continued)

Pedon	Horizon	Depth	COLE	Related Distribution	Plasmic Fabric (125X)	Comments and Features
4	B21t	13-27	.16	Porphyroskelic	Moderate Ma-skelsepic	Argillans and ferriargillans in rhombahedral chert pores. Moderate striated and some continuous argillans around some skeleton grains.
	B22t	27-41	.14	Porphyroskelic	Skel-masepic	Argillans and ferriargillans in rhombahedral chert pores. Moderate striated argillans around skeleton grains.
8	A11	0-5	ND	Porphyroskelic	Weak Ma-skelsepic	Some ferriargillans in chert pores.
	A12	5-19	.14	Porphyroskelic	Ma-skelsepic	Occasional argillan in chert pore. Moderate striated argillans around some skeleton grains.
11	B2t	19-35	.14	Porphyroskelic	Skel-masepic	Moderate striated argillans around some skeleton grains.
	A11	0-8	.18	Agglomeroplasmic	Argillasepic	Occasional ferriargillan in pores of chert fragments.

Table 13. (Continued)

Pedon	Horizon	Depth	COLE	Related Distribution	Plasmic Fabric (125X)	Comments and Features
	A12	8-20	.11	Porphyroskelic	Weak Skel-masepic	Argillans and ferriargillans present in pores of chert fragments.
	B21t	20-35	ND	Porphyroskelic	Strong Skel-masepic	Ferriargillans present in pores of chert fragments. Strong striated argillans around chert fragments.
	B22t	35-50	ND	Porphyroskelic	Strong Skel-masepic	Occasional argillans in chert pores. Strong striated argillans around skeleton grains. Common Fe nodules.
	B22t	50-65	.22	Porphyroskelic	Strong Skel-masepic	Strong striated argillans around skeleton grains. Abundant Fe nodules.
	B3tca	65-80	.23	Porphyroskelic	Strong Skel-masepic	Strong striated with some moderate continuous argillans around skeleton grains and pores. Abundant Fe nodules and some carbonate nodules.

† Terminology of Brewer (1976).

generally show good agreement with micromorphic stress features. The strongest expression of stress orientation was observed in the B2t and B3tca horizons of Pedon 11, which also had the greatest COLE values. According to criteria established by Franzmeier and Ross (1968) Pedons 11, 9 and 8 all have COLE values in the very critical range indicating very high shrink-swell potential. COLE values for Pedon 1 are somewhat lower but are still in the critical range. With the high shrink-swell of these soils it would not be surprising for illuvial argillans to be absent. The absence of good illuvial features could be attributed either to a lack of stable ped surfaces for clay accumulation, or to the disruption and destruction of illuvial argillans by stress activity. Nettleton et al. (1969) have indicated that the shrink-swell pressures in soils with COLE values as low as 0.04 could be sufficient to preclude micromorphic identification of oriented illuvial clay.

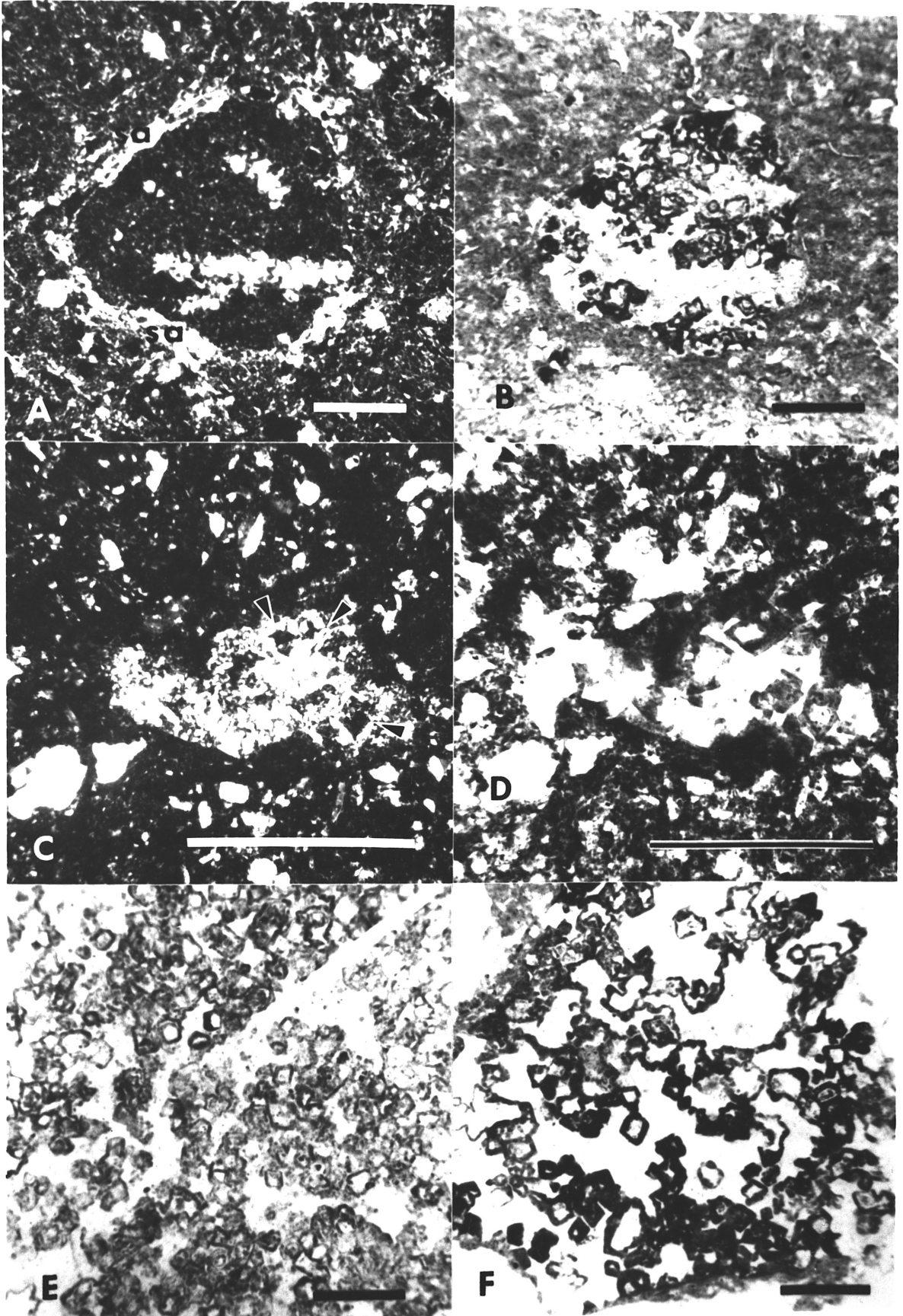
Most of the argillans observed were located around skeleton grains although some did occur along voids. Due to the lack of stable ped surfaces in clay-rich soils with high shrink-swell activity, skeleton grains and coarse fragments may provide a relatively stable surface. If illuviation argillans were to occur in such a soil, skeleton grain surfaces would be a likely location. Skeleton grain surfaces, however, are also prime locations for the development of stress argillans. Although many of the argillans did appear to be the result of primarily shrink-swell stresses, careful examination did reveal features more characteristic of illuviation argillans. Many of the argillans that showed strong striated orientation had abrupt

boundaries with the matrix material and a lack of sub-cutanic striations. Stress argillans usually are thin (about one or two plasma aggregates thick, 5-10 μ m) and have more diffuse boundaries. When the features are strongly oriented, they also commonly have accompanying sub-cutanic stress orientation. A number of the observed argillans occurred only on one side of a skeleton grain. Such features usually form completely around a given grain, if it is in fact formed due to stress forces, rather than from illuviation.

Although a few continuous, argillans with band extinction were observed along voids and skeleton grains, the best expression of these features in all four pedons was within the pores of chert fragments (Fig. 33). Two of the four pedons had a dolomite component in the limestone which had coprecipitated with chert. The dissolution and leaching of carbonates from these soils left rhombohedral-shaped pores (dolomite pseudomorphs) within chert fragments. Since these microenvironments are protected from the shrink-swell activity in the soil by the rigid chert framework, illuvial clay which has moved into and accumulated within the pores is well preserved. These features show good band extension characteristic of illuvial clay. They can sometimes be traced to oriented plasma of similar color and birefringence in the host material.

In pedons 8 and 1, plasma separations have been somewhat masked by organic matter and Fe oxides respectively. Organic C contents of the A12 and B2t horizons in pedon 8 are 3.5% and 2.7% respectively (Appendix E). While plasma separations (skelsepic or masepic plasmic fabric) can be seen at a magnification of 125X, examination at 30X

Fig. 33. Illuviation argillans present in rhombahedral pores vacated by dissolved dolomite crystals. A and B are from the B22t horizon of the Gillespie Co. pedon (#4) under cross-polarized and plane light respectively. C and D are from the A11 horizon of the Comal Co. pedon (#1) under cross-polarized and plane light respectively. E and F are from the A1 and B21t horizons respectively of the Gillespie Co. pedon (#4) as photographed under plane light. Note in C the band extinction of the argillans (arrows). Note also in A the striated argillan (sa) around the chert fragment.



reveals only argillasepic fabric (A12) or weak expression of the masepic fabric (B2t) even though COLE values are quite high (.14).

The plasmic fabric in pedon 1 similarly reveals plasma separations at higher magnification (125X) but argillasepic fabrics at lower magnification (30X). These asepic fabrics actually tend toward undulic, presumably due to the abundance of Fe-oxides. The Fe-oxide levels in this pedon are much higher than any of the other soils with argillic horizons, ranging from 2.3% Fe₂O₃ in the A11 to 4.3% in the B22t (see Appendix F). The percentages of total clay and fine clay in this pedon are similar to those in pedon 4 which has strongly expressed skelmasepic fabrics, easily observed even at low magnification. It is postulated that the effect of abundant Fe-oxides in pedon 1 are twofold regarding the relative lack of observed stress features. First, as just mentioned, the Fe-oxides simply obscure the observation of the features. Secondly, the Fe-oxides may actually cause stabilization of the clays, reducing their shrink-swell activity. The argillic horizon of this pedon was well aggregated into fine and very fine subangular blocks and thin-sections reveal an abundant macroporosity, suggestive of high aggregate stability.

An alternative explanation for the relative lack of stress features in pedon 1 relative to pedon 4 might be the abundance of gravel-size chert fragments (50-75% by weight in the argillic) in the former. Magier and Ravina (1982) have correlated higher porosity, lower bulk density, and more friable structures in Terra Rosa soils with abundant coarse fragments. They suggest that rock fragments may provide a "skeleton" resistant to compaction.

CONCLUSIONS

The climate gradient extending across the Edwards Plateau has pronounced effects on the nature of the soils formed in this region. In the dryer, western portion of the Edwards Plateau, the soils are calcareous and calcic and petrocalcic horizons are common. In the humid eastern portion of the area non-calcareous sola are the general rule, and argillic horizons are common on stable landscapes. The texture and mineralogy of these soils are such that they have high shrink-swell activity which tends to obliterate or inhibit formation of illuvial argillans. Illuvial clay films are, however, preserved in pores of skeletal fragments where they are protected from shrink-swell stresses.

Soils across the area appear to have sola which have formed from limestone parent materials which were different from the subjacent limestone. The explanation for this is illustrated in Fig. 34. It is necessary to dissolve between 10 and 100 times a given volume of limestone to form a unit volume of non-calcareous residuum. It is therefore likely that previously overlying limestone strata with contrasting residue character have been weathered to form the parent material of these soils. Hard crystalline limestone beds may serve as deterrents to further residue accumulation. Where these hard beds occur immediately subjacent to the solum, they may be mistaken for the soil parent material.

Measurement of current rates of additions of airborne dust to the Edwards Plateau indicates that accumulations could be significant in

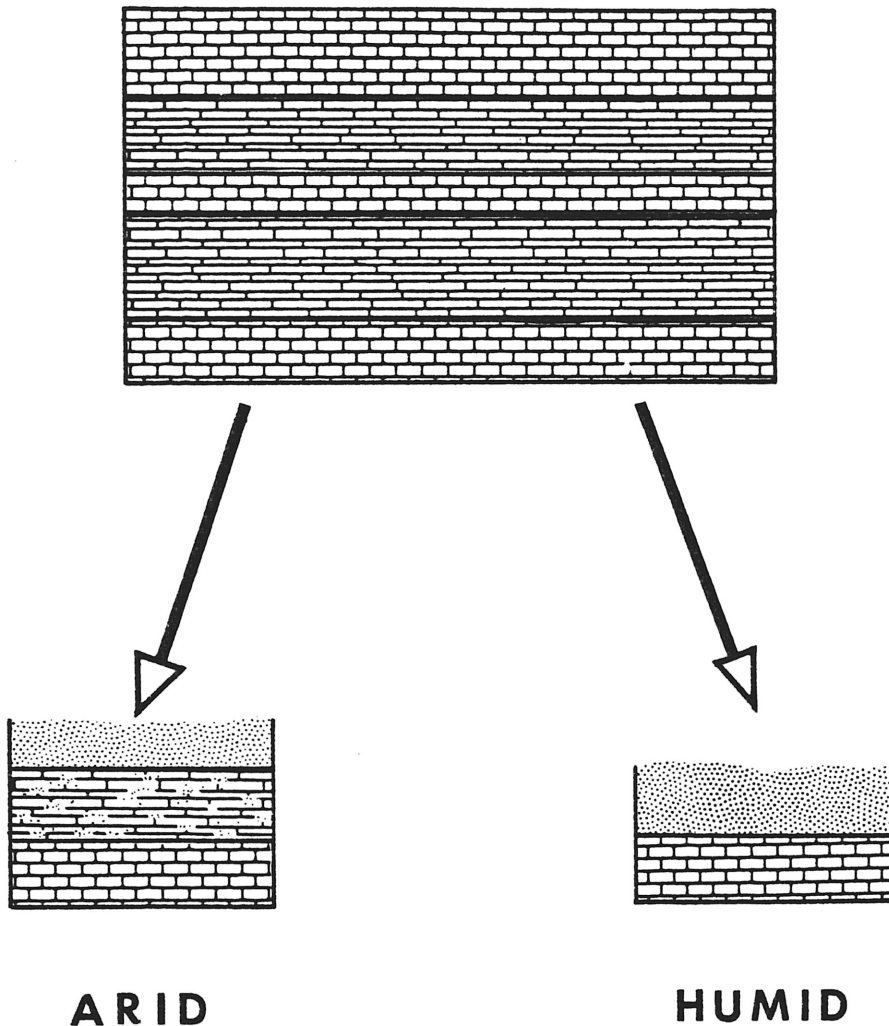


Fig. 34. Schematic diagram illustrating the weathering of numerous strata of limestone during the accumulation of a residual solum. One or more of the overlying strata may have contrasting residues from the limestone underlying the solum. Soils in the more humid eastern portion of the area tend to have deeper sola while soils in the more arid region tend to have shallower sola which may overlies petrocalcic horizons.

these shallow soils. The particle size, mineralogy, and elemental composition of the dusts do not contrast sufficiently with the residual soil material to be useful in estimating dust accumulations. The smooth conchoidally fractured surfaces of quartz and feldspar grains in the dusts, as revealed by SEM, are distinctively different from residual soil materials. Their absence from the upper soil horizons, however, indicates that particulate dusts are not noticeably accumulating in the soils. Rates of geologic erosion by water and/or wind must be sufficiently high to remove dusts added to the surface.

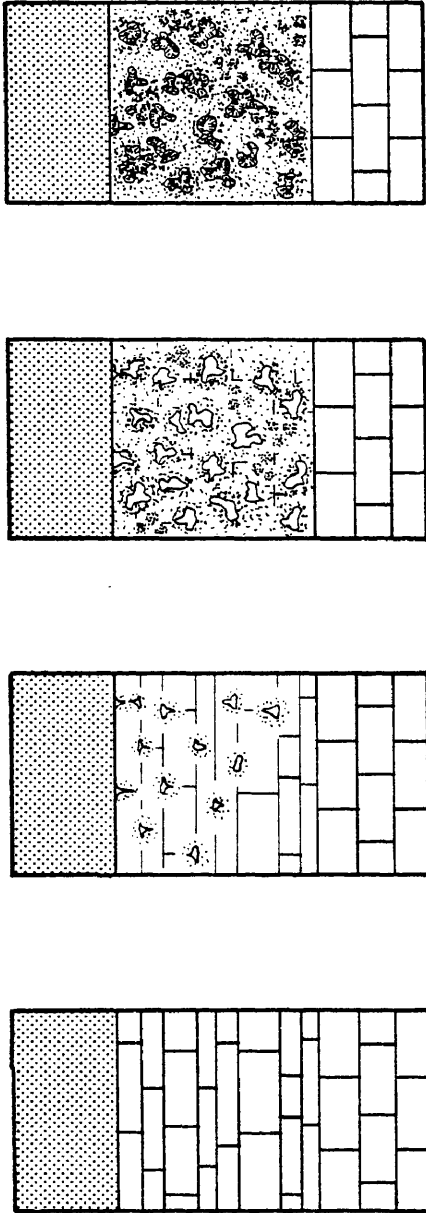
The petrocalcic horizons occurring in soils of the Edwards Plateau appear to be forming through a process of limestone alteration by in situ dissolution and reprecipitation of carbonates. This is in distinct contrast to the model proposed by Gile et al. (1966) where carbonates are translocated and accumulate within a solum which is initially non-indurated.

Evidence for the in situ petrocalcic formation includes:

1. Petrocalcic horizons have very low (0.9-8%) non-carbonate residue contents.
2. Contrasting particle size, mineralogy, and elemental contents exist between the carbonate-free petrocalcic residues and the overlying non-indurated sola.
3. Labile minerals (fluorite) which would not persist in a soil leached of carbonates (and subsequently enriched with carbonates) are present in some petrocalcics.

4. Total fluorite levels and fluorite PSD indicate that processes of translocation and in situ precipitation within the petrocalcic horizon have occurred.
5. Secondary silica within petrocalcic horizons indicates enrichment in soluble components.

The pedogenic nature of these petrocalcic horizons has been confirmed both through micromorphological investigation and stable carbon isotope analysis. The proposed sequence for petrocalcic formation is illustrated in Fig. 35. Stage 0 represents the unaltered limestone precursor to the petrocalcic horizon. Stage 1 shows the development of pores within the limestone with concurrent micritization of the adjacent limestone. In stage 2, the porosity has greatly increased and has developed the characteristic convoluted pattern and the matrix of the limestone has been nearly completely pedogenically altered to a micritic fabric. Zones of nodular or clotted micritic fabric are also present. In stage 3, the petrocalcic zone has been completely altered to a convoluted or nodular micritic fabric and the pores have been partially or completely filled with pedogenic carbonates in the forms of needles, blades, prisms or equant blocks. The primary petrocalcic fabric may also include zones where micrite has been recrystallized to a neomorphic microspar (not shown in Fig. 35). Once pores become plugged, a lamninar cap may form at the upper surface of the petrocalcic horizon, similar to stage IV of Gile et al. (1966).



0

1

2

3

Fig. 35. Four sequential stages in the formation of petrocalcic horizons by in situ pedogenic alteration of limestone and enrichment with pedogenic carbonates. Stage 0 shows the unaltered limestone precursor to the petrocalcic horizon. Stage 3 shows the completely formed petrocalcic horizon.

LITERATURE CITED

- Adkins, W. S. 1978. The Mesozoic systems in Texas. In The geology of Texas, Volume I: Stratigraphy. Bur. of Econ. Geol. Bull. No. 3232. The Univ. of Texas, Austin.
- Alexander, A. E. 1934. Petrology of the great dustfall of November 13, 1933. Monthly Weather Rev. 62:15.
- American Association of Petroleum Geologists. 1973. Geological highway map of Texas. United States geological highway map series, Map No. 7. Tulsa, Oklahoma.
- Arkley, R. J. 1963. Calculation of carbonate and water movement in soil from climatic data. Soil Sci. 96:239-248.
- Blank, H. R., and E. W. Tynes. 1965. Formation of caliche in situ. Geol. Soc. Am. Bull. 76:1387-1392.
- Brasher, B. R., D. P. Franzmeier, V. T. Valassis, and S. E. Davidson. 1966. Use of saran resin to coat natural soil clods for bulk density and water retention measurements. Soil Sci. 101:108.
- Bretz, J. H., and L. Horberg. 1949. Caliche in southeastern New Mexico. J. Geology 57:491-511.
- Brewer, R. 1976. Fabric and mineral analysis of soils. Krieger Pub. Co., Huntington, N.Y.
- Brown, C. N. 1956. The origin of caliche on the northeastern Llano Estacado Texas. J. Geol. 64:1-15.
- Buol, S. W. 1964. Present soil forming factors and processes in arid and semi-arid regions. Soil Sci. 99:45-49.
- Bur. of Econ. Geol. 1979. Geologic atlas of Texas. The Univ. of Texas, Austin.
- Choun, H. F. 1936. Dust storms in the southwest plains area. Monthly Weather Rev. 64:195-199.
- Delany, A. C., A. C. Delany, D. W. Parkin, J. J. Griffin, E. D. Goldberg, and B. E. F. Reimann. 1967. Airborne dust collected at Barbados. Geochim. Cosmochim. Acta. 31:885-909.
- Dreimanis, A. 1962. Quantitative gasometric determination of calcite and dolomite by using Chittick apparatus. J. Sediment. Petrol. 32: 520-529.

- Dunham, R. J. 1962. Field trip guidebook reinterpretation of sedimentation and diagenesis of the Permian Capitan Reef and associated rocks, New Mexico and Texas. Shell Development Co. Special Rep. 4. Houston, Texas.
- Fisher, W. L. 1974. Geologic atlas of Texas: San Antonio sheet. Bur. of Econ. Geol. The Univ. of Texas, Austin.
- Fisher, W. L. 1981a. Geologic atlas of Texas: Llano sheet. Bur. of Econ. Geol. The Univ. of Texas, Austin.
- Fisher, W. L. 1981b. Geologic atlas of Texas: Sonora sheet. Bur. of Econ. Geol. The Univ. of Texas, Austin.
- Flach, K. W., W. D. Nettleton, L. H. Gile, and J. G. Cady. 1969. Pedocementation: Induration by silica, carbonates, and sesquioxides in the Quaternary. *Soil Sci.* 107:442-453.
- Franzmeier, D. P., and S. J. Ross, Jr. 1968. Soil swelling: Laboratory measurement and relation to other soil properties. *Soil Sci. Soc. Am. Proc.* 32:573-577.
- Gardiner, L. R. 1972. Origin of the Mormon Mesa caliche, Clark County, Nevada. *Geol. Soc. Amer. Bull.* 83:143-155.
- Gile, L. H. 1961. A classification of ca horizons in soils of a desert region, Dona Ana County, New Mexico. *Soil Sci. Soc. Am. Proc.* 25:52-61.
- Gile, L. H., and R. B. Grossman. 1979. The desert project soil monograph: Soils and landscapes of a desert region astride the Rio Grande Valley near Las Cruces, New Mexico. SCS, USDA. U.S. Government Printing Office, Washington, D. C.
- Gile, L. H., F. F. Peterson, and R. B. Grossman. 1966. Morphological and genetic sequences of carbonate accumulation in desert soils. *Soil Sci.* 101:347-360.
- Gillam, W. S. 1937. The formation of lime concretions in the Moody and Crofton series. *Soil Sci. Soc. Am. Proc.* 2:471-477.
- Harper, W. G. 1957. Morphology and genesis of Calcisols. *Soil Sci. Soc. Am. Proc.* 21:420-424.
- Hassett, J. J., D. W. Gregg, and J. B. Fehrenbacher. 1976. Formation of calcium carbonate concretions in natric horizons of Illinois soils. *Soil Sci.* 122:202-205.
- Hawker, H. W. 1927. A study of the soils of Hidalgo County, Texas and the stages of their lime accumulation. *Soil Sci.* 23:475-485.

- Hawley, J. W., and R. B. Parsons. 1980. Glossary of selected geomorphic and geologic terms. West Technical Service Center, Soil Conservation Service - USDA. Portland, Oregon.
- Hendy, C. H. 1971. The isotopic geochemistry of speleothems. I. The calculation of the effects of different modes for formation on the isotopic composition of speleothems and their applicability as paleoclimatic indicators. *Geochim. Cosmochim. Acta.* 35:801-824.
- Holmgren, G. S., R. L. Juve, and R. C. Geschwender. 1977. A mechanically controlled variable rate leaching device. *Soil Sci. Soc. Am. J.* 41:1207-1208.
- Jacka, A. D. 1977. Deposition and diagenesis of the Fort Terrett formation (Edwards group) in the vicinity of Junction, Texas. In D. G. Bebout and R. B. Loucks (eds.) *Cretaceous carbonates of Texas and Mexico.* Bur. of Econ. Geol. The Univ. of Texas, Austin.
- Jackson, M. L. 1974. Soil chemical analysis--advanced course. 2nd. ed. Pub. by author, Dept. Soil Science, Univ. of Wisconsin, Madison.
- Jackson, M. L., F. R. Gibbons, J. K. Syers, and D. L. Mokma. 1972. Eolian influence on soils developed in a chronosequence of basalts of Victoria, Australia. *Geoderma* 8:147-163.
- Jackson, M. L., T. W. M. Levelt, J. K. Syers, R. W. Rex, R. N. Clayton, G. D. Sherman, and G. Uehara. 1971. Geomorphological relationships of tropospherically derived quartz in the soils of the Hawaiian islands. *Soil Sci. Soc. Am. Proc.* 35:515-525.
- James, N. P. 1972. Holocene and Pleistocene calcareous crust (caliche) profiles: Criteria for subaerial exposure. *J. Sediment. Petrol.* 42:817-836.
- Jenny, H. 1941a. Calcium in the soil: III. Pedological relationships. *Soil Sci. Soc. Am. Proc.* 6:27-37.
- Jenny, H. 1941b. Factors of soil formation: A system of quantitative pedology. McGraw-Hill, New York.
- Jenny, H., and C. D. Leonard. 1934. Functional relationships between soil properties and rainfall. *Soil Sci.* 38:363-381.
- Junge, C. E., and R. T. Werby. 1958. The concentration of chloride, sodium, potassium, calcium, and sulfate in rainwater over the United States. *J. Meteorology* 15:417-425.
- Kahle, C. F. 1977. Origin of subaerial Holocene calcareous crusts: role of algae, fungi and sparmicritisation: *Sedimentology* 24:413-435.

- Keller W. D. 1976. Scan electron micrographs of kaolins collected from diverse environments of origin - I. Clays Clay Min. 24:107-113.
- Kilmer, V. J., and L. T. Alexander. 1949. Methods of making mechanical analysis of soils. Soil Sci. 68:15-24.
- Lodge, J. P., Jr., J. B. Pate, W. Basbergill, G. S. Swanson, K. C. Hill, E. Lorange, and A. L. Lazrus. 1968. Chemistry of United States precipitation: Final report on the national precipitation sampling network. National Center for Atmospheric Research. Boulder, Colo.
- Loucks, R. G., A. J. Scott, D. G. Bebout, and P. A. Mench. 1978. Lower Cretaceous carbonate tidal facies of Central Texas. Bur. Econ. Geol. Res. Note 10. The Univ. of Texas, Austin.
- Lozo, F. E., H. F. Nelson, K. Young, O. B. Shelburne, and J. R. Sandidge. 1959. Symposium on Edwards limestone in Central Texas. Bur. Econ. Geol. Pub. No. 5905. The Univ. of Texas, Austin.
- Magier, J., and I. Ravina. 1982. Effect of coarse fragments on physical conditions of a clay soil (Terra-Rossa). Agron. Abstr. p. 234.
- Martin, R. J. 1936. Dust storms of February and March 1936 in the United States. Monthly Weather Rev. 64:87-89.
- McFarlan, E., Jr. 1977. Lower Cretaceous sedimentary facies and sea level changes, U.S. Gulf Coast. In D. G. Bebout and R. G. Loucks (eds.), Cretaceous carbonates of Texas and Mexico. Bur. of Econ. Geol. The Univ. of Texas, Austin.
- Metcalf, A. L. 1967. Late Quaternary mollusks of the Rio Grande Valley, Caballo Dam, New Mexico to El Paso, Texas. Univ. Texas at El Paso Science Series 1, Texas Western Press.
- Mokma, D. L., J. K. Syers, M. L. Jackson, R. N. Clayton, and R. W. Rex. 1972. Aeolian additions to soils and sediments in the South Pacific Area. J. Soil Sci. 23:147-162.
- Nelson, H. F. 1973. The Edwards Reef complex and associated sedimentation in Central Texas. Bur. Econ. Geol. Guidebook No. 15. The Univ. of Texas, Austin.
- Nettleton, W. D., K. W. Flach, and B. R. Brasher. 1969. Argillic horizons without clay skins. Soil Sci. Soc. Am. Proc. 33:121-125.
- Nikiforoff, C. 1937. General trends of the desert type of soil formation. Soil Sci. 43:105-131.

- Price W. A., M. K. Eliás, and J. C. Frye. 1946. Algae reefs in cap rock of Ogallala formations on Llano Estacado Plateau, New Mexico and Texas. *Am. Assoc. Petroleum Geol. Bull.* 30:1742-1746.
- Rabenhorst, M. C., J. E. Foss, and D. S. Fanning. 1982. Genesis of Maryland soils formed from serpentinite. *Soil Sci. Soc. Am. J.* 46:607-616.
- Read, J. F. 1974. Calcrete deposits and Quaternary sediments, Edel Province, Shark Bay, Western Australia. p. 250-282: *In Evolution and diagenesis of Quaternary carbonate sequences, Shark Bay, Western Australia: Am. Assoc. Petroleum Geol. Memoir* 22.
- Redmond, C. E., and J. E. McClelland. 1959. The occurrence and distribution of lime in Calcium Carbonate Solonchak and associated soils of eastern North Dakota. *Soil Sci. Soc. Am. Proc.* 23:61-65.
- Reeves, C. C., Jr. 1970. Origin, classification and geologic history of caliche on the southern high plains, Texas and eastern New Mexico. *J. Geol.* 78:352-362.
- Rex, R. W., J. K. Syers, M. L. Jackson, and R. N. Clayton. 1969. Eolian origin of quartz in soils of Hawaiian islands and in Pacific pelagic sediments. *Science* 163:277-279.
- Robinson, W. O. 1936. Composition and origin of dust in the fall of brown snow, New Hampshire and Vermont, February 24, 1936. *Monthly Weather Rev.* 64:86.
- Rodda, P. U., W. L. Fisher, W. R. Payne, and D. A. Schofield. 1966. Limestone and dolomite resources, lower Cretaceous rocks, Texas. *Bur. of Econ. Geol. Rep. of Invest. No. 56.* The Univ. of Texas, Austin.
- Rose, P. R. 1978. Edwards group, surface and subsurface, Central Texas. *Bur. of Econ. Geol. Rep. of Invest. No. 74.* The Univ. of Texas, Austin.
- Rostad, H. P. W., and R. J. St. Arnaud. 1970. The nature of carbonate minerals in two Saskatchewan soils. *Can J. Soil Sci.* 50:65-70.
- Sehgal, J. L., and G. Stoops. 1972. Pedogenic calcite accumulations in arid and semiarid regions of the Indo-Gangetic Alluvial Plain of Erstwhile Punjab (India). *Geoderma* 8:59-72.
- Sherman, G. D., and H. Ikawa. 1958. Calcareous concretions and sheets in soils near South Point, Hawaii. *Pacific Sci.* 12:255-257.
- Simonson, R. W. 1959. Outline of a generalized theory of soil genesis. *Soil Sci. Soc. Am. Proc.* 23:152-156.

- Smith, R. M., P. C. Twiss, R. K. Krauss, and J. M. Brown. 1970. Dust deposition in relation to site season, and climatic variables. *Soil Sci. Soc. Am. Proc.* 34:112-117.
- Snyder, C. T., and W. B. Langbein. 1962. The Pleistocene lake in Spring Valley, Nevada and its climatic implication. *J. Geophys. Res.* 67:2385-2394.
- Sobecki, T. M. 1980. The distribution and genesis of calcic horizons in some soils of the Texas Coast Prairie. M.S. Thesis. Texas A&M Univ., College Station.
- Soil Survey Staff. 1975. Soil taxonomy: A basic system of soil classification for making and interpreting soil surveys. *Agric. Handbook No. 436.* SCS, USDA. U.S. Government Printing Office, Washington, D. C.
- Steele, J. G., and R. Bradfield. 1934. The significance of size distribution in the clay fraction. *Am. Soil Survey Assoc. Bull.* 15:88-93.
- Stuart, D. M., and R. M. Dixon. 1973. Water movement and caliche formation in layered arid and semiarid soils. *Soil Sci. Soc. Am. Proc.* 37:323-324.
- Stuart, D. M., M. A. Fosberg, and G. G. Lewis. 1961. Caliche in southwestern Idaho. *Soil Sci. Soc. Amer. Proc.* 25:132-135.
- Syers, J. K., M. L. Jackson, V. E. Berkheiser, R. N. Clayton, and R. W. Rex. 1969. Eolian sediment influence on pedogenesis during the Quaternary. *Soil Sci.* 107:421-427.
- Texas State Climatologist. 1974. *Climatography of Texas: Mean annual rainfall 1941-1970.* Office of the Texas State Climatol. Misc. Pub. No. 1. College Station.
- Thomas, C. M. 1965. Origin of pisolites. *Amer. Assn. Petrol. Geol.* 50th Annual Meeting, New Orleans, LA. Abstr. p. 99.
- Thorntwaite, C. W. 1948. An approach towards a rational classification of climate. *Geogr. Rev.* 38:55-94.
- Tompkins, R. E. 1980. Origin and occurrence of selected worldwide calcrete deposits. Ph.D. dissertation, Texas A&M Univ., College Station.
- USDA. 1957. Annual P-E index in Texas and Oklahoma. Pub. No. 4-L-12734.

- USDA, SCS. 1972. Soil survey laboratory methods and procedures for collecting soil samples. Soil Survey Investigations Rep. No. 1., U.S. Government Printing Office, Washington, D. C.
- U.S. Department of Commerce. 1968. Climatic atlas of the United States. U.S. Government Printing Office, Washington, D. C.
- U.S. Salinity Laboratory Staff. 1954. Diagnosis and improvement of saline and alkalai soils. L. A. Richards (ed.). USDA Handbook 60, U.S. Government Printing Office, Washington, D.C.
- Warn, G. F., and W. H. Cox. 1951. A sedimentary study of dust storms in the vicinity of Lubbock, Texas. *Am. J. Sci.* 249:553-568.
- White, E. M. 1971. Secondary carbonate accumulation between structure units in subsoils. *Proc. South Dakota Acad. Sci.* 50:75-78.
- Wilding, L. P., N. E. Smeck, and L. R. Drees. 1977. Silica in soils: Quartz, cristobalite, tridimite, and opal. pp 471-552. In J. B. Dixon and S. B. Weed (eds.), *Minerals in soil environments*. Soil Sci. Soc. Am., Madison, Wisconsin.
- Winchell, A. N., and E. R. Miller. 1918. The dustfall of March 9, 1918. *Am. J. Sci.* 46:599-609.
- Winchell, A. N., and E. R. Miller. 1922. The great dustfall of March 19, 1920. *Am. J. Sci.* 203:349-364.
- Winchell, A. N., and E. R. Miller. 1924. The dustfall of February 13, 1923. *J. Agric. Res.* 29:443-450.
- Windom, H. L. 1969. Atmospheric dust records in permanent snowfields: Implications to marine sedimentation. *Geol. Soc. Am. Bull.* 80: 761-782.
- Yaalon, D. H., and E. Ganor. 1973. The influence of dust on soils during the Quaternary. *Soil Sci.* 116:146-155.

APPENDIX A
PEDON DESCRIPTIONS

Pedon: S81TX-091-1

Soil name: Rumple

Classification: Udic Argiustoll; clayey skeletal, mixed, thermic

Physiography: Broad level hilltop (200 meters across) in gently undulating landscape; <1% slope

Parent material: Hard dolomitic cherty limestone of the Edwards formation

Vegetation: Pasture

Elevation: 265 meters

Location: Comal County, Texas; William Pfeuffer ranch; In pasture 40 yds east of Rt. 308, 0.6 miles south of entrance to ranch, 0.15 miles north of junction with county road; about 5 miles north of New Braunfels, approximately 98°6' W 29°48' N

Described by: M. C. Rabenhorst, L. T. West, Terry J. Moore, and Charles Batte. 20 August, 1981

Horizon	Depth (cm)	Colors for moist soil
A11	0-7	Dark brown (7.5YR 3/2) silt loam; weak fine platy parting to moderate medium granular structure; friable; many fine roots; slightly acid; clear smooth boundary
A12	7-20	Dark brown (7.5YR 3/2) cherty silty clay loam; moderate fine subangular blocky parting to moderate medium and fine granular structure; friable; common fine roots; approximately 15% chert fragments; slightly acid; clear smooth boundary
B21t	20-31	Dark reddish brown (2.5YR 3/3) cherty silty clay; moderate medium and fine subangular blocky structure; friable; common fine roots; thin continuous clay films on ped surfaces; approximately 40% chert fragments; slightly acid; clear smooth boundary
B22t	31-51	Dark reddish brown (2.5YR 3/4) cherty clay; moderate fine and very fine subangular blocky structure; friable; common fine roots; thin discontinuous clay films on ped surfaces; approximately 60% chert fragments; neutral; abrupt smooth boundary

S81 TX-091-1 (Continued)

R 51⁺ Gray (2.5Y 6/1) hard dolomitic limestone, zones with larger crystals have been solution pitted and have soil material in cavities; zones which have very fine crystals are very hard and massive and have no cavities

Remarks: A few limestone and chert fragments were present on the soil surface. Most of the coarse fragments in the soil were chert although a few large limestone floaters were observed. The solum thickness of this pedon is very close to the 50 cm depth cutoff for lithic subgroups. It is the opinion of local soil scientists that soils in this landscape position do on the average have sola thicknesses greater than 50 cm.

Pedon: S81TX-105-1

Soil Name: Ector/Upton

Classification: Petrocalcic Calciustoll; fine-loamy, mixed, thermic, shallow

Physiography: Nearly level Mesa Top, <1% slope with southern aspect

Elevation: 730 meters

Parent Material: Soft limestone of the Buda formation

Vegetation: Rangeland; shrub species mainly sotol, redberry juniper, saccahuista, agarita and mesquite; Grass species mainly three-awn, buffalograss, hairy tridens, red grama and sideoats grama; also various forbes

Location: Crockett County, Texas; Austin Millspaugh Ranch; enter through the Pie Pierce Ranch, on Mesa Top; between north and northwest shooting fingers of SW portion of mesa between Howards Creek and Government Canyon; About 4 miles NNE (as crow flies) of intersection of Rt. 2083 and the unpaved road at Howards Creek; approximately 101°27' W, 30°32' N

Described by: M. C. Rabenhorst, L. P. Wilding, C. C. Girdner, and C. Wiedenfeld. 23 July, 1981

Horizons	Depth (cm)	Colors for dry soil unless otherwise stated
A11	0-2	Grayish brown (10YR 5/2) silt loam, very dark grayish brown (10YR 3/2) moist; weak thin platy parting to moderate medium and fine granular structure; slightly hard; many fine roots; about 10% coarse fragments; violently effervescent; clear smooth boundary
A12	2-12	Dark grayish brown (10YR 4/2) gravelly silty clay loam, very dark grayish brown (10YR 3/2) moist; moderate medium subangular blocky and granular structure; hard; many fine roots; approximately 20% unoriented coarse fragments; strongly effervescent; abrupt wavy boundary

S81TX-105-1 (Continued)

C1cam & A1	12-24	White (10YR 8/2) indurated carbonate material containing about 10% grayish brown (10YR 5/2) loam, dark brown (10YR 3/3) moist, within fractures 1/2 to 2 cm wide; abrupt wavy boundary
C2cam	24-45	White (10YR 8/1) indurated carbonate material (10 YR 8/2) moist
Rca or C3cam	45-55	Light yellowish brown (10YR 6/7) indurated carbonate material

Remarks:

No hard limestone was encountered within 55 cm. The lowest horizon could not be conclusively identified on field evidence as being soft limestone with some enrichment with secondary carbonates or as a petrocalcic horizon. An intermittent seam of browner material (10YR 5/3 dry, 4/3 moist) 2 to 3 cm thick was observed between the C1cam and A1 horizon and the C2cam horizon.

Pedon: S81TX-171-1

Soil Name: Eckrant

Classification: Lithic Haplustoll; clayey-skeletal, montmorillonitic, thermic

Physiography: Level hilltop, high point in landscape

Elevation: 630 meters

Parent material: Hard dolomitic limestone of the Ft. Terret member of the Edwards Limestone

Vegetation: Pasture; Live oak, post oak, elm, three-awn

Location: Gillespie County, Texas. Roger Dittmar ranch; approximately 13 miles west of Fredericksburg on Rt. 290; Turn south onto the Dittmar ranch and follow road past Dittmar residence approximately 1 mile to top of hill; pedon sampled 100 ft east of road (Sheet 41 Gillespie Co. Report).

Described by: M. C. Rabenhorst, L. T. West, and Terry J. Moore. 19 August, 1981

<u>Horizon</u>	<u>Depth (cm)</u>	Colors are for moist soil
A11	0-8	Very dark brown (10YR 2/2) silty clay loam; weak fine and very fine granular structure; very friable; many fine and very fine roots; mildly alkaline; clear smooth boundary
A12	8-20	Very dark brown (10YR 2/2) stony silty clay; moderate very fine granular structure; very friable; many fine and very fine roots; approximately 80% coarse fragments; mildly alkaline; clear wavy boundary
R1	20-28	Hard dolomitic limestone bedrock; some calcareous browner material present in some fractures (<5%); clear smooth boundary
R2	23-43 ⁺	White (10YR 8/1) hard dolomitic limestone bedrock

Remarks: This site contained a number of chert and limestone fragments on the soil surface.

Pedon: S81TX-171-2

Soil Name: Similar to Speck

Classification: Lithic Haplustalf; clayey, mixed, thermic

Physiography: Nearly level bench, downslope from hillcrest; approximately 3 to 6 meters lower in elevation than adjacent hilltop; <1% slope

Elevation: 625 meters

Parent material: Hard dolomitic limestone of the Ft. Terret member of the Edwards Limestone

Vegetation: Pasture; Live oak, post oak and elm; three-awns and buffalograss

Location: Gillespie County, Texas. Rodger Dittmar ranch; approximately 13 miles west of Fredericksburg on Rt. 290; Turn south onto the Dittmar ranch and follow road past Dittmar residence approximately 1 mile just before reaching the hilltop; pedon sampled on level bench 100 feet west of the road (Sheet 41 Gillespie Co. Report)

Described by: M. C. Rabenhorst, L. T. West, and Terry J. Moore. 19 August, 1981

Horizon	Depth (cm)	Colors are for moist soil
A11	0-13	Dark brown (7.5YR 3/2) silt loam; weak medium subangular blocky parting to moderate medium granular structure; friable; many roots; neutral; clear smooth boundary
B21t	13-27	Dark reddish brown (2.5YR 3/4) clay; moderate medium subangular blocky structure; firm; medium continuous clay films on ped surfaces; slightly acid; clear smooth boundary
B22t	27-41	Dark reddish brown (2.5YR 3/4) clay; moderate medium prismatic parting to subangular blocky structure; Very firm; medium continuous clay films present on ped surfaces; some worm casts observed; slightly acid; abrupt smooth boundary

S81TX-171-2 (Continued)

R 41⁺ White (10YR 8/2) and light gray (5Y 7/1) partially weathered hard dolomitic limestone bedrock

Remarks: Many chert fragments were observed on the soil surface but there were very few coarse fragments within the solum. This soil is very similar to the Speck soil (in fact mapped within a Speck unit) but lacks a mollic epipedon.

Pedon: S81TX-265-1

Soil name: Eckrant variant

Classification: Lithic Haplustoll; clayey, montmorillonitic, thermic

Physiography: High broad nearly level divide; <1% slope

Elevation: 700 meters

Parent material: Soft limestone of the Segovia member of the Edwards formation

Vegetation: Pasture; shin oak, live oak, and prickly pear; curly mesquite, three-awn, and Texas wintergrass are dominant grasses

Location: Kerr County, Texas; Black Bull Ranch; Rt. 41, 10.0 miles west of junction with Rt. 27. After entering Black Bull ranch take pasture road east 1.3 miles from the entrance road. Site is 232 paces north of Rt. 41.

Described by: M. C. Rabenhorst, L. T. West, and Terry J. Moore. 19 August, 1981

Horizon	Depth (cm)	Colors are for moist soil
A11	0-5	Very dark brown (10YR 2/2) silty clay; weak medium subangular blocky parting to weak medium and fine granular structure; friable; many fine roots; neutral; clear smooth boundary
A12	5-20	Very dark brown (10YR 2/2) silty clay; moderate medium and fine subangular blocky parting to moderate fine granular structure; friable; many fine roots; neutral; abrupt smooth boundary
R&A13	20-33	Very dark brown (10YR 2/2) clay; moderate medium and fine subangular blocky parting to moderate fine granular structure; hard; many fine roots; slightly effervescent; approximately 50% limestone fragments having a horizontal orientation in the pedon; a few veins of browner material like the underlying horizon present; clear wavy boundary

S81TX-265-1 (Continued)

- R & Bca 33-43 Dark yellowish brown (10YR 4/4) clay; weak fine sub-angular blocky parting to moderate fine granular structure; soft; few fine roots; violently effervescent; approximately 70% limestone fragments showing horizontal orientation; abrupt smooth boundary.
- R 43-61⁺ White (10YR 8/1) and light gray (2.5Y 7/2) soft limestone

Remarks:

While this pedon contained a zone of browner material within the zone of rock fragments, some soils in the vicinity were observed to have calcareous cambic horizons above the rock material. This soil is like the Eckrant except that it lacks the abundance of coarse fragments in the upper horizons; the browner cambic like material at 33-43 cm is also atypical for Eckrant soils.

Pedon: S81TX-267-1

Soil name: (Mereta)

Classification: Petrocalcic Calciustoll; clayey, mixed, thermic, shallow

Physiography: Slightly undulating ridgetop

Elevation: 698 meters

Parent material: Soft limestone of the Segovia member of the Edwards formation

Vegetation: Wooded pasture; Three-awn, Texas wintergrass, side-oats grama, curly mesquite, prickly pear, live oak, blueberry juniper

Location: Kimble County, Texas; 11 miles west of Junction on I10 and then south (across the Llano River) on the Edward Dunbar Ranch; 99°55'53" W 30°26'24" N according to the Bailey Creek 7.5' Quadrangle map

Described by: M. C. Rabenhorst, L. P. Wilding, and C. L. Girdner. 24 July, 1981.

Horizon	Depth (cm)	Colors for dry soil unless otherwise stated
A11	0-1	Dark grayish brown (10YR 4/2) silt loam, very dark grayish brown (10YR 3/2) moist; weak medium platy parting to moderate fine and medium granular structure; soft; many fine roots; approximately 15% coarse fragments; slightly effervescent; abrupt smooth boundary
A12	1-6	Very dark grayish brown (10YR 3/2) silty clay loam, very dark brown (10YR 2.5/2) moist; moderate medium subangular blocky parting to fine and medium granular structure; hard; common fine roots; approximately 15% coarse fragments; non-calcareous matrix with spots slightly effervescent; abrupt wavy boundary
Ccam&A1	6-20	White (10YR 8/2) massive indurated carbonate material with some vertical fractures; fractures contain very dark grayish brown (10YR 3/2) silty clay, very dark brown (10YR 2.5/2) moist; the fine material is also found beneath the indurated carbonate and above the underlying rock; the A1 material has moderate fine granular structure and is non-calcareous; many fine roots in the A1 material; abrupt boundary

S81TX-267-1 (Continued)

- R1ca 20-28 White (10YR 8/2) case hardened soft limestone overlain by a thin (1-8 mm) laminar cap of pale brown (10YR 6/3) secondary carbonates
- R2ca 28-39 White (10YR 8/1) soft limestone; somewhat softer than the R1
- R3ca 39-56 White (2.5Y 8/2) soft limestone

Remarks:

The site has an undulating surface topography and this pedon was sampled at a high spot. Nearby areas in local low spots appear to be deeper cracking soils. A few hard crystalline limestone boulders occur on the surface in the vicinity but no such material was encountered in this pedon. The parent material of this pedon appears to be a soft limestone. The R material sampled appears to have some enrichment with secondary carbonate. Many of the coarse fragments on the soil surface appear to be case hardened, soft limestone material. Field identification of a petrocalcic horizon needs laboratory verification, as the possibility exists that the massive material is a soft limestone rather than a petrocalcic horizon. If soil actually lacks a petrocalcic horizon, then it would be classified as a Lithic Haplustoll. It is also possible that the material identified as soft limestone is in fact petrocalcic material.

Pedon: S81TX-271-1

Soil name: Ector Variant (Olmos)

Classification: Petrocalcic Calciustoll; loamy-skeletal, mixed, thermic, shallow

Physiography: Stable upland; 1% slope to the east

Elevation: 380 meters

Parent material: Limestone; may be soft limestone overlying the hard limestone of the Salmon Peak formation

Vegetation: Rangeland; dominantly blackbrush and guajillo with some ceniza, prickly pear; also red grama, three-awn, and sideoats grama grasses

Location: Kinney County Texas, 300 ft. N of Rt. 2523 approximately 2.2 miles east (along Rt. 2523) from the Val Verde County line, 0.4 miles east of ranch gate (Sheet 17 Kinney Co. Report)

Described by: M. G. Rabenhorst, L. P. Wilding, C. L. Girdner, and Jack Stevens. 20 July, 1981

Horizon	Depth (cm)	Colors for dry soil unless otherwise stated
A1	0-13	Grayish brown (10YR 5/2) to dark grayish brown (10YR 4/2) stony silt loam, very dark brown (10YR 2.5/2) moist uncrushed, (10YR 2/2) crushed; 60% coarse fragments by volume mostly shattered flags of petrocalcic material oriented mainly horizontally and have pendants of secondary carbonate on the lower side; weak fine and medium granular structure; soft; many fine roots in upper 1 cm and at the Ccam contact, otherwise many medium roots; strongly effervescent; abrupt wavy boundary
C1cam	13-26	Numerous small white (10YR 8/1) sequences of laminae overlying more massive cemented carbonate; maximum thickness of laminar material less than 1 cm; this layer contained some interconnecting voids with a dendritic pattern which are incompletely filled with roots and A1 material; clear wavy boundary
C2cam	26-43	Several white (10YR 8/2) to pinkish white (7.5YR 8/2) sequences of laminae overlying more massive cemented carbonate; clear smooth boundary

S81TX-271-1 (Continued)

- C3cam 43-53 White (10YR 8/1) cemented massive carbonate; somewhat softer than above, can be cut with a spade with difficulty; clear smooth boundary
- C4cam 53-75⁺ White (10YR 8/1) cemented massive carbonate; softer than above, can be easily cut with a spade

Remarks: Topographic surface of underlying limestone is very irregular; a large massive limestone boulder was exposed at the surface 1 meter from the pit while no hard limestone was encountered within 75 cm in the pit. Most of the coarse fragments on the surface were petrocalcic material although some hard limestone boulders were also observed. This pedon was associated with areas of deeper soils containing little or no coarse fragments at the surface suggesting localized areas of inwash. The upper laminar surface of the C1cam contained a number of fractures in an exposed area of roughly 2 square feet. Upper surface of the C1cam was very hard and may easily be mistaken for limestone bedrock. Because of this, the soils of this area have been mistakenly mapped as Ector. This pedon is similar to the Kimbrough soil mapped in the county except that this pedon is in a skeletal particle size family. It is similar to the Olmos series mapped in Val Verde County except that the Olmos soil has a carbonatic mineralogy and is in a hyperthermic temperature regime.

Pedon: S81TX-325-1

Soil name: Speck

Classification: Lithic Argiustoll; clayey, montmorillonitic, thermic

Physiography: Near top of a broad divide; nearly level, approximately 1% slope

Elevation: 375 meters

Parent material: Hard limestone of the Edwards Formation

Vegetation: Wooded pasture; Cedar and live oak; three-awn and silver bluestem

Location: Medina County, Texas; Ralph Snavely ranch; Take road traveling NW out of Rio Medina 6.5 miles from the junction with route 471 and then turn north 55 yards to sampling location (sheet 20 Medina Co. Report).

Described by: M. C. Rabenhorst, L. T. West, and Terry J. Moore. 21 August 1981

Horizon	Depth (cm)	Colors are for moist soil
A11	0-5	Black (10YR 2/1) gravelly silty clay loam; moderate medium subangular blocky structure; slightly hard; many fine roots; approximately 20% coarse fragments, slightly acid; clear smooth boundary
A12	5-19	Black (10YR 2/1) gravelly silty clay; strong medium subangular blocky structure; very hard; common fine roots; approximately 20% coarse fragments; slightly acid; clear wavy boundary
B2t	19-35	Dark reddish brown (10YR 3/3-ped interiors, 2/2-ped surfaces) clay; moderate medium prismatic parting to strong medium subangular blocky structure; very hard; common fine roots; thin discontinuous clay films only on prism faces; neutral; abrupt wavy boundary
R	35+	Light gray (2.5Y 7/2) and white (10YR 8/1) hard limestone bedrock

S81TX-325-1 (Continued)

Remarks:

The upper 1 cm of the A11 horizon was sampled separately as a mulch. This material was lighter in color (10YR 2/2, 3/2 dry), had weak fine platy structure, was soft, and had a lower clay content than the bulk of the A11 horizon. Pressure faces were observed in both the A12 and B2t horizons making identification of illuviation clay films difficult in the field. This soil may be a Lithic Vertic Argiustoll, depending on COLE values determined.

Pedon: S81TX-371-1

Soil name: Upton

Classification: Typic Paleorthid; loamy-skeletal, mixed, thermic, shallow

Physiography: Mesa top, <1% slope

Elevation: 930 meters

Parent material: Hard limestone; Washita group undifferentiated

Vegetation: Rangeland; shrub species including mesquite, lechugilla and creosote bush; grasses dominantly three-awn and burrograss with lesser amounts of black grama, tobosa, rough tridens and fluffgrass

Location: Pecos County, Texas; mesa top on one of the south extensions of Big Mesa 5.2 miles east of intersection of I10 and route 67; approximately 14 miles east of Ft. Stockton (Sheet 52 in Pecos Co. Report).

Described by: M. C. Rabenhorst, L. P. Wilding, B. L. Allen, and C. L. Girdner. 22 July, 1981

Horizon	Depth (cm)	Colors for dry soil unless otherwise stated
A11	0-3	Light gray (10YR 7/2) gravelly silt loam, dark grayish brown (10YR 4/2) moist; weak thin platy breaking to moderate fine granular structure; soft; many fine roots; violently effervescent; clear smooth boundary
A12	3-16	Pale brown (10YR 6/3) gravelly silt loam, brown (10YR 4/3) moist; moderate medium subangular blocky and granular structure; slightly hard; common fine roots; approximately 35% coarse fragments most of which are fragments of fractured petrocalcic horizon which have no preferred orientation; violently effervescent; abrupt wavy boundary
Clcam	16-31	White (10YR 8/2) carbonate cemented material comprised of several sequences of laminae; some fines similar to A1 horizon present within fractures and between laminar zones; few roots within vertical fractures and between successive laminar zones

S81TX-371-1 (Continued)

- C2cam 31-62 White (10YR 8/2) and very pale brown (10YR 7/3) carbonate cemented material comprised of several sequences of laminar zones; some fine material similar to A1 horizon found between laminae; lower part contains some limestone fragments which have been incorporated into the horizon.
- R 62-75⁺ White (10YR 8/1) hard limestone bedrock

Remarks: Range in depth to the petrocalcic ranged between 10 and 20 cm. Within the petrocalcic horizon, at least 5 sets of laminae were observed, each ranging from 5-10 cm in thickness with some fine material similar to the A1 horizons occurring between them. C2cam horizon was divided into an upper and lower part for sampling.

Pedon: S81TX-371-2

Soil name: (Kimbrough) mapped as Lozier

Classification: Petrocalcic Calciustoll; coarse-loamy, mixed, thermic, shallow

Physiography: Nearly level summit of a gradually rising knob

Elevation: 1100 meters

Parent material: Hard limestone of the Washita group, undifferentiated

Vegetation: Rangeland; Brush canopy is about 18% and is dominated by white thorn acacia, creosote, lechugilla, mesquite and agarita; grass species are primarily three-awn, hairy grama, and red grama.

Location: Pecos County, Texas; Asa Stone Ranch; Approximately 30 miles west of Ft. Stockton on Rt. 290 to Huvey Rd; South on Huvey Road 10.6 miles to a fork, take east fork 1.8 miles to gate on west side of road; sampling location is on top of knob approximately 1/4 mile west of Huvey Road.

Described by: M. C. Rabenhorst, L. P. Wilding, B. L. Allen, and C. L. Girdner. 22 July, 1981

Horizon	Depth (cm)	Colors for dry soil unless otherwise stated
A11	0-3	Grayish brown (10YR 5/2) gravelly silt loam, very dark grayish brown (10YR 3/2) moist; weak thin platy parting to weak fine granular structure; soft; many fine roots; approximately 20% coarse fragments; violently effervescent; clear smooth boundary
A12	3-10	Brown (10YR 5/3) gravelly silt loam, dark brown (10YR 3/3) moist; moderate fine subangular blocky breaking to moderate medium and fine granular structure; slightly hard; common fine roots; approximately 15% coarse fragments; some thin carbonate films present along ped surfaces and the surfaces of some small stones; violently effervescent; abrupt wavy boundary
Ccam&A1	10-22	White (10YR 8/2) carbonate cemented material containing vertical fractures which are coated with secondary carbonates; the upper surface is smooth while the lower surface has pendants of secondary carbonates; within the fractures is some fine material, similar in texture and color to the A12 horizon; abrupt wavy boundary

S81TX-371-2 (Continued)

- C1cam 22-25 Pinkish white (7.5YR 8/2) and very pale brown (10YR 8/3) laminar cap material; strongly indurated and extremely hard; shows distinct horizontal laminae of <1 mm in scale; abrupt smooth boundary
- C2cam&R 25-29 Pale brown (10YR 6/3) and white (10YR 8/2) indurated carbonate material; contains some zones and fragments of hard limestone; identification of the material as petrocalcic as opposed to soft limestone is unsure
- R1 29-34 White (2.5Y 8/2) hard limestone seam with a thin (2-3 mm) coating of secondary carbonate on the upper surface
- C3cam&R 34-37 Very pale brown (10YR 8/3) indurated carbonate material surrounding fragments of pale yellow (2.5Y 8/4) hard limestone
- R2 37-42⁺ White (10YR 8/1) very hard and massive limestone bedrock

Remarks: Some large limestone boulders occur in the upper 25 cm of the pedon and are coated with 1-3 mm of secondary carbonates on all sides; Many chert fragments were noticed on the surface but not within the solum indicating their origin to be a lag concentrate. A few rhyolite pebbles were noticed on the surface. Their origin is most likely the Barrilla Mountains to the west of this site. This suggests that there may be some igneous influence on this soil.

Pedon: S81TX-385-1

Soil name: Rumple variant

Classification: Udic Haplustalf; clayey-skeletal, montmorillonitic, thermic

Physiography: Stable upland on top of a narrow divide between the Frio and Nueces rivers; <1% slope

Elevation: 715 meters

Parent material: Hard cherty limestone of the Devils River formation

Vegetation: Pasture; cedar, live oak, post oak, dropseed and three-awn

Location: Real County, Texas; Sidney Wells ranch; on Route 337, 10.25 miles west of junction with route 83 at Leaky; North of Rd. just inside the gate and 50 feet west under some trees

Described by: M. C. Rabenhorst, L. T. West, Terry J. Moore. 18 August, 1981

<u>Horizon</u>	<u>Depth (cm)</u>	Colors are for moist soil
A11	0-8	Very dark brown (10YR 2/2) cherty silty clay loam; weak medium granular structure; friable; many fine roots; neutral; clear smooth boundary
A12	8-20	Dark brown (10YR 3/2) cherty silty clay loam; weak medium subangular blocky parting to weak medium granular structure; friable; many fine roots; neutral; clear smooth boundary
B21t	20-35	Dark reddish brown (5YR 3/4) cherty clay; moderate fine subgranular blocky structure; firm; common fine and medium roots; medium continuous clay films on ped surfaces; approximately 40% chert fragments; neutral; gradual smooth boundary
B22t	35-65	Dark reddish brown (2.5YR 3/4) cherty clay; moderate medium subangular blocky structure; firm; common fine and medium roots; medium continuous clay films on ped surfaces; approximately 30% chert fragments; neutral; clear smooth boundary

S81TX-385-1 (Continued)

B3tca 65-80 Reddish brown (5YR 4/4) cherty clay; moderate medium subangular blocky structure; firm; few medium roots; medium discontinuous clay films; matrix material non-calcareous and neutral; white nodules strongly effervescent; approximately 35% chert fragments, some with carbonate coatings; abrupt irregular boundary

R 80-84⁺ Light gray (5Y 7/1 and 7/0) hard limestone bedrock

Remarks: This soil is like the Rurple but lacks a mollic epi-pedon. This soil should possibly be classified in the implied subgroup of Mollic Haplustalfs but presently Soil Taxonomy makes no such accommodation, thus requiring this pedon to be classified as an Udic Haplustalf. This pedon contains many chert fragments both within the soil and on the surface. These fragments range between 1 cm and 25 cm along the long axis.

Pedon: S81TX-435-1

Soil name: (Boracho/Kimbrough)

Classification: Petrocalcic Calciustoll; loamy-skeletal, mixed, thermic shallow

Physiography: Nearly level upland, <1% slope

Elevation: 705 meters

Parent material: Hard limestone of the Segovia member of the Edwards Limestone

Vegetation: Rangeland; shrub species mainly mesquite and various cactus species; grasses mainly perennial three-awn and Texas wintergrass; also a number of forbes present

Location: Sutton County, Texas; Lea Allison Ranch; approximately 18 miles east of Sonora, 3/4 mile South of the North Llano River; 100°20'56" W 30°31'18" N according to the Buffalo Well SE 7.5' quadrangle map. On top of a broad hill, 250 yds east of the windmill (Sheet 52 Sutton Co. Report)

Described by: M. C. Rabenhorst, L. P. Wilding, and C. L. Girdner. 24 July, 1981

Horizon	Depth (cm)	Colors for dry soil unless otherwise stated
A11	0-2	Dark brown (10YR 3/3) stony silt loam, very dark brown (10YR 2/2) moist; moderate fine and very fine granular structure; soft; many fine roots; approximately 30% coarse fragments; slightly effervescent; clear smooth boundary
A12	2-15	Very dark grayish brown (10YR 3/2) gravelly silty clay loam, very dark brown (10YR 2.5/2) moist; moderate fine subangular blocky and granular structure; hard; approximately 50% coarse fragments. Fragments are mainly petrocalcic material and limestone coated with secondary carbonates; some fine films of secondary carbonates present in the lower part of the horizon; strongly effervescent; abrupt wavy boundary

S81TX-435-1

- C1cam 15-30 White (10YR 8/1) and pinkish white (7.5YR 8/2) indurated carbonate material; fractured in upper part with vertical fractures approximately 15 cm apart; Some (<10%) brownish "B bodies" present within the carbonate material with some localized concentrations of spherical carbonate nodules approximately 2 mm in diameter; abrupt wavy boundary
- C2cam 30-34 Very pale brown (10YR 8/3) and pale brown (10YR 6/3) continuous laminar cap of secondary carbonate; actual range in thickness is 5-20 mm; abrupt boundary
- R1ca 34-39 Very pale brown (10YR 7/4) and yellow (10YR 7/6) soft limestone which has some enrichment with white (10YR 8/2) secondary carbonate
- R2 39⁺ Very pale brown (10YR 7/3) very hard limestone bedrock containing yellow (10YR 7/6) mottles
- Remarks: It is uncertain whether the limestone encountered at 39 cm was thick massive bedrock or a thinner seam of hard material.

Pedon: S81TX-435-2

Soil name: (Mereta variant)

Classification: Petrocalcic Calciustoll; clayey-skeletal, montmorillonitic, thermic, shallow

Physiography: High broad interfluvial, <1% slope

Elevation: 668 meters

Parent material: Soft limestone of the Segovia member of the Edwards formation

Vegetation: Rangeland; buffalograss and cedar

Location: Extreme SW corner of Sutton County, Texas; Bobby Martin ranch, 0.7 miles north of route 189 approximately 6 miles east of intersection with route 1989. 100°51'53" W 30°17'43" N according to the Flat Rock Draw SE, Texas 7.5' quadrangle (Sheet 90 Sutton Co. Report)

Described by: M. C. Rabenhorst, L. T. West, and Terry J. Moore. 18 August, 1981

Horizon	Depth (cm)	Colors for dry soil unless otherwise stated
A11	0-4	Very dark brown (10YR 2/2) moist, stony silty clay loam; moderate medium granular structure; friable; many fine and very fine roots; strongly effervescent; abrupt smooth boundary
A12	4-14	Very dark brown (10YR 2/2) moist, silty clay; weak medium subangular blocky breaking to weak medium granular structure; friable; many fine roots; strongly effervescent, abrupt wavy boundary
A13&Ccam	14-22	Very dark brown (10YR 2/2) moist stony silty clay; weak medium subangular blocky breaking to weak medium granular structure; friable; many fine roots between coarse fragments; approximately 60% coarse fragments; violently effervescent; abrupt wavy boundary
C1cam or Cr1	22-32	White (10YR 8/1) carbonate cemented material; massive; upper part appears case hardened; lower part also has zones which are very pale brown (10YR 7/3); clear smooth boundary

S81TX-435-2 (Continued)

C2cam or 32-45⁺ White (2.5Y 8/1) cemented carbonate material; mas-
Cr2 sive

Remarks: From field observations, it is uncertain whether the material below 22 cm is petrocalcic or soft limestone. Similar questions exist regarding the coarse fragments in the A13 horizon. Hard limestone was not encountered within the pit. A nearby caliche pit had no hard limestone within 10 ft of the soil surface. Downslope from the sampled pedon, hard limestone was exposed. Some areas in the sampling vicinity has large quantities of large coarse fragments (up to 0.5 meters across) on the surface while other adjacent areas had very little. If the carbonate material is interpreted to be petrocalcic, then the correct classification of the soil would be as a Petrocalcic Calciustoll. If however the material was considered lithic (barely digable with a spade) this soil would more correctly be classified as Lithic Calciustoll. If a lithic contact was not recognized, then the soil would be a Typic Calciustoll.

Pedon: S81TX-443-1

Soil name: Upton variant

Classification: Ustollic (Typic) Paleorthid; loamy-skeletal, carbonatic, thermic, shallow

Physiography: Stable upland divide, <1% slope

Elevation: Approximately 900 meters

Parent material: Hard fossiliferous limestone of the Santa Elena formation

Vegetation: Rangeland; brush species mainly creosotebush, Dalea sp., tasajillo, and lechuguilla; grasses include three-awn, hairy tridens, fluffgrass, chino grama, and sideoats grama

Location: Terrell County, Texas; approximately 6.5 miles SW of Sanderson; Approximate geographic grid coordinates 30°04' N, 102°29' W. On mesa top between Washboard Canyon and Hagler Canyon (Sheet 50 Terrell Co. Report)

Described by: M. C. Rabenhorst, L. P. Wilding, and C. L. Girdner. 21 July, 1981

Horizon	Depth (cm)	Colors for dry soil unless otherwise stated
A11	0-10	Very pale brown (10YR 7/3) stony silt loam, brown (10YR 5/3) moist; weak thin platy parting to moderate medium granular structure; slightly hard; many fine roots; a few biological casts present; about 20% coarse fragments, half of which are limestone coated with secondary carbonates and half of which are petrocalcic fragments, showing no preferred orientation; some filaments of secondary carbonate present; violently effervescent; clear irregular boundary
A12	10-18	Very pale brown (10YR 7/3) stony silt loam, brown (10YR 5/3) moist; weak medium granular structure; soft; common fine roots; approximately 60% coarse fragments, mostly broken fragments of petrocalcic material which is oriented horizontally; violently effervescent; abrupt irregular boundary

S81TX-443-1 (Continued)

- C1cam 18-23 Numerous sequences of hard laminar material 2-5 mm thick over pale yellow (2.5Y 8/4) massive and softer cemented carbonates 2-3 cm in thickness; this horizon contains fine earth material similar to the A1 in between the horizontal layers and flags, the total volume being less than 5%; the fine earth is very pale brown (10YR 7/3), brown (10YR 5/3) moist, with weak fine granular structure and soft consistence; few roots between flags or successive laminar sequences, mainly parallel to the laminar surfaces; abrupt wavy boundary
- C2cam 23-35 Numerous sequences of laminar and light gray (10YR 7/2) massive cemented carbonate 2-4 cm in thickness; this horizon contains <5% fine earth material similar to the A1 horizon in between layers; some primary hard limestone is incorporated in this horizon and increases in amount with depth to roughly 50%; few roots between successive laminar zones; abrupt wavy boundary
- R 35-50+ Light gray (2.5Y 7/2) and very pale brown (10YR 7/4) hard fossiliferous limestone, overlain at surface by a thin laminar cap of secondary carbonate

Remarks:

The thickness of the A11 horizon ranged from 2-10 cm in the immediate sampling area. There is substantial lateral variability in the sampling vicinity. Within 50 meters of the sampling site soils were observed which had almost no coarse fragments on the surface suggesting a position of local inwash while other areas had large areas of bedrock 2-7 meters wide exposed at the surface. Although this pedon is mapped in the Upton series, the OC values as determined in the lab are too high to meet the requirements for a Typic Paleorthid. This is however marginal since the depth to the petrocalcic horizon is 18 cm which is the break between Typic and Ustollic subgroups.

Pedon: S81TX-465-1

Soil name: Langtry variant

Classification: Lithic Calciustoll; loamy-skeletal, mixed, thermic

Physiography: Nearly level narrow upland divide, <1% slope

Elevation: 500 meters

Parent material: Hard limestone of the Devils River formation

Vegetation: Rangeland; shrub species are mainly catclaw acacia and prickly pear; grasses include sideoats grama, red grama, three-awn, Hall's panicum and hairy tridens.

Location: Val Verde County, Texas; On the Rose Ranch, 13.7 miles N of Comstock on Rt. 163, 40 yds west of fence and 50 yds S of gate.

Described by: M. C. Rabenhorst, L. P. Wilding, C. L. Girdner, and Jack Stevens. 21 July, 1981

Horizon	Depth (cm)	Colors for dry soil unless otherwise stated
A11	0-5	Grayish brown (10YR 5/2) stony silt loam, very dark brown (10YR 2/2) moist; moderate fine and medium granular structure; soft; many fine roots; slightly effervescent; 50 percent coarse fragments; clear irregular boundary
A12ca	5-18	Dark grayish brown (10YR 4/2) stony silt loam, very dark brown (10YR 2.5/2) moist; weak fine granular structure; soft; common fine roots between coarse fragments; 80 percent coarse fragments by volume, flaggy and horizontally oriented; fragments are coated with secondary carbonates ranging from 1 mm to 1 cm in thickness and coating both upper and lower surfaces; some have pendants on lower surfaces; interstices are filled with fine earth; slightly effervescent; abrupt wavy boundary
Ccam over R	18-25	Very pale brown (10YR 8/3 and 7/3) laminar cap over hard rock; laminar cap is continuous and has a maximum thickness of about 1 cm; upper surface of limestone is solution pitted

S81TX-465-1 (Continued)

R 25-35⁺ Light gray (2.5Y 7/2) hard limestone bedrock; what few fractures are present contain infillings of secondary carbonates.

Remarks: This pedon is too low in carbonates to be in a carbonatic family. For this reason, it does not fit the Langtry series or Ector series.

APPENDIX B
COLLECTION AND CHARACTERIZATION
OF AIRBORNE DUSTS IN TEXAS

Like many semi-arid and arid regions, Central and West Texas are subject to airborne dust additions to the soils. These additions occur both during dust storm events and as more gradual, continuous depositions. Warn and Cox (1951) have reported particle size and $> 2 \mu\text{m}$ mineralogy for samples collected during dust storms at Lubbock, Texas. Smith et al., (1970) have reported monthly deposition rates and limited characterization of dust collected at two Texas locations.

In the Edwards Plateau land resource area, shallow and often skeletal soils are underlain by Cretaceous limestone, marl, and calcareous shale and sandstone. Because of the shallow nature of these soils, the potential contribution of dust to the total soil material was substantial. As part of an effort to estimate the impact of airborne dust on pedogenesis in this region, dust traps were installed and monitored, and samples were characterized.

MATERIALS AND METHODS

Seven locations were selected so as to span the 500 km study while at the same time be in proximity to towns where local SCS personnel could assist in monitoring the traps (Fig. 1). Specific sites were chosen to minimize local dust inputs according to the following criteria: 1) maximum distance from any local dust source such as trails, paved and dirt roads, cultivated fields, industrial activity, etc.; 2) upwind direction (with respect to prevailing winds) of any local dust source; 3) vegetated soil surface; and 4) high landscape positions. The traps were an open bucket design as illustrated in Fig. 2. Three layers of 2.5-cm polystyrene balls were placed in the

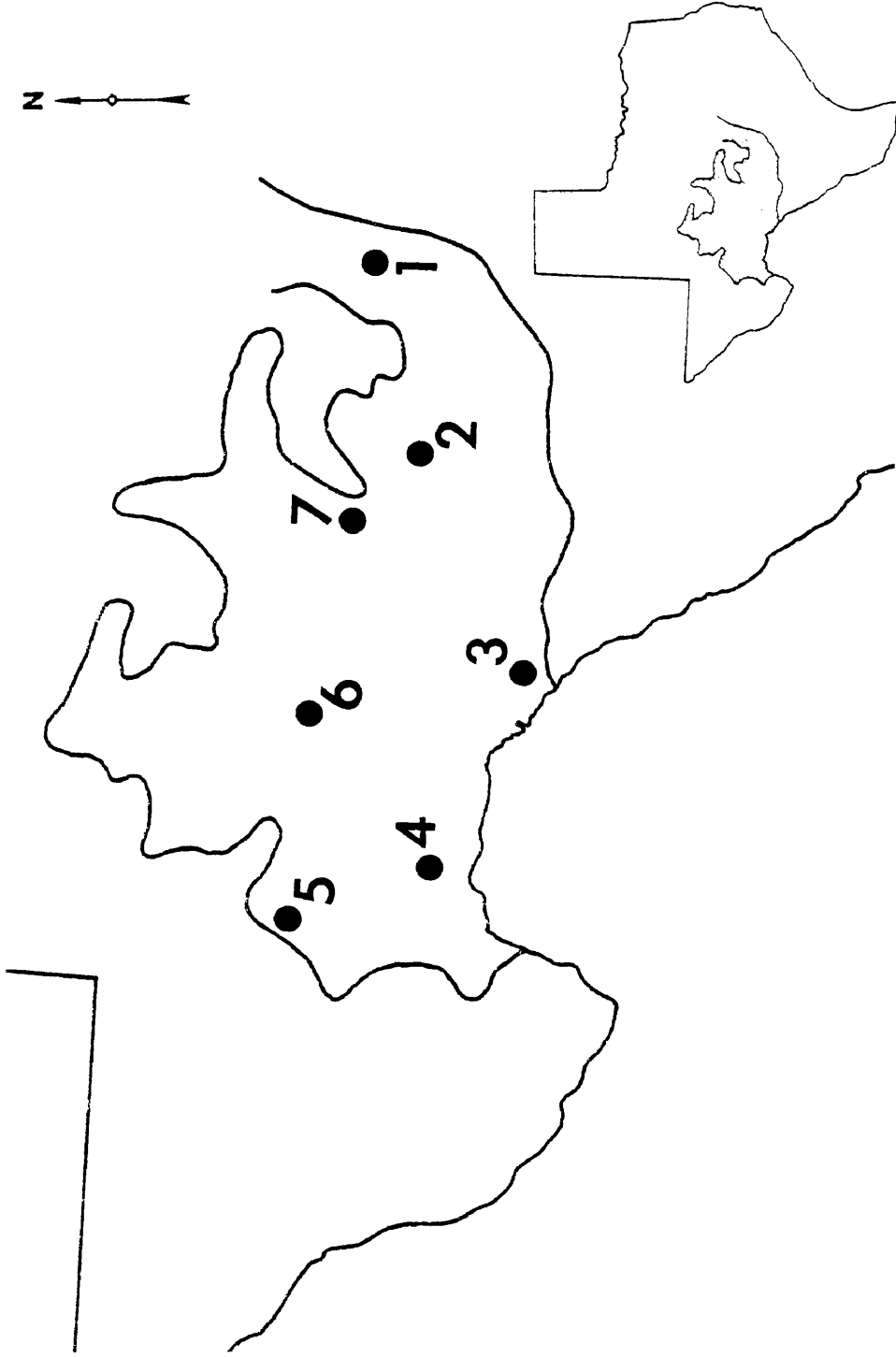


Fig. B1. Dust trap locations across the Edwards Plateau region of Central and West Texas.

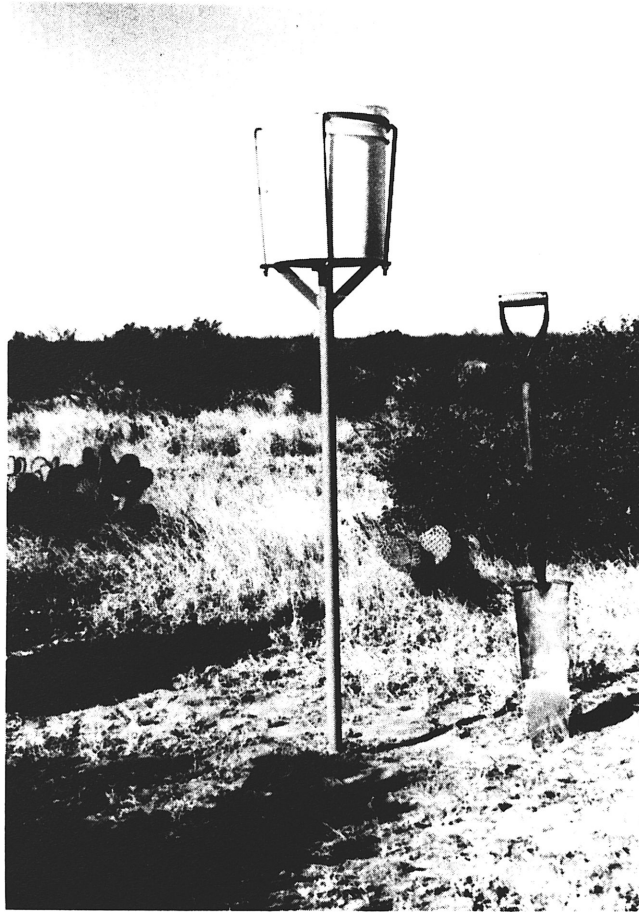


Fig.B2. Open bucket style dust trap used in this study. Top of bucket is 1.5 meters above the ground surface.

bucket to further help trap dust particles and to prevent collected dust from being carried out of the dry buckets by eddies. The tops of the buckets were situated 1.5 meters above the ground surface. Small barb-wire fences were built around the traps to protect against grazing animals. Dusts were collected every four months on or about January 1, May 1, and September 1. Dates were chosen to approximate seasonal changes in weather patterns and dust infall in Texas (Smith, et al., 1970). The buckets were removed from the support stands and liquid-tight lids were affixed while still in the field. They were then mailed directly to the laboratory for processing and analysis.

Because buckets were open, both wet and dry infall was collected. Most of the buckets contained some water (0.5 - 4 liters) when received at the laboratory. Algae and other microorganisms that had grown were removed by adding a quantity of 30% H_2O_2 to the buckets until the final solution was 6% H_2O_2 . To buckets which were dry or only slightly moist, 2 liters of 6% H_2O_2 were added. Peroxide digestion occurred for 3 to 5 weeks at room temperature. Plastic balls were then removed and rinsed with distilled water. Larger organic materials such as leaves and insects were removed by passing the suspension through a 60 mesh sieve. Upon organic matter removal, the suspension was passed through a nuclepore filter under vacuum. Solids were then transferred to 100 ml centrifuge tubes for fractionation by centrifugation and sedimentation. The silt fractions were dried at 60°C and weighed. Clays were freeze-dried and weighed. Filtrates were analyzed for Ca, Mg, Na and K by atomic adsorption or flame emission spectroscopy. Electrical conductivity measurements were also

made on filtrates. Preliminary analyses for anions showed levels too low to be meaningfully determined by wet chemical techniques, and were thus not determined.

Twenty mg-samples of clay were Mg and K saturated for each sample and plated onto glass slides for X-ray diffraction (XRD) analysis. Mg saturated specimens were placed in a desiccator over ethylene glycol before examination by XRD. K-saturated specimens were run at 25°C, and after heating to 350°C and 500°C. Random oriented mounts were used for XRD examination of silts. Selected medium silt (5 - 20 μm) samples were analyzed using scanning electron microscopy (SEM) and X-ray microanalysis (electron microprobe). Specimens were mounted on 10 mm carbon stubs and were carbon coated. Samples were examined using a JEOL JSM-35U scanning microscope equipped with energy dispersive and wavelength dispersive chemical analysis systems and interfaced with a TRACOR mini-computer.

RESULTS AND DISCUSSION

Total Dust Infall

Values for total dust infall for each location and collection period are presented in Table 1. The total quantity of sample collected during any period is quite small, making analysis somewhat difficult. An analysis of variance and subsequent application of Duncan's multiple range test showed there were no significant differences between locations. However, each of the three collection periods had total infall values significantly different from the

Table B1. Total dust infall at seven Texas locations during three collection periods in 1981.

Location	Period 1		Period 2		Period 3		Σ	
	g/bucket	g/m ²	g/bucket	g/m ²	g/bucket	g/m ²	g/bucket	g/m ²
1	.3148	4.93	.2743	4.30	.2189	3.43	.8079	12.7
2	.3979	6.24	.2150	3.37	.2606	4.08	.8736	13.7
3	.2973	4.66	.2510	3.39	.1405	2.20	.6888	10.8
4	.3339	5.23	.2641	4.14	.1697	2.66	.7677	12.0
5	.3319	5.20	.3200	5.02	.1385	2.17	.7904	12.4
6	.3105	4.87	.2475*	3.88*	.1964	3.08	.7544	11.8
7	.3255	5.10	.2910	4.56	.1807	2.83	.7972	12.5
\bar{X}	.3303	5.18	.2661	4.17	.1865	2.92	.7829	12.3

* Bucket collected after 3 months. Value reported is estimated for 4 months.

others. The greatest quantities were collected during the winter-spring period (Jan.-April). Smith et al. (1970) also showed a maximum collection during these months for their Texas location at Riesel.

The total yearly infall across the study area was about 12 g/m². This is only about half of the yearly infall reported by Smith et al. (1970) at their two Texas locations. These differences may reflect differences in collection efficiency due to trap design. More likely however, the differences are due to our traps being placed at greater height so there is less local influence (0.6 m for Smith et al., 1970; 1.5 m for this study). Gile and Grossman (1979) reported average collection rates of between 10 and 60 g/m²/yr for traps placed at 90 cm near Las Cruces, New Mexico. Quantities collected were 2 and 5 fold greater for two traps placed at 30 cm compared to those at 90 cm.

Particle Size Distribution of Dust

Particle size distribution (PSD) data are presented in Table 2. A cursory examination of this data suggests a high degree of uniformity. A chi-square test for independence indicates that PSD of the samples collected during each of the three periods were not dependent on location (not significantly different) even with α levels of 0.10, 0.20, and 0.50, respectively.

The average clay content for all three collection periods was consistently high (56-60%). Since clay-size particles are not highly subject to detachment by wind, the clay is most likely entering the traps as silt-size aggregates of clay rather than as individual particles. Due to aggregate destruction during processing, however, this cannot be verified.

The clay content of the dust is also considerably greater than in the surface horizons of surrounding soils further suggesting that the dust is not of local origin. The percentage of $< 2 \mu\text{m}$ material are somewhat greater than the 30-48% reported by Smith et al. (1970), especially since their values include all dissolved material, resulting in even lower clay percentages. The lower heights of the sampling apparatus used by Smith et al. (1970) are probably responsible for a general skewness toward a coarser PSD, as well as the greater collection rate discussed earlier.

Table B2. Particle size distribution of dust collected during three collection periods in 1981.

Location	<2 μm	2-5 μm	5-20 μm	> 20 μm
1	48.7	6.8	23.4	21.1
2	55.5	6.0	24.4	14.1
3	64.3	5.3	25.9	4.5
4	62.7	6.0	22.5	8.8
5	65.2	5.9	24.4	4.5
6	62.2	3.8	24.9	9.1
<u>7</u>	<u>61.0</u>	<u>6.4</u>	<u>24.9</u>	<u>7.7</u>
\bar{X}	60.0	5.7	24.3	10.0
1	65.6	7.6	17.5	9.3
2	54.8	5.9	33.3	6.0
3	57.6	9.3	28.9	4.2
4	55.9	5.8	28.0	10.4
5	57.1	8.8	25.7	8.5
6	57.5	7.0	23.8	11.9
<u>7</u>	<u>59.1</u>	<u>8.8</u>	<u>26.2</u>	<u>5.9</u>
\bar{X}	58.2	7.6	26.2	8.0
1	59.9	5.5	19.5	15.1
2	60.4	7.3	22.1	10.2
3	58.4	6.3	29.8	5.5
4	50.3	6.5	30.5	12.7
5	52.1	6.1	34.3	7.5
6	57.2	4.2	30.3	8.3
<u>7</u>	<u>58.2</u>	<u>4.4</u>	<u>27.3</u>	<u>10.1</u>
\bar{X}	56.6	5.8	27.7	9.9

Mineralogical Composition

Semi-quantitative interpretations of XRD analyses are presented in Tables 3 and 4. The diffraction patterns for the clay samples were somewhat difficult to interpret in that most of the clays showed poor crystallinity and/or poor orientation. The clays from all seven locations were quite uniform in composition; they were primarily mica and quartz with lesser amounts of smectite, kaolinite and feldspar. Samples collected during the 3rd period had observably greater amounts of both smectite and kaolinite.

The medium silt mineralogy was extremely uniform both among sampling locations and collection periods. This fraction was dominantly quartz with moderate amounts of alkali feldspars. Only slight differences in the presence or absence of mica and kaolinite were observed. This high degree of mineralogical uniformity for the dust samples as well as the particle size homogeneity strongly suggest that the dusts being deposited across the 500 km of this area have the same origin. Optical examination of the silts showed some opaline phytoliths to be present which would not be detected by XRD (Wilding et al., 1977; Smith et al., 1970).

No carbonate minerals were observed in any of the clay or silt fractions examined. This may be the result of either dissolution of carbonates during peroxide digestion and filtration, or to simply a lack of carbonates in the airborne material (see section on analysis of filtrates for further discussion).

Table B3. Semi-quantitative interpretations of XRD patterns for the clay (< 2 μm) mineralogy of dusts collected during three collection periods in 1981.

Location	Mica	Quartz	Smectite	Kaolinite	Feldspar
1	XXX	XXX	tr	tr	tr
2	XXX	XXX	XX	-	-
3	XXX	XXX	XX	X	-
4	XXX	XXX	tr	-	tr
5	XXX	XXX	X	X	-
6	XXX	XXX	XX	X	tr
7	XXX	XXX	XX	X	tr
1	XXX	XXX	X	tr	tr
2	XXX	XXX	tr	tr	-
3	XXX	XXX	X	X	-
4	XXX	XXX	XX	X	X
5	XXX	XXX	XX	X	tr
6	XXX	XXX	X	X	tr
7	XXX	XXX	X	-	tr
1	XXX	XXX	X	XX	-
2	XXX	XXX	X	tr	-
3	XXX	XXX	XX	XX	tr
4	XXX	XXX	XX	XX	X
5	XXX	XXX	XX	XX	tr
6	XXX	XXX	XX	XX	X
7	XXX	XXX	XX	XX	X

tr - trace
X - low <10%
XX - moderate 10-30%
XXX - high 30-70%
XXXX - dominant >70%

Table B4. Semi-quantitative interpretations of XRD patterns for mineralogy of the medium silt (5-20 μm) fraction of dust collected during three collection periods.

Location	Quartz	Na Feldspar	K Feldspar	Mica	Kaolinite
1	XXXX	X	XX	X	tr
2	XXXX	X	XX	-	tr
3	XXXX	X	XX	-	tr
4	XXXX	X	XX	-	tr
5	XXXX	X	XX	-	-
6	XXXX	X	XX	-	-
7	XXXX	X	XX	-	-
1	XXXX	X	XX	tr	-
2	XXXX	X	XX	-	-
3	XXXX	X	XX	-	-
4	XXXX	X	XX	-	-
5	XXXX	X	XX	X	-
6	XXXX	X	XX	tr	-
7	XXXX	X	XX	X	X
1	XXXX	X	XX	X	-
2	XXXX	X	XX	-	-
3	XXXX	X	XX	-	-
4	XXXX	X	XX	-	-
5	XXXX	X	XX	-	-
6	XXXX	X	XX	X	-
7	XXXX	X	XX	tr	-

tr - trace

X - low <10%

XX - moderate 10-30%

XXX - high 30-70%

XXXX - dominant >70%

SEM and Microprobe Analysis

Medium silts from sites 2, 3 and 5 collected during each of the three periods were examined using SEM and the electron microprobe for semi-quantitative chemical analysis. Grains rich in Si, Al and K (and containing little else) were considered K-feldspars, while quartz grains contained only Si. Quartz, K-feldspars and Na-feldspars (identified by the presence of Si, Al and Na) were all detected in the medium silts analyzed (although Na feldspars were less common). A variety of grain surface morphologies was observed for each mineral. Two main types of quartz were observed and representative grains are shown in Fig. 3. One group is characterized by relatively smooth surfaces and conchoidal fracture while the other is characterized by rough, pitted weathered surfaces. However, these same two morphologies were also observed for K-feldspars (Fig. 4), making mineralogical identification by morphology alone impossible. Most of the smooth grains observed were in fact K-feldspars. Some of the feldspar grains had weathered surfaces showing prominent cleavage traces which were diagnostic. The variety of forms for both quartz and feldspars may indicate multiple source areas for the dust.

Analysis of Filtrates

Values for water soluble cations from filtrates are presented in Table 5. Data have been reported on a unit area basis. On the average, total quantities of Na and K are 3-fold and 7-fold higher respectively, than estimates of elemental deposition from rainfall alone

Fig. B3. Various morphologies of quartz grains identified using the electron microprobe: A and B show smooth surfaces and conchoidal fractures; C and D show rough pitted surfaces.

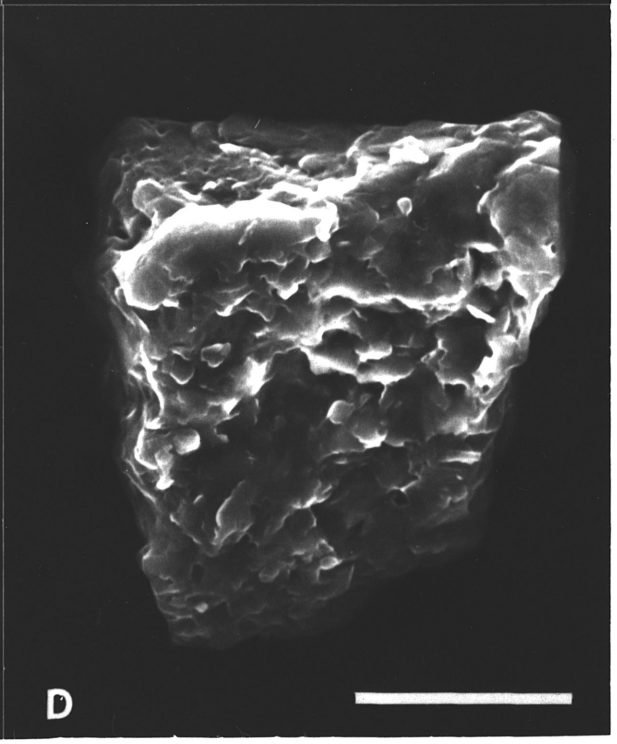
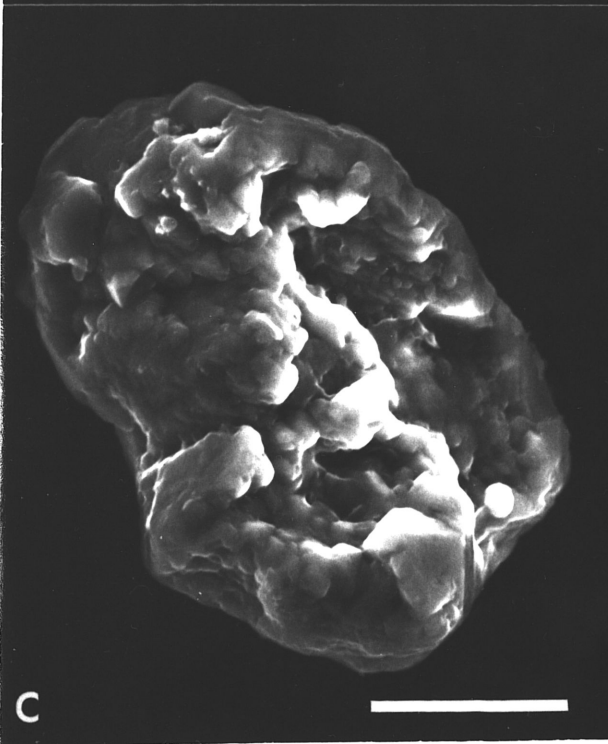
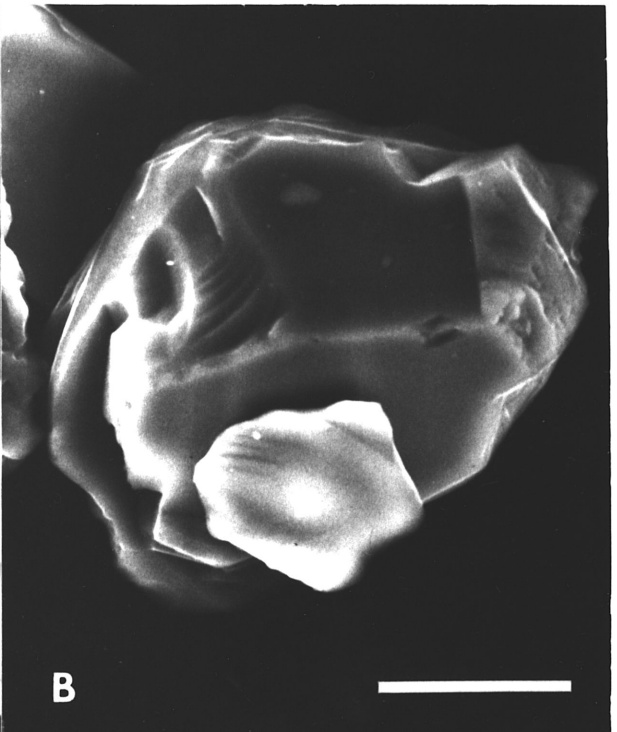


Fig. B4. Various morphologies for K-feldspar grains identified using the electron microprobe: A and B show weathering traces along well defined cleavage planes; C and D show smooth conchoidally fractured surfaces and rough pitted surfaces respectively, which are also characteristic of quartz grains observed.

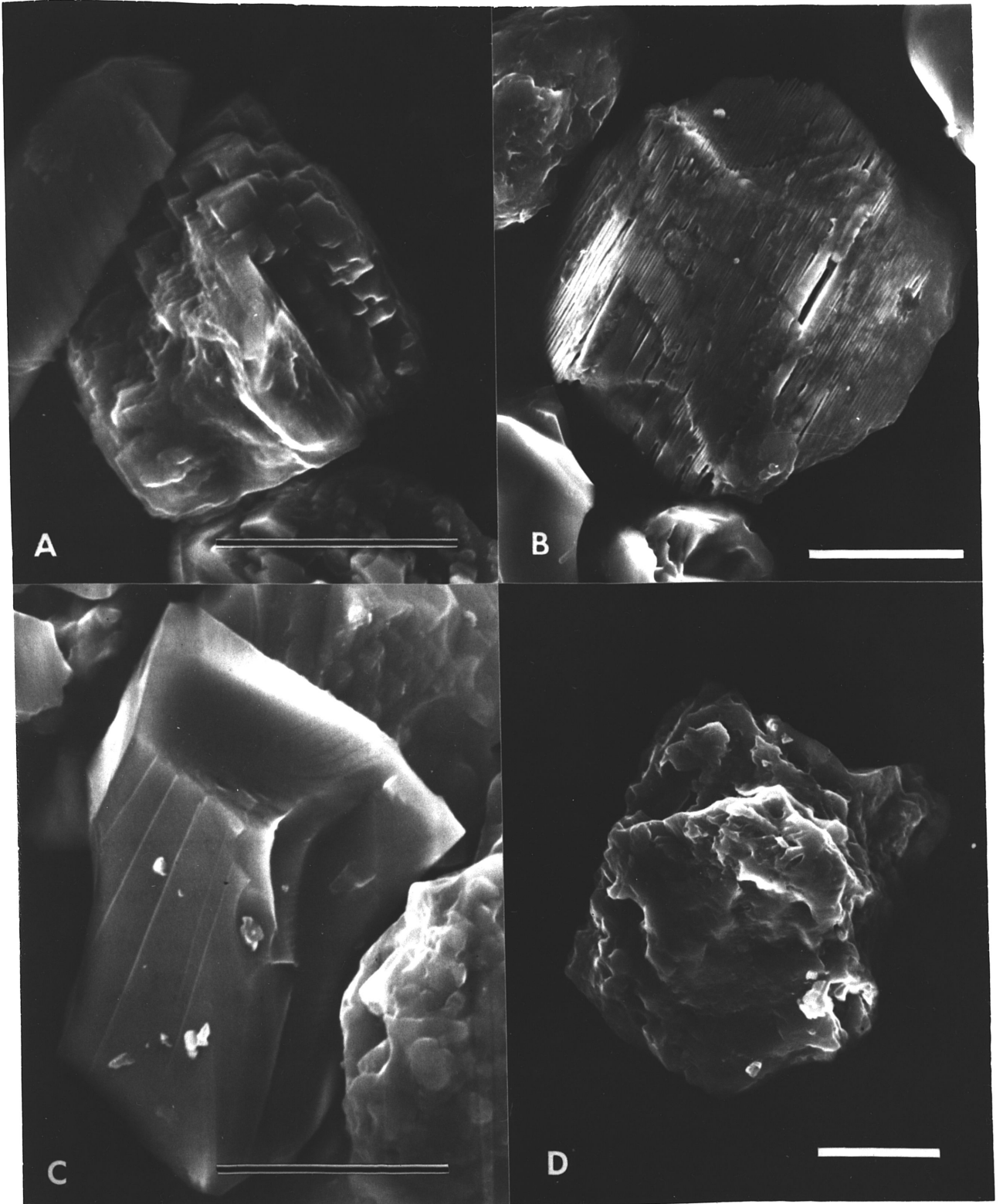


Table B5. Total water soluble cations collected at seven Texas locations during the year 1981.

Location	Ca	Mg	K	Na
	----- mg/m ² -----			
1	1090	180	980	730
2	760	110	780	890
3	830	70	300	970
4	950	70	540	1860
5	980	50	260	930
6	910	60	430	1020
<u>7</u>	<u>850</u>	<u>160</u>	<u>1060</u>	<u>730</u>
\bar{X}	910	100	620	1020

(Junge and Werby, 1958; Lodge et al., 1968). Higher values for samples may be the result of leaves, insects, pollen or other organic materials collected in the traps and partially decomposed by H₂O₂ treatment. The Ca levels in the filtrates are only 15-30% of the levels for calcite saturation, so any particulate carbonates would quickly be dissolved. Measured calcium values, however, were roughly equal to estimates expected from rainfall alone. It is possible, therefore, that much if not most of the Ca collected in the dust traps is entering as dissolved Ca and not as particulate carbonates. Furthermore, if particulate carbonates were being added with the dust and subsequently dissolving, a correlation might be expected between dissolved Ca values and total dust infall. No significant correlation exists ($r^2 = 0.002$). Therefore, if particulate carbonate is contributing to the total dissolved Ca, it must be of minor importance

relative to other sources (i.e., rainwater). If even half of the Ca were carbonate derived (which is unlikely), it would constitute only 5-13% of the total dust weight. In the desert project Gile and Grossman (1979) reported average particulate carbonate percentages ranging from 0.4 to 5.7% in dust samples collected during the dry period in New Mexico, but total Ca infall was comparable to values observed in this study.

CONCLUSIONS

The high degree of uniformity in mineralogy, particle-size distribution and total quantity for dust blown onto the Edwards Plateau region implies a common source for the dust. The present rate of addition ($12 \text{ g/m}^2/\text{yr}$) translates to approximately 1 mm/100 yrs. Although long term extrapolations should not be made from current rates, there is reason to suspect that potential impact on soil formation is significant. Comparisons with soils and residues from underlying limestones are presently necessary to assess the actual long term contribution and impact of dusts on soil development.

APPENDIX C
pH EFFECTS ON CLAY RESIDUES
DURING CARBONATE DISSOLUTION

While studying the genesis of carbonate enriched soils over Cretaceous limestone in Central and West Texas, attention was given to both carbonate and non-carbonate components in the system. In order to document parent material origin and uniformity and mineralogical transformations during pedogenesis, there was need to collect non-carbonate residues from limestone bedrock and petrocalcic horizons.

Carbonates are commonly removed from soil materials by some variation of Jackson's (1969) method employing pH 5 N sodium acetate (NaOAc) buffer. Grossman and Millet (1961) have modified this method for use with large sample sizes. Unfortunately, this procedure is quite slow, taking up to two months or longer for large samples of carbonate cemented materials. It is also estimated that roughly 40 liters of pH 5.0 N NaOAc solution would be required to dissolve 1 kg of limestone. A more rapid technique was therefore desired.

Early workers used strong acids to remove carbonates and were unaware of or unconcerned with the problem of mineral alterations of sensitive clays such as smectite (Bray, 1937; Grim et al., 1937). Attempts to overcome this problem have involved the use of complexing agents such as EDTA (Glover, 1961) and cation exchange resins (Ray et al., 1957). Ostrom (1961) treated several different clays with various concentrations of hydrochloric and acetic acids to determine "safe" concentrations. She concluded that Hectorite, a sensitive 2:1 layer mineral, was not altered by solutions of 0.3 M HOAc or 0.1 M HCl, so long as some carbonates remained present (presumably serving as a pH buffer). Incomplete dissolution, however, is risky due to microsite variability in mineralogy and porosity of the limestone which might

result in collection of a non-representative residue. Furthermore, the pH of the dissolving solution varies widely between the start and completion of the dissolution. In contrast, use of a buffered solution eliminates wide fluctuations in pH during the course of dissolution.

A more rapid dissolution of indurated materials can be accomplished by (1) grinding the sample to increase surface area, or (2) using solutions with a higher hydrogen ion activity. Increased grinding can appreciably change the particle size distribution of residues. Thus, the purpose of this study was to determine the optimum pH of a buffered acid for dissolving limestone and petrocalcic materials that would minimize reaction time without appreciable clay mineral alterations.

MATERIALS AND METHODS

Two calcareous samples known to contain smectite were selected for the study. The first (sample #1) was a Cretaceous limestone of the Segovia formation of the Edwards group collected in western Kerr County, Texas. The second sample (sample #2) was a C-horizon sampled 4 meters below the surface of Aquic Haplustoll in the Texas Coast Prairie (See Table 1 for analyses). Sample #1 was selected due to its similarity to samples to be examined during the soil genesis study mentioned previously. Sample #2 was chosen for its high smectite content. Samples were treated with NaOAc solutions of pH 5.0, 4.5, 4.0, 3.5, 3.0, and 2.5. Due to the buffering effect of NaOAc, the concentrations of the solutions were reduced in order to attain

Table C1. Percent CaCO_3 equivalent and carbonate free particle size distribution for the two samples studied.

Sample	CaCO_3	2.0-0.05 mm	0.05-0.002 mm	<0.002 mm
	%	----- % -----		
1	93.4	6.3	54.4	39.3
2	6.2	3.4	26.1	70.5

solutions of low pH. The NaOAc solutions were therefore 1, 1, 0.5, 0.5, 0.25, and 0.1 molar respectively. For sample #1, 200 g of limestone (enough to provide sufficient residue for analysis) was ground to pass a #18 sieve (1 mm) and placed in a 20 liter plastic bucket to which was added 1850 ml of NaOAc buffer solution. Large containers were used in order to contain the frothing which occurred. For sample #2, 20 g of soil (< 2 mm) was placed in a 250 ml beaker to which was added 150 ml of NaOAc buffer solution. Suspension pHs were monitored daily and maintained at the given pH by adding acetic acid. Residues were kept in the solutions for two weeks after which pHs were adjusted to 5.0 with Na_2CO_3 . High levels of Ca acetate formed during the dissolution of the limestone causing an increased buffering effect and a rise in pH. Hence, solutions for treatments at pH 3.0 and 2.5 were decanted one time after carbonates were dissolved (less than 1 day) and fresh NaOAc solution was added in order to keep the pH at the desired level. Sample #2 was treated with pH 5.5 NaOAc, 0.3 M and 3 M HOAc, and 0.1 N and 1 N HCl in addition to the NaOAc solutions discussed above. A method similar to Ostrom (1961) was used except that the carbonates were completely dissolved.

Samples were fractionated using conventional sedimentation techniques. Clays ($< 2 \mu\text{m}$) were plated onto ceramic tiles by suction and analyzed by X-ray diffraction (XRD) under the following treatments: Mg saturation, air dry (25°C); Mg saturation, ethylene glycol solvated; K saturation; air dry (25°C); K saturation, 350°C ; K saturation; 550°C . Specimens were scanned from 2° to $30^\circ 2\theta$ at a speed of $1^\circ 2\theta/\text{min}$ on a Philips X-ray diffractometer equipped with a single crystal monochromator and a theta compensating slit, using $\text{Cu K}\alpha$ radiation. The cation exchange capacity (CEC) of selected clays was determined by Ca saturation and subsequent displacement with Mg as described by Jackson (1969).

RESULTS AND DISCUSSION

X-Ray Diffraction (XRD)

Representative XRD patterns of both samples are shown in Figs. 1 and 2. Sample #1 shows substantial resistance both to expansion and collapse of the expansible components, presumably due to the presence of hydroxy-interlayers. In contrast, the smectite of sample #2 both expands upon glycolation and collapses when heated indicating little if any stable hydroxy interlayer material present. The sharpness and intensity of the $15\overset{\circ}{\text{A}}$ smectite peak when Mg saturated (air dry) and resistance to collapse of the peak to $10\overset{\circ}{\text{A}}$ when K saturated were used as criteria to evaluate acid alteration of the smectite component.

For NaOAc buffer treatments in the pH range of 5.5-2.5, no observable differences were noted in XRD patterns. Examples of XRD patterns (Mg and K air dry) for selected treatments of sample #2 are

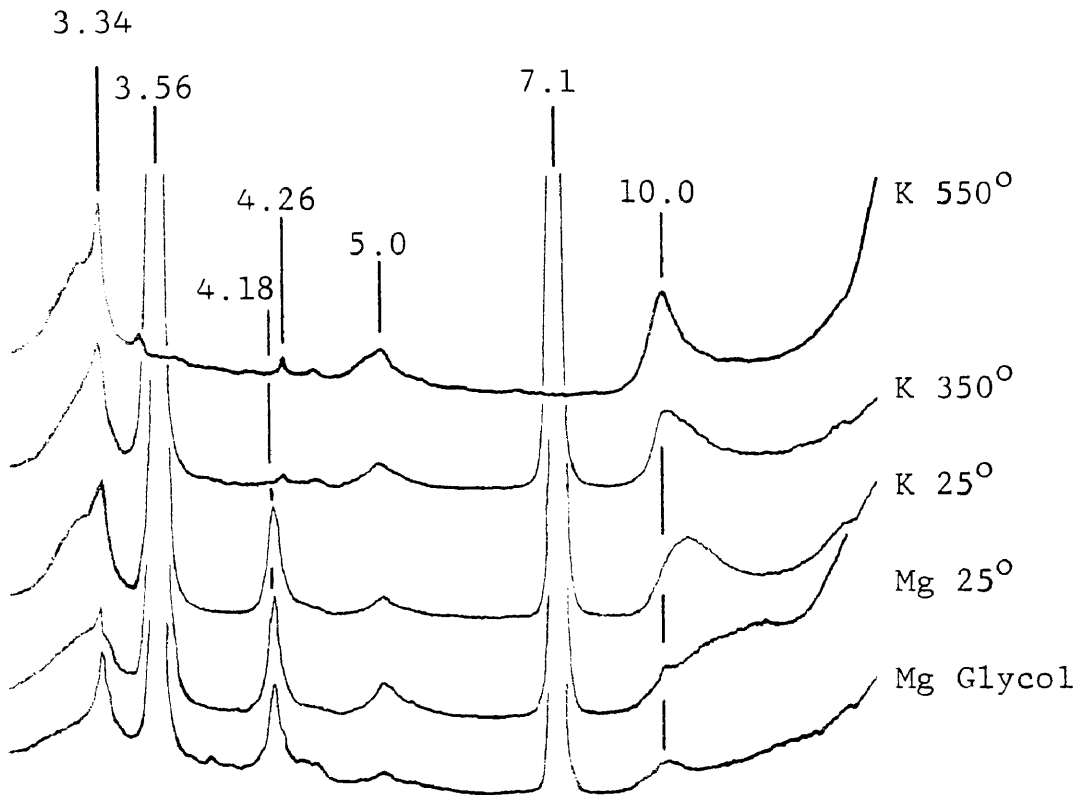


Fig. C1. Diffraction patterns for the clay (<2 μ m) fraction of the non-carbonate residue remaining after dissolution of a Cretaceous limestone (sample #1) in pH 5.0 1N NaOAc.

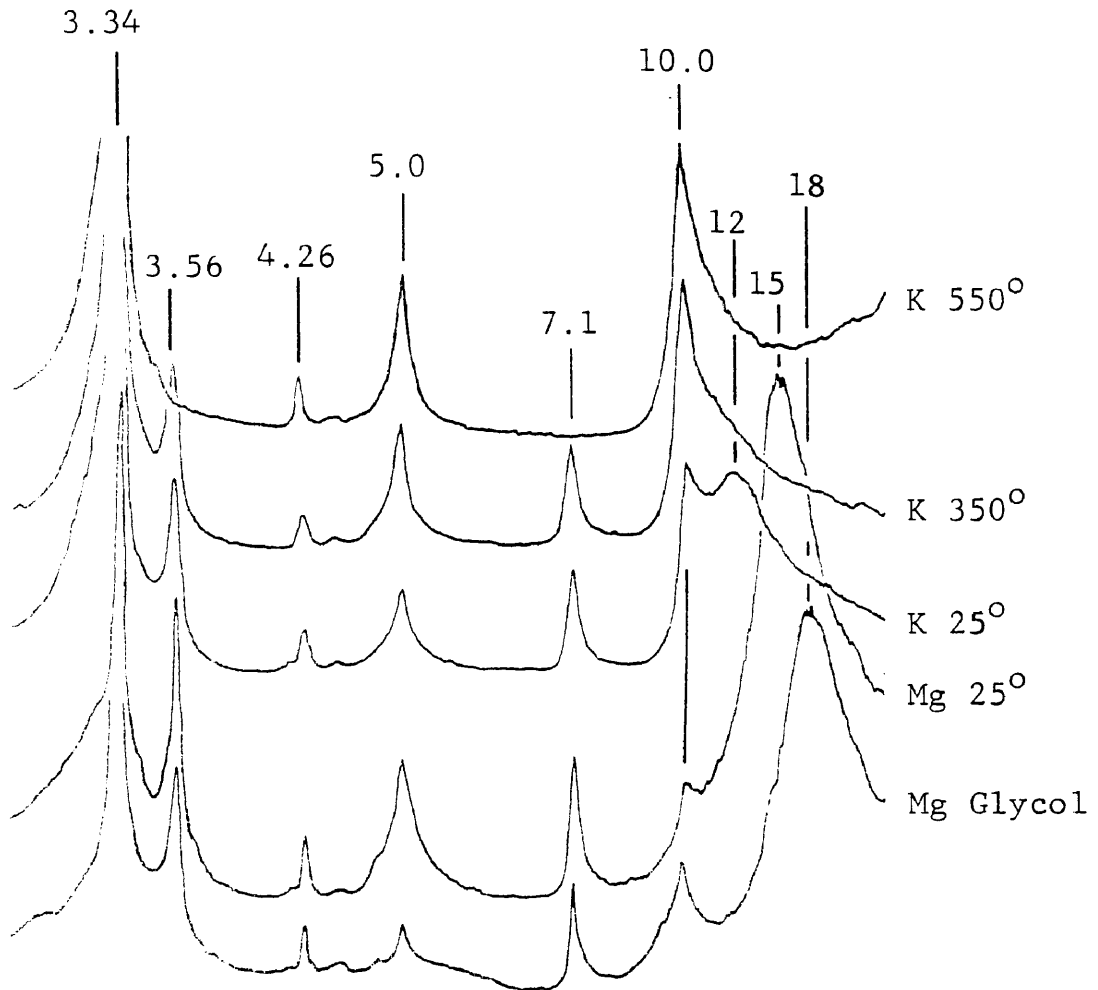


Fig. C2. Diffraction patterns for the clay (<2 μ m) fraction of a deep calcareous C horizon from an Aquic Haplustoll (sample #2) following removal of carbonates in pH 5.0 1N NaOAc.

illustrated in Figs. 3 and 4. Only the 1N HCl treatment resulted in distinct differences in XRD line profiles. The 001 smectite peak ($15\overset{\circ}{\text{A}}$) for the Mg air-dry specimen treated with 1N HCl was slightly sharper and less intense than the other treatments. The K air dry pattern for the untreated clay shows part of the smectite collapsing from $15\overset{\circ}{\text{A}}$ to $10\overset{\circ}{\text{A}}$ indicating a higher charged component, and part of the smectite only partially collapsing to a broad peak centered at approximately $12\overset{\circ}{\text{A}}$ indicating either a lower charged component or some thermally unstable hydroxy interlayers present in part of the smectite. Patterns for all samples except the 1N HCl treatment are similar. The 1N HCl treatment resulted in a smaller portion of the smectite collapsing completely to $10\overset{\circ}{\text{A}}$ and a more intense peak at $12\overset{\circ}{\text{A}}$. This is interpreted to be the result of the formation of low stability (thermally unstable) Al-hydroxy polymers in the smectite interlayers. The strong acid treatment probably caused Al to be released to solution from the clay structure. It is postulated that subsequent adjustment of the pH to 5.0 induced formation of Al-hydroxy polymers between the basal layers of the smectite. Heating the specimens to 350° caused collapse to $10\overset{\circ}{\text{A}}$ such that there were no observable differences between any of the treatments.

Cation Exchange Capacity (CEC)

Cation exchange capacity data for clays of sample #2 indicate a reduction in charge as a result of the acid treatments (Table 2). Compared to the untreated clay sample, there is a 6% reduction in CEC

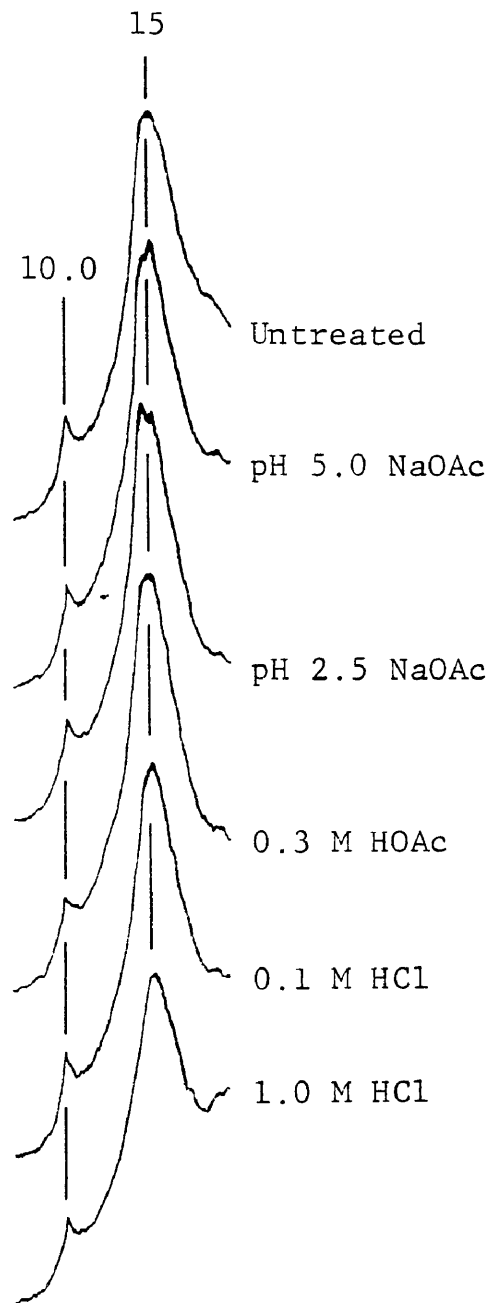


Figure C3. Diffraction line profiles for Mg-saturated air-dry clay (<2μm) specimens of sample #2 following various treatments for carbonate removal.

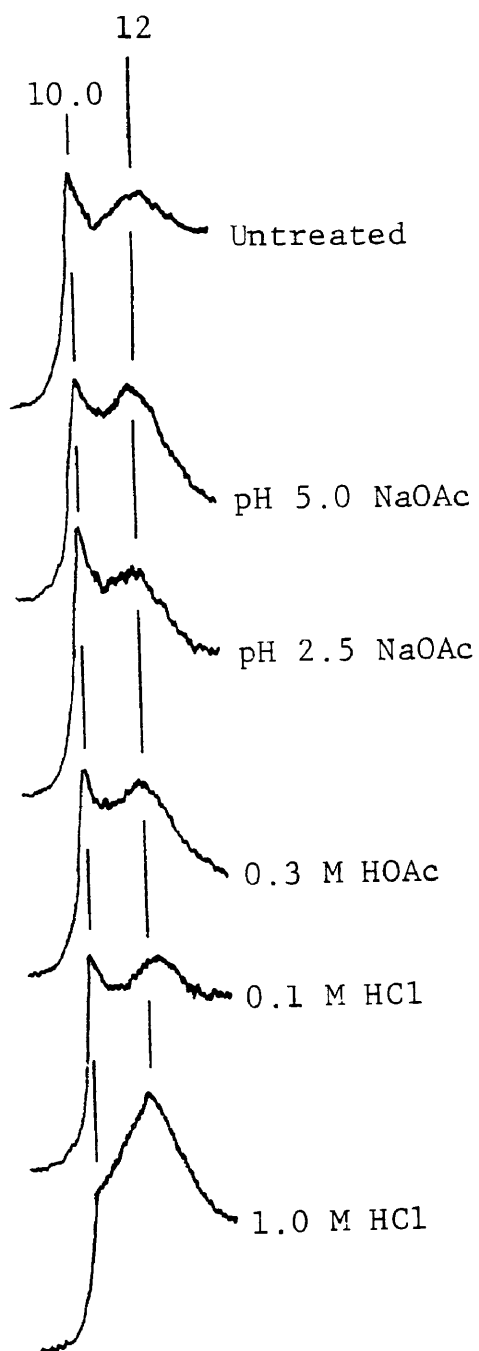


Fig. C4. Diffraction line profiles for K-saturated air-dry clay (<2μm) specimens of sample #2 following various treatments for carbonate removal.

Table C2. Cation exchange capacity values for clay fractions of samples after various treatments for carbonate removal.

Treatment	Sample 1	Sample 2
	Limestone Residue	III Cca
	-----meq/100 g-----	
Untreated	-	62.8 ± .1
pH 5.0 NaOAc	26.1 ± .1	59.0 ± .4
pH 2.5 NaOAc	28.0 ± .2	58.4 ± .5
1 M HCl	-	55.8 ± .2

as a result of removing carbonates at pH 5.0 but there is no significant change between 5.0 and 2.5. The 1N HCl treatment further reduced the CEC to 89% of the untreated sample. The initial decrease in CEC at pH 5.0 may be due to the formation of some hydroxy interlayers, although not detected by XRD. Further reduction in CEC by the 1N HCl treatment is positively correlated with formation of Al-hydroxy interlayers as discussed previously. The small increase in CEC between pH 5.0 and 2.5 of sample #1, if in fact real and not due to chance variation, may be attributed to partial removal of Al-hydroxy interlayers from the smectite. Evidence for the latter was not confirmed by XRD.

In summary, any clay mineral structural changes that are a consequence of carbonate removal by NaOAc buffered solutions appears to occur even with the least drastic treatments at pH 5.0 or 5.5. Little evidence is available that further structural alterations occur with increasing hydrogen ion activity to pH 2.5. Any structural alterations that may be occurring during these dissolution treatments were too subtle to be detected by XRD analyses. In conclusion, for the

purposes of XRD, NaOAc buffers in the pH range from 2.5 to 5.0 can be safely utilized to dissolve free carbonates for clay mineral residue analyses.

APPLICATION

Subsequent to this study 46 samples of limestone and petrocalcic horizons have been dissolved using pH 4.5 NaOAc buffer. One kg samples were ground to gravel size (< 8 mm) in order to preserve the indigenous particle size distribution of the residue. The samples were placed in 20 liter plastic buckets to which were added 4.5 liters of pH 4.5 NaOAc buffer. The pH was maintained by adding HOAc. Four liters of distilled water was added to keep calcium acetate from precipitating. Approximately 2 liters of glacial HOAc is necessary to dissolve 1 kg of limestone or petrocalcic material. Nearly all the samples (with the exception of four dolomite samples and a few samples rich in secondary silica) were completely dissolved within two weeks. This procedure drastically reduces the length of time necessary to dissolve carbonates from these materials from the 2 months or so required with pH 5.0 NaOAc buffer. The time could presumably be shortened even further by lowering the pH of the buffer.

APPENDIX D
IDENTIFICATION OF PEDOGENIC
CARBONATES USING STABLE CARBON ISOTOPES

While some pedogenic forms of carbonates such as concretions, pendants, and laminar caps are readily identifiable, in some soils formed from carbonate-rich parent materials it is often difficult to distinguish between carbonates inherited from the parent material (lithogenic) and those formed in situ (pedogenic). This is especially a problem when the carbonates occur in a massive indurated form which is easily confused with soft limestone materials or in a finely divided form distributed throughout the soil matrix.

Since the differentiation of these forms has been difficult, the accurate quantification of pedogenic carbonates has been even more elusive. This is a particular problem since this criterion is used in Soil Taxonomy in the definition of the calcic and petrocalcic horizon. Soil scientists are therefore in need of an approach to the identification of pedogenic carbonates that will be both definitive and quantitative.

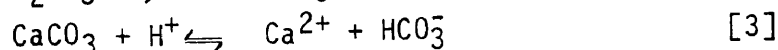
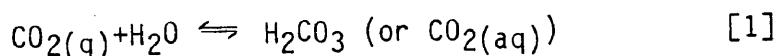
Several workers have applied stable carbon isotope methodology to the study of carbonate materials (Salomons, 1975; Salomons and Mook, 1976; Salomons et al., 1978; Magaritz and Amiel, 1980; Magaritz et al., 1981; Hendy et al., 1972; Leamy and Rafter, 1972). In their study of soil carbonates, Salomons and Mook (1976) assumed a "closed system" where equilibrium was not maintained between the soil solution and the gaseous soil CO₂. As will be discussed later, this does not well approximate most soil conditions. Magaritz and Amiel (1980) corrected these deficiencies by assuming the soil to be an "open system" where equilibrium is maintained between the soil solution and the soil CO₂ gas, thus providing for theoretically sound application to pedological studies.

The objectives of this study were: 1) to apply stable carbon isotope theory and methodology to the identification and quantification of pedogenic carbonates in soils formed over limestone in the Edwards Plateau region of Texas, and 2) to correlate isotopic determination with micromorphological observations in order to better utilize micromorphology in the differentiation of pedogenic and lithogenic carbonates.

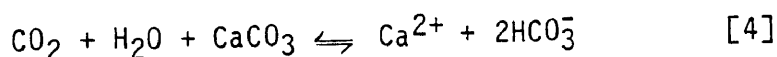
THEORY

Chemical Equilibrium

The dissolution and precipitation of calcium carbonate in an aqueous solution open to CO₂ gas can be expressed in the following equations:



These can be summarized by the single equation:



Thus, as the pCO₂ of a system increases, the solubility of CaCO₃ in that system also increases (Garrels and Christ, 1965). Also according to equation [4], half of the carbon in the dissolved HCO₃⁻ is derived from the CaCO₃, the remainder coming from the dissolved CO₂ gas.

If the system is "closed," that is, the solution containing dissolved CO₂ does not remain in contact (for chemical equilibrium)

with a reservoir of gaseous CO_2 during and after its reaction with CaCO_3 yielding HCO_3^- (aq), then the proportion of carbonate-derived carbon in the dissolved bicarbonate will remain equal to the proportion of CO_2 -derived carbon. Such is the case when rainwater enters the soil, or becomes charged with CO_2 , and then moves beneath the solum and into the groundwater where it dissolves carbonate. If, however, the system is "open," that is, the solution dissolving the CaCO_3 does remain in contact with a reservoir of gaseous CO_2 , the above relation regarding the source of carbon in the aqueous HCO_3^- no longer pertains. Rather, an equilibrium will exist between the HCO_3^- (aq) and the CO_2 (g) reservoir (Hendy, 1971). Such is the case where rainwater enters the soil, dissolves carbonate and then remains in the moist but unsaturated solum. Since the proportion of C in the CO_2 (g) reservoir is large relative to that in solution (equilibrium constant K for equation [1] is $10^{-1.47}$) (Garrels and Christ, 1965) with time, virtually all of the carbon in the HCO_3^- (aq) will have originated in the CO_2 gas. If for some reason the HCO_3^- charged soil solution was not permitted to reach equilibrium with the soil CO_2 prior to precipitation, such as might occur if a higher pH induced a more rapid precipitation or if the solution were somehow partially isolated from the soil CO_2 gas, a lower proportion of the carbonate C would have its origin in the soil CO_2 . Generally, however, once the CaCO_3 has become dissolved and is in solution as HCO_3^- , carbonate precipitation can be induced by either a lowering of the $p\text{CO}_2$ or by evaporation.

Isotopic Equilibria and Fractionation

Isotopic equilibria also exist between the various carbon containing phases of the system. The isotopic fractionation factor α between two phases A and B is defined as:

$$\alpha_{AB} = \frac{(^{13}\text{C}/^{12}\text{C})_{\text{phase A}}}{(^{13}\text{C}/^{12}\text{C})_{\text{phase B}}} \quad [5]$$

If phase A is enriched in the heavy isotope, then α will be somewhat greater than one.

According to normal physical chemical processes, an equilibrium based isotopic fractionation occurs between phases in the $\text{CO}_2\text{-H}_2\text{O-CaCO}_3$ system. This is due to differences in the molecular weight of the isotopes which affect their vibrational, rotational and translational energy components (Broecker and Oversby, 1971). Theoretical values of fractionation factors have been formulated by calculating the partition functions for the various phases (Bottinga, 1968).

Empirical values for the fractionation factors have also been measured by several workers. These values have been summarized in Table 1. Both bicarbonate and carbonate species in equilibrium with CO_2 gas are enriched in ^{13}C . Actual isotope enrichment can be calculated from the relation:

$$\alpha_{AB} = \frac{\delta^{13}\text{C}_{(A)} + 1000}{\delta^{13}\text{C}_{(B)} + 1000}$$

Table D1. Isotopic fractionation factors between phases in the system
 $\text{CO}_2 - \text{H}_2\text{O} - \text{CaCO}_3$.

PHASES A-B	α_{AB}	T°C	d α /dT°	Source
$\text{CO}_2(\text{aq}) - \text{CO}_2(\text{g})$	0.9989	25		Vogel et al. 1970
$\text{HCO}_3^-(\text{aq}) - \text{CO}_2(\text{g})$	1.0077	20		†Vogel 1961
	1.0083	25		†Abelson & Hoering 1961
	1.00838	20	-.000109	Emrich et al. 1970
	1.0076	20	-.000083	†Deuser & Degens 1967
	1.0089	14	-.00006	Wendt 1968
$\text{CaCO}_3(\text{s}) - \text{CO}_2(\text{g})$	1.010	25		†Baertschi 1957
	1.0093	22		†Vogel 1959
	1.0107	20	+.000148	‡Bottinga 1968
	1.01017	20	+.000063	Emrich et al. 1970
$\text{CaCO}_3(\text{s}) - \text{HCO}_3^-(\text{aq})$	1.00185	20	+.000035	Emrich et al. 1970
	1.0009	25		Rubinson & Clayton 1969

† After Friedman and O'Neil, 1977.

‡ Calculated

where
$$\delta^{13}\text{C} = \frac{(^{13}\text{C}/^{12}\text{C})_{\text{sample}} - (^{13}\text{C}/^{12}\text{C})_{\text{std}}}{(^{13}\text{C}/^{12}\text{C})_{\text{std}}} \times 1000 \quad [7]$$

Values are usually reported relative to those of the Pee Dee belemnite (PDB standard) (Craig, 1957).

There is also a kinetic fractionation which occurs during irreversible chemical reactions such as the photosynthetic process (Craig, 1953). This is related to the dissociation energy barrier (i.e., bond strength) which causes a discrimination against the heavy isotopes of carbon in the products (Broeker and Oversby, 1971). This results in plants with different metabolic pathways having different proportions of the carbon isotopes, and in organic carbon forms being much depleted in the heavy isotope relative to carbonate carbon.

The carbon in C_3 plants (most temperate region terrestrial plants) has $\delta^{13}\text{C}$ values in the range of -24 to -34 per mill with a mean of about -27 per mill. The carbon in C_4 plants (many arid plants, salt marsh species, and some tropical grasses) has $\delta^{13}\text{C}$ values in the range of -9 to -16 per mill with a mean of about -12 per mill. Plants with the CAM (Crassulacean Acid Metabolism) pathway are intermediate with $\delta^{13}\text{C}$ values in the range -9 to -19 per mill with a mean of -17 per mill (Hoefs, 1980). In contrast, most marine limestones have much higher $\delta^{13}\text{C}$ values. Keith and Weber (1964) reported the mean $\delta^{13}\text{C}$ of 272 selected marine limestones and fossil samples to be +0.56‰ with a standard deviation of 1.55. Fresh-water limestones had lower values (mean = -4.93‰) and were somewhat more variable (std. dev. = 2.75).

The Soil System

As a result of microbial respiration during the decomposition of organic materials and the respiration of plant roots, the $p\text{CO}_2$ of the soil air is much greater than atmospheric levels. This causes an increase in calcite solubility. While $\delta^{13}\text{C}$ values for atmospheric CO_2 usually average around -7‰ (Keeling, 1958), values for soil CO_2 are much lower. During periods of microbial activity (adequate moisture and temperatures) the isotopic ratios in the soil CO_2 generally reflect those of the soil organic matter, which in turn are dependent on the native vegetation. Rightmire and Hanshaw (1973) report $\delta^{13}\text{C}$ values for soil CO_2 closely resembling (slightly higher than) those for soil organic matter.

Within soils, the $p\text{CO}_2$ generally increases with depth (Boynton and Reuther, 1938; Lyda & Burnett, 1975; Baker & Cook, 1974). This means that CaCO_3 precipitation within the soil profile is generally not a result of a lowering of the $p\text{CO}_2$ as carbonate-charged waters move downward. Water loss through evapotranspiration is the primary mechanism in the formation of pedogenic carbonates.

As water is removed from the soil by drainage and evapotranspiration, the soil air replaces the vacated pore space. Depending on the water holding capacity of the soil, the depth of wetting and the rate of evapotranspiration, it may require a few days to several weeks for the soil to become dry. During this time, equilibrium is established and maintained between the gaseous CO_2 in the soil air and the

dissolved HCO_3^- in the soil solution. This corresponds to the "open system" described earlier.

As rainwater enters the soil and CO_2 from the soil air is dissolved, there is an isotopic fractionation such that:

$$\delta^{13}\text{C}_{(\text{CO}_2(\text{aq}))} = \delta^{13}\text{C}_{(\text{CO}_2(\text{g}))} + \varepsilon_1 \quad [8]$$

where ε_1 is the fractionation factor between $\text{CO}_2(\text{g})$ and $\text{CO}_2(\text{aq})$ (Table 1). The H_2CO_3 in the soil solution reacts with CaCO_3 from the parent material (with a given $\delta^{13}\text{C}$ value) according to equation [4]. At this point, the $\delta^{13}\text{C}$ for the $\text{HCO}_3^-(\text{aq})$ is about half way between the $\delta^{13}\text{C}$ for the parent CaCO_3 and that of the H_2CO_3 . However, since the soil solution maintains contact with the soil air, an isotopic equilibrium is established between the dissolved HCO_3^- and the CO_2 gas. The $\delta^{13}\text{C}$ for the HCO_3^- is thus independent of $\delta^{13}\text{C}$ of the parent carbonate and can be described by:

$$\delta^{13}\text{C}_{(\text{HCO}_3^-(\text{aq}))} = \delta^{13}\text{C}_{(\text{CO}_2(\text{aq}))} + \varepsilon_2 \quad [9]$$

where ε_2 is the fractionation factor between $\text{CO}_2(\text{aq})$ and $\text{HCO}_3^-(\text{aq})$.

Since the precipitation of CaCO_3 proceeds relatively slowly compared to the processes maintaining isotopic equilibrium (Hendy, 1971), as precipitation of CaCO_3 is induced by evaporation, the equilibrium between the $\text{HCO}_3^-(\text{aq})$ and $\text{CO}_2(\text{g})$ is maintained. The isotope content of the pedogenic carbonate is described by:

$$\delta^{13}\text{C}_{(\text{CaCO}_3)} = \delta^{13}\text{C}_{(\text{HCO}_3^-(\text{aq}))} + \varepsilon_3 \quad [10]$$

or

$$\delta^{13}\text{C}_{(\text{CaCO}_3)} = \delta^{13}\text{C}_{(\text{CO}_2(\text{g}))} + \varepsilon_1 + \varepsilon_2 + \varepsilon_3 \quad [11]$$

where ε_3 is the fractionation factor between $\text{HCO}_3^-(\text{aq.})$ and $\text{CaCO}_3(\text{s.})$. The isotope content of the pedogenic carbonate is therefore directly dependent on the $\delta^{13}\text{C}$ of the soil CO_2 gas plus the sum of the fractionation factors which is +10.2 ‰ (Magaritz & Amiel, 1980; Emrich et al., 1970). Since the $\delta^{13}\text{C}$ of the most marine carbonates is near zero, while that of pedogenic carbonates is considerably lower, the proportions of these two phases in the soil can be determined isotopically using an equation by Salomons and Mook (1976):

$$\% \text{ pedogenic} = \frac{\delta^{13}\text{C}_{(\text{soil})} - \delta^{13}\text{C}_{(\text{par. mat.})}}{\delta^{13}\text{C}_{(\text{ped.})} - \delta^{13}\text{C}_{(\text{par. mat.})}} \times 100 \quad [12]$$

The $\delta^{13}\text{C}$ values for the soil carbonate and parent material carbonate can be measured directly. The $\delta^{13}\text{C}$ value for the pedogenic carbonate can be calculated by measuring the $\delta^{13}\text{C}$ of the soil organic matter from which one can estimate the $\delta^{13}\text{C}$ of the soil CO_2 (gas) and subsequent application of the appropriate fractionation factor.

It should be pointed out that this "open system" is much simpler than the "closed system" mentioned earlier. Instead of the pedogenic carbonate having a fixed $\delta^{13}\text{C}$ value, dependent only on the $\delta^{13}\text{C}$ of the $\text{CO}_2(\text{gas})$ reservoir, carbonates precipitated in a closed system exhibit changing $\delta^{13}\text{C}$ values as precipitation proceeds, after the fashion of the Rayleigh distillation process (Hendy, 1971).

MATERIALS AND METHODS

The western part of the Edwards Plateau region of Texas is dominated by shallow soils underlain by Cretaceous limestone. Pedons at seven locations in this area were sampled as shown in Fig. 1. Samples from major horizons and prominent carbonate features as well as the underlying bedrock were collected and dried at 35°C. Samples from A horizons were crushed to pass a 2 mm sieve and the > 2 mm material was removed. Percent CaCO₃ was determined gasometrically using the Chittick procedure (Dreimanis, A., 1962). Carbonate and organic $\delta^{13}\text{C}$ values were determined in the Department of Oceanography, Texas A&M University, using a Nuclide 60° sector isotope mass spectrometer. Oriented clods were impregnated and thin sections were prepared for micromorphological examination.

RESULTS AND DISCUSSION

Data for the 7 pedons sampled are presented in Table 2. The $\delta^{13}\text{C}$ values for the soil organic matter, soil carbonates, and parent material carbonates were measured directly from samples collected. The percent pedogenic carbonate of total soil carbonate was calculated twice using equations 11 and 12. Values were first calculated on the assumption that the $\delta^{13}\text{C}$ of the soil CO₂ was equal to that of the soil organic matter. Since published data suggest that values for CO₂ might be slightly higher than for organic matter (Rightmire and Hanshaw, 1973) values were then calculated a second time assuming that the $\delta^{13}\text{C}$ of the soil CO₂ was 1‰ higher than that of the soil

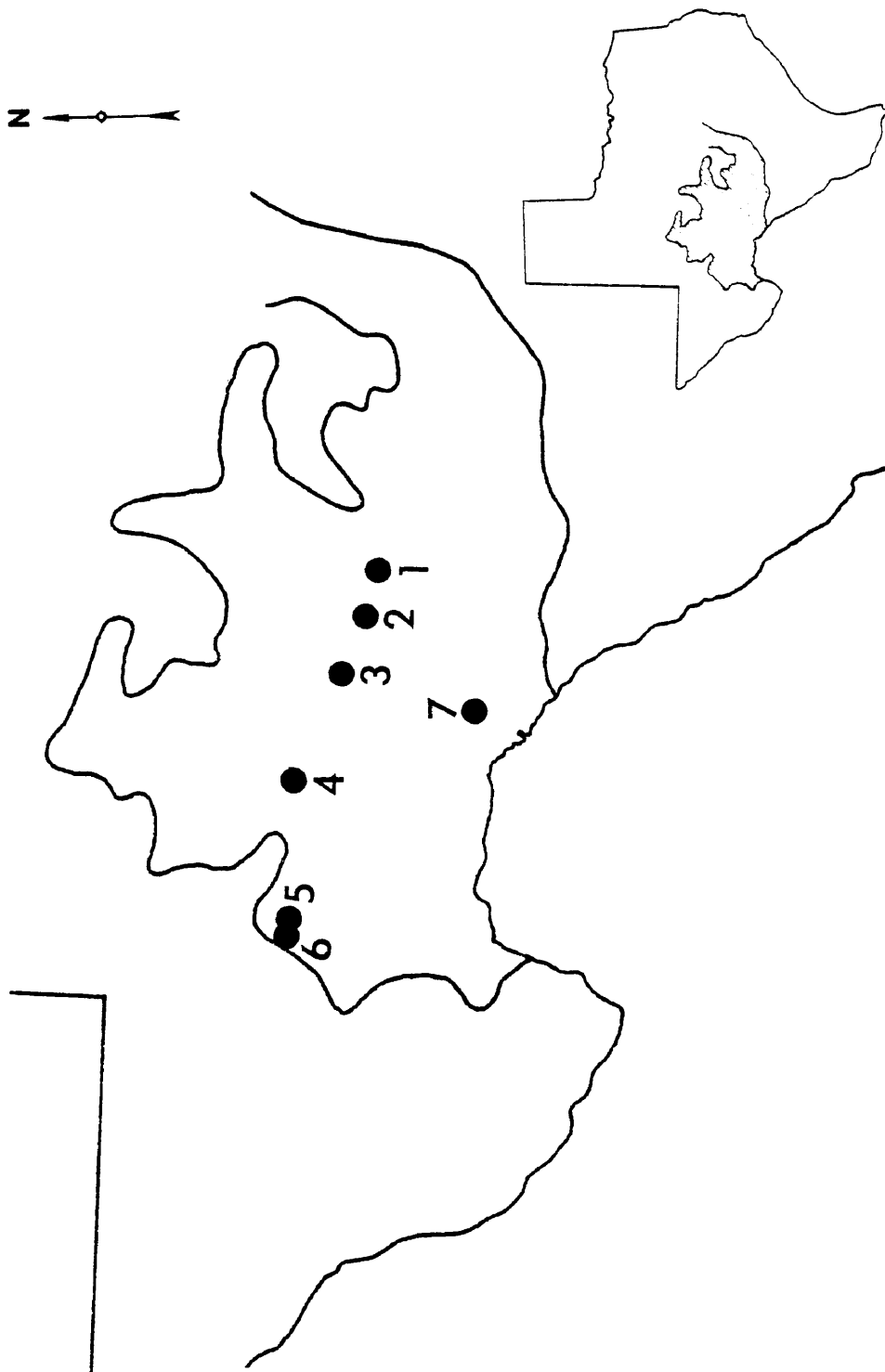


Fig. D1. Locations of seven pedons sampled for carbon isotope analysis in the Edwards Plateau land resource area.

Table D2. Percent pedogenic carbonates of total soil carbonates in seven pedons calculated using the stable carbon isotope method.

Horizon	Depth (cm)	CaCO ₃ %	Pedogenic Carbonates in Total Soil Carbonate			
			$\delta^{13}\text{C}^{\dagger}$ of Org. C. -----°/----- -----°/-----	$\delta^{13}\text{C}^{\dagger}$ of CaCO ₃	$\delta^{13}\text{C}$ of CO ₂ = org. C -----°/-----	$\delta^{13}\text{C}$ of CO ₂ 1°/-----°>Org.C -----°/-----
Site #1 (Kimble Co.)						
A11	0 - 8	25.7	-16.3	-3.9	68	80
A12	8 -12	34.9		-3.7	64	76
Ccam	12-15	85.6		-3.2	58	68
R	15+	95.5		+0.6		
Site #2 (Sutton Co.)						
A1	0 -15	10.2	-15.2	-3.1	56	73
C1cam lam- inar cap	15-18	85.4		-2.8	49	64
C1cam con- cretions	25-30	82.6		-2.1	33	42
C2cam lam- inar cap	30-31	85.4		-2.1	33	42
C2cam	31-32	89.8		-4.2	81	106
C2cam	32-34	89.3		-4.3	84	109
C3cam	34-39	94.2		-5.5	112	145
R	39+	98.5		-0.7		
Site #3 (Sutton Co.)						
A11	0 - 4	14.6	-17.1	-5.2	75	88
A12	4 -10	20.0		-5.7	82	96

Table D2. (Continued)

Horizon	Depth (cm)	CaCO ₃ %	Pedogenic Carbonates in Total Soil Carbonate			
			$\delta^{13}\text{C}^{\dagger}$ of Org. C. -----°/oo-----	$\delta^{13}\text{C}^{\dagger}$ of CaCO ₃ -----	$\delta^{13}\text{C}$ of CO ₂ = org. C ----- % -----	$\delta^{13}\text{C}$ of CO ₂ 1°/oo>Org.C -----
Alca	10-12	28.6		-4.6	65	76
R	12+	94.1		-0.4		
Site #4 (Crockett Co.)						
A1	0 - 5	27.3	-16.6	-0.2	13	15
Secondary pendants		89.9		-4.8	77	89
Ccam	5 - 9	90.4		-5.7	91	105
R	9+	95.1		+0.8		
Site #5 (Pecos Co.)						
A11	0 - 3	18.9		-1.4	31	36
A12	3 -16	23.0	-16.9	-1.7	35	40
C1cam lam- inar cap	16-17	81.9		-1.3	30	34
C1cam be- neath lam- inar cap	17-31	86.3		-4.9	77	88
C2cam lam- inar cap	31-32	82.0		-2.1	40	46
C2cam be- neath lam- inar cap	32-50	92.3		-4.8	75	87
R	62-75	94.0		+1.0		

Table D2. (Continued)

Horizon	Depth (cm)	CaCO ₃ %	Pedogenic Carbonates in Total Soil Carbonate			
			$\delta^{13}\text{C}^\dagger$ of Org. C. -----°/‰-----	$\delta^{13}\text{C}^\dagger$ of CaCO ₃	$\delta^{13}\text{C}$ of CO ₂ = org. C ----- % -----	$\delta^{13}\text{C}$ of CO ₂ 1°/‰>Org.C ----- % -----
Site #6 (Pecos Co.)						
A1	0 - 7	30.9	-17.8	-3.4	53	60
Ccam lam- inar cap	7 - 8	84.7		-1.6	32	36
Ccam be- neath lam- inar cap	8 -15	84.9		-4.6	66	75
R	15+			+1.3		
Site #7 (Val Verde Co.)						
A11	0 - 5	4.0		-3.5	56	66
A12	5 -18	4.7	-16.8	-4.4	69	80
Secondary pendants		83.0		-2.1	37	43
Laminar cap (upper)	18-19	85.8		-2.3	39	46
Laminar cap (lower)	19-20	85.6		-2.3	39	46
R	20-35+	92.8		+0.5		

† ‰ relative to PDB

organic matter. A range in values is therefore established within which the true value probably lies.

Finely Divided Carbonates

Carbonates in A horizons are for the most part disseminated and are not concentrated in nodules or concretions. The percent pedogenic carbonates in these soil carbonates is generally quite high ranging between approximately 40-90% for 5 of the pedons. These are somewhat higher values than reported for A horizons of Calciorthids of the Jordan Valley (Magaritz, 1980). Only one pedon (site #4) shows very low values (<20%). The high levels of pedogenic carbonates in the A horizons reflect repeated cycles of wetting and drying, and subsequent dissolution and reprecipitation of the carbonate phases. The dissolved and reprecipitated phases lose the character of the parent lithogenic carbonates and acquire the character of soil formed pedogenic carbonates (decreasing δ^{13} values). The values for percent pedogenic carbonates in A horizons can be converted to percent by volume using measured values for total CaCO_3 and assumed values of 1.1 and 20% for bulk density and percent by volume of coarse fragments, respectively (average values for soils in this region). These values are presented in Table 3. Three of the 7 pedons have in excess of 5% by volume pedogenic carbonates in the A horizon. These carbonates, as mentioned earlier, are not segregated into identifiable secondary forms but occur in a finely divided form. They therefore do not in themselves meet the conditions outlined in Soil Taxonomy for a calcic horizon, occurring over limestone. It must have 5% by volume of

Table D3. Percent pedogenic carbonates by volume for A horizons based on % pedogenic carbonates by volume of disseminated carbonates, an assumed bulk density of 1.1 and 20% coarse fragments.

Site	% Pedogenic carbonates by volume
1	6 - 10
2	2
3	4 - 8
4	1
5	2 - 3
6	6 - 7
7	1

identifiable secondary carbonates such as pendants, concretions or soft powdery forms (Soil Survey Staff, 1975).

Identifiable Secondary Carbonate Forms

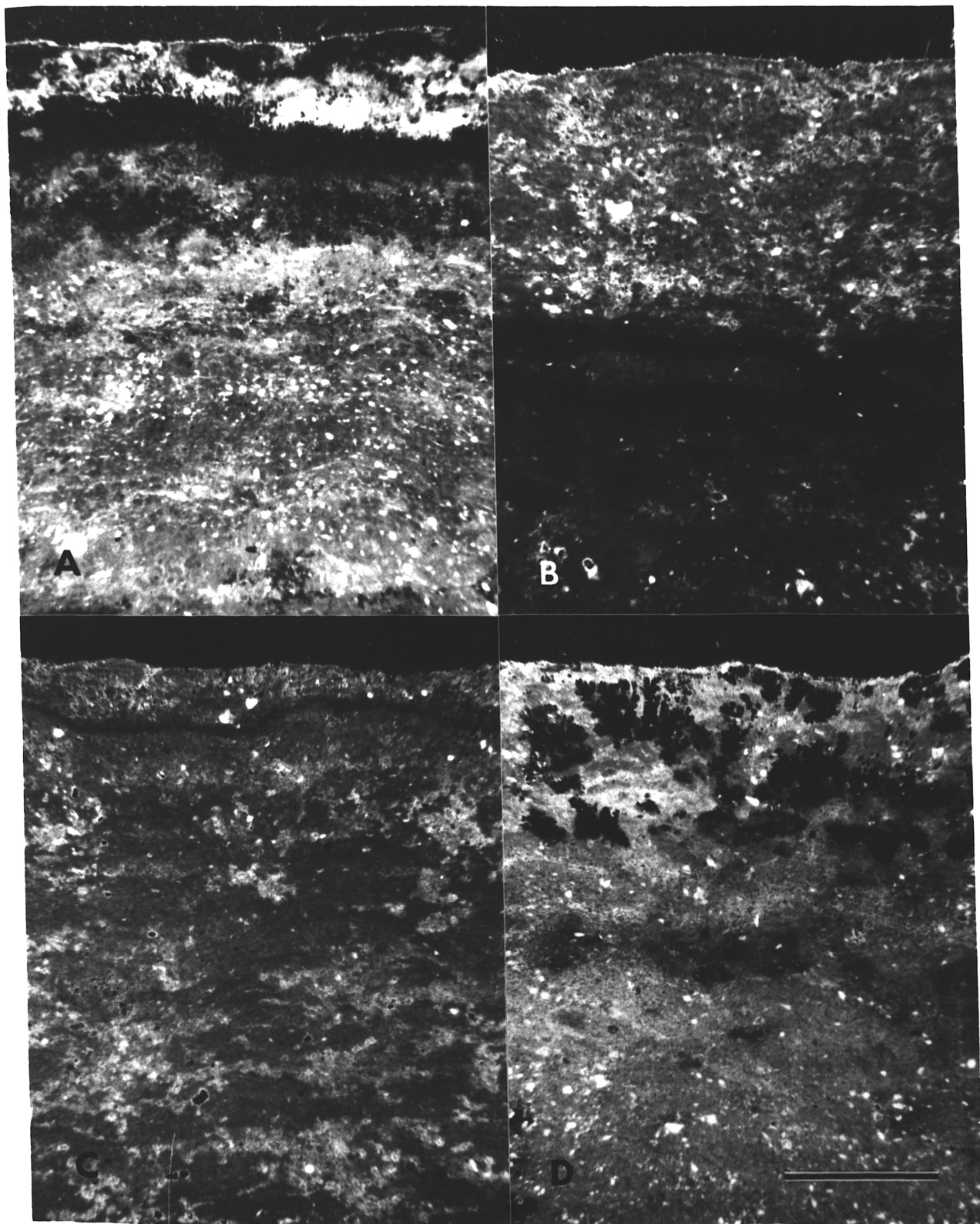
Laminar caps

Laminar cappings on petrocalcic horizons have been described by Gile et al. (1966) as the final stage (IV) in the formation of petrocalcic horizons. After a zone has become impermeable to the downward movement of carbonate enriched waters, lateral movement along this surface causes sheet or laminar like precipitation of carbonates at this interface. These easily recognizable forms range in thickness from millimeters to centimeters. Six samples of laminar caps from

four pedons (sites 2, 5, 6 and 7) were analyzed for carbon isotope ratios. In all cases, the calculated percent pedogenic carbonates was much lower than other pedogenic carbonate materials in the same pedon. In some cases, plugged materials only a few millimeters beneath the laminar cap had pedogenic carbonate percentages twice those in the laminar zone. Examination of thin-sections for these laminar zones do not reveal identifiable lithogenic carbonate forms (Fig. 2) which might have caused a lower value. Theoretically, these laminar zones should have pedogenic carbonate levels approaching 100%, rather than values in the observed range 25-46%. The consistently low values over several locations, and in several cases more than one occurrence within a given pedon, indicates that this is not an artifact of a particular location but must represent an authentic difference in the mode or environment of formation relative to other pedogenic carbonates.

Back calculations indicate the CO₂ gas in equilibrium with these precipitating laminar caps would have $\delta^{13}\text{C}$ values approximately -11.8 to -13.0‰ which are intermediate between soil organic matter ($\delta^{13}\text{C}$ of about -17‰) and atmospheric CO₂ (-7‰). Water moving through the soil upon arrival of the laminar surface may not have had sufficient time for isotopic equilibration with soil CO₂. Furthermore, the impervious nature of this laminar material causes precipitation of carbonate at the surface, rather than in protected pores. The lack of capillary pores at the surface allows more rapid drying at the surface and a subsequent rapid precipitation of carbonate (relative to soil or limestone pores which hold water by capillarity). It is postulated that this process does not permit time for

Fig. D2. Thin sections of laminar cap zones from 4 pedons. A is from site #2; B is from the Clcam of site #5; C is from site #6; D is from site #7. Note the lack of fossils and the presence of foliar laminations, quartz skeletal grains, and manganese stains. Line scale is 1 mm. Cross-polarized light.



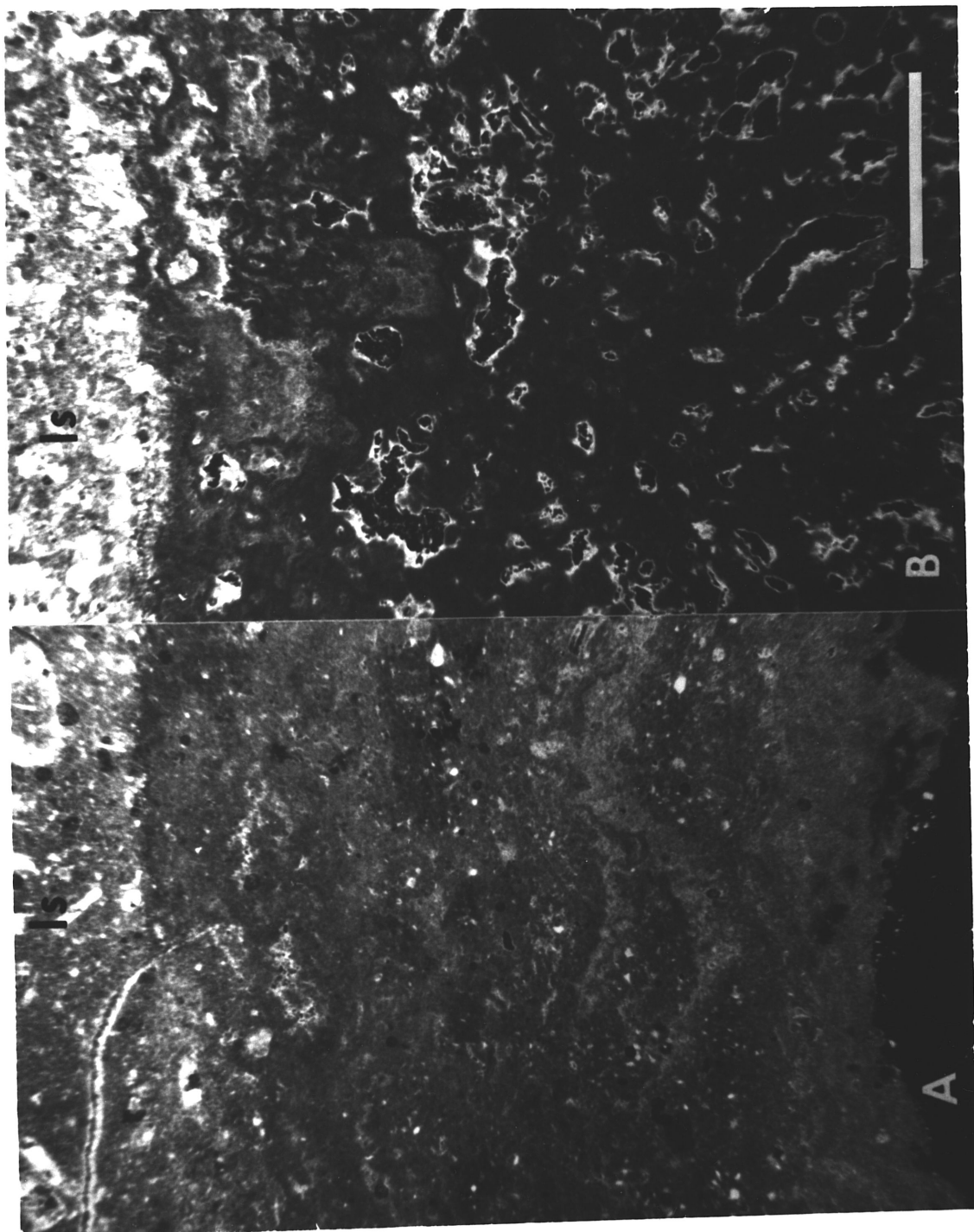
adequate isotopic exchange and for equilibrium to be reached prior to precipitation.

Secondary pendants

Carbonate charged waters adhering to the lower surfaces of gravels and cobbles within a soil often precipitate to form secondary carbonate pendants on the lower side of these fragments. Pendants from two locations (sites 4 and 7) were analyzed for carbon isotope ratios. The pendants from these two pedons had distinctly different micromorphological fabrics and distinctly different calculated values for percent pedogenic carbonates. Figure 3 shows the micro-fabrics of the two samples.

The pendants at site 7 have rather low values for percent pedogenic carbonates which are in the range observed for the laminar caps. The micro-fabric of this sample is also strongly reminiscent of the fabrics observed in the laminar caps including laminar foliations, incorporation of sand and silt size quartz and manganese stains. The mode of formation for this pendant is therefore assumed to be similar to that of the laminar caps. Pendants from site 4 have a characteristic micritic fabric which is more porous and lacks the quartz grains and manganese stains found at site 7. Higher calculated pedogenic carbonate values (77-89%) as well as the micro-fabric indicate that these pendants have a different mode of formation than those at site 7. The higher porosity of this material (and perhaps other soil characteristics) has likely permitted slower drying and precipitation of pedogenic carbonate closer to isotopic equilibrium with the soil CO₂.

Fig. D3. Thin section micrographs of secondary pendants from two different pedons. A is from site #7 and shows foliations, quartz skeletal grains, and Mn stains similar to laminar cap material; B is from site #4 and shows a characteristic convoluted fabric. Note contrast with primary limestone (1s). Line scale is 1 mm. Cross-polarized light.



Concretions

Carbonate nodules with distinctly concentric zoning are termed concretions. Concretions were observed only at site 2 and were found in a horizontal fissure between two successive layers of petrocalcic material. The $\delta^{13}\text{C}$ value for these concretions (and therefore their calculated pedogenic carbonates) is equal to that of the immediately subjacent laminar cap material (25-30%). The microfabric is also similar to the laminar caps examined. The concentric foliations are morphologically and probably genetically akin to the horizontal laminations of the laminar zone. They also show Fe and Mn staining and have sand and silt size quartz incorporated into the matrix (Fig. 4). The similarities in micro-fabric and carbon isotope ratios indicate that these concretions have formed in a manner similar to that of the laminar caps.

Massive Petrocalcic Materials

Five of the pedons sampled (sites 1, 2, 4, 5 and 6) contained massive carbonate materials which were tentatively identified in the field as pedogenic petrocalcic materials although definitive or diagnostic field evidence was not available. Many of these materials were located beneath a laminar zone. Carbon isotope analysis verifies that these carbonates were in fact dominantly pedogenic in origin ranging from 58-68% in site 1 to 91-100% in site 4. Micro-fabrics in these materials are distinctly unlike those of lithogenic limestones and include 4 characteristic types which are illustrated in Fig. 5. These

Fig. D4. Concretions found in the Clcam horizon at site #2. Note concentric laminations, quartz skeletal grains, and Fe and Mn staining. Line scale is 1 mm. Cross-polarized light.

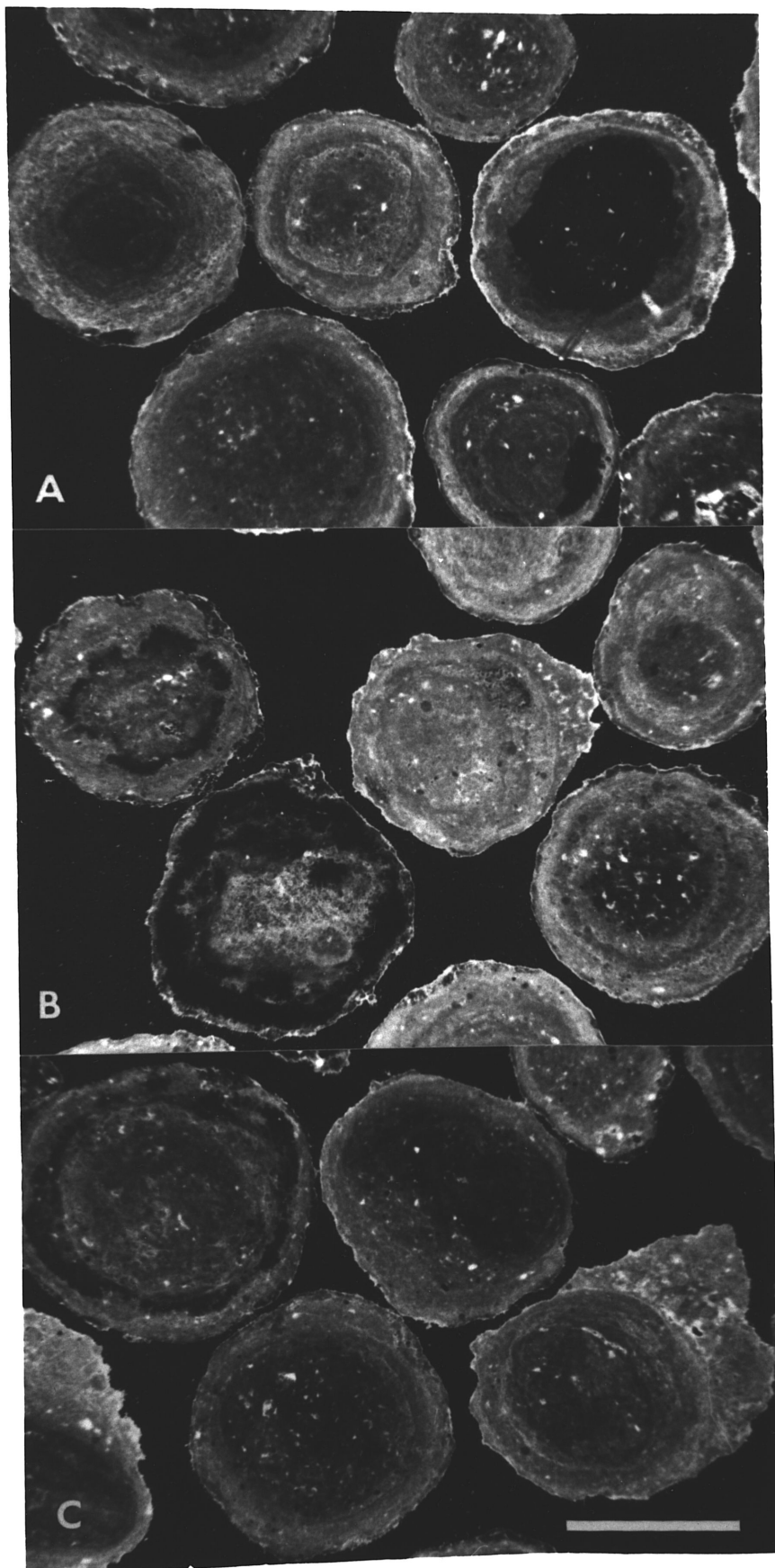
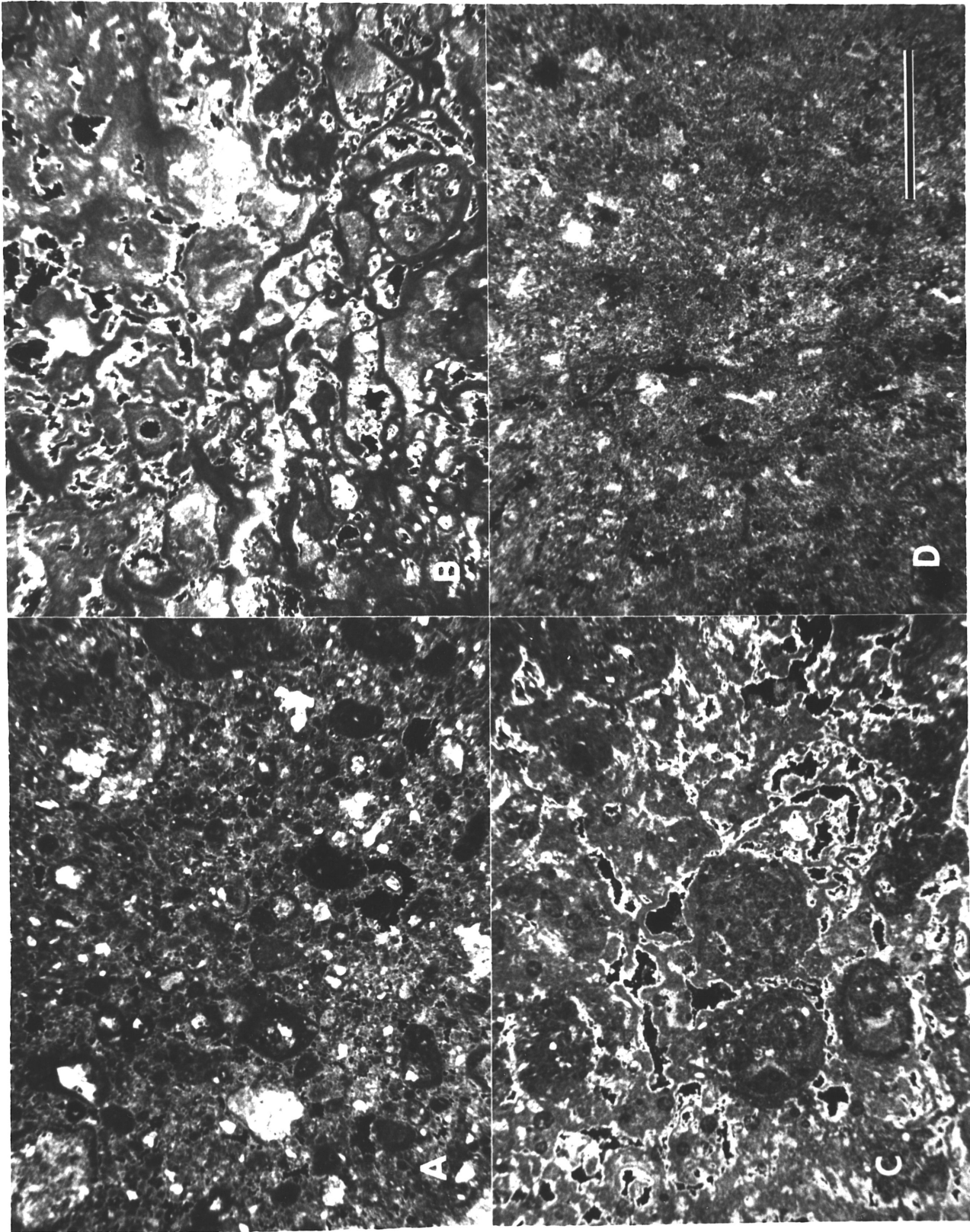


Fig. D5. Representative micro-fabrics of massive petrocalcic (pedogenic) materials. A is from the C1cam horizon of pedon #5 and shows the nodular fabric; B and C are from the C2cam and C3cam respectively of pedon #2 and show the convoluted fabric with a micritic network; C also shows the development of pisolites; D is from the C2cam of pedon #5 and illustrates the recrystallized fabric. Line scale is 1 mm. Cross-polarized light.



materials which are generally porous have provided an environment for slow carbonate precipitation (relative to the laminar cap environment) which permits more thorough isotopic exchange approaching equilibrium.

CONCLUSION

While the use of carbon isotope analysis appears to be a useful tool for the confirmation and quantification of pedogenic carbonates in soil environments, it is not without limitations. Certain pedogenic forms of carbonates such as laminar caps and some pendants and concretions, appear to form in such a manner and environment that isotopic equilibrium is not maintained with the soil CO_2 . This results in significant underestimation of the pedogenic component. Uncemented soil matrix and more porous petrocalcic materials, however, do appear to provide an environment for carbonate precipitation where isotopic equilibrium is more closely approximated.

Several distinctive micromorphological fabrics were observed in petrocalcic materials which were confirmed by isotopic analysis to be of pedogenic origin. These microfabrics may be considered to be diagnostic in the identification of massive pedogenic carbonate materials.

APPENDIX E
SOIL CHARACTERIZATION LABORATORY DATA

APPENDIX F
FREE IRON OXIDE LEVELS FOR SELECTED PEDONS AND HORIZONS

APPENDIX F

Free Iron Oxide Levels for Selected Pedons and Horizons

Lab #	Pedon	Horizon	Depth	Free Fe Oxide as Fe ₂ O ₃
			(cm)	%
1213	7	A1	0 -13	1.1
1225	15	A11	0 - 5	1.0
1226	15	A12	5 -18	1.0
1235	9	A11	0 - 3	0.4
1236	9	A12	3 -16	1.1
1260	11	A11	0 - 8	1.4
1261	11	A12	8 -20	1.1
1262	11	B21t	20-35	2.0
1263	11	B22t	35-50	2.6
1264	11	B22t	50-65	2.7
1265	11	B3tca	65-80	1.7
1277	4	A1	0 -13	1.1
1278	4	B21t	13-27	2.1
1279	4	B22t	27-41	2.9
1281	1	A11	0 - 7	2.3
1282	1	A12	7 -20	2.6
1283	1	B21t	20-31	3.4
1284	1	B22t	31-51	4.3
1287	8	A11	0 - 5	1.7
1288	8	A12	5 -19	2.1
1289	8	B2t	19-35	2.9

APPENDIX G

PARTICLE SIZE DISTRIBUTION FOR LIMESTONE
AND PETROCALCIC RESIDUES

APPENDIX G

Particle Size Distribution for Limestone
and Petrocalcic Residues

Lab #	Site	Horizon	% CO ₃ -free Residue	<.2µm	.2- 2µm	2-20µm	20-50µm	50µm- 2mm	%>2mm
----- t% -----									
1210	2	Ccam&A1	0.90	42.7	13.6	20.6	16.2	6.9	0
1211 upper	2	Ccam	1.42	37.6	14.0	21.6	19.1	7.7	0
1211 lower	2	Ccam	0.80	37.3	15.4	26.2	12.2	8.9	0
1212	2	Rca&Ccam	0.87	30.7	18.4	24.8	16.7	9.4	0
1214	7	C1cam	1.56	21.6	12.9	16.0	11.0	38.5	0.1
1215	7	C2cam	1.68	18.3	16.1	20.1	9.1	36.4	0.6
1216	7	C3cam	2.00	18.2	11.9	17.5	12.0	40.4	2.3
1217	7	C4cam	4.79	33.6	18.1	18.8	11.8	17.7	0.04
1220	6	Ccam&A1	1.51	55.4	13.9	23.1	6.9	0.7	0
1221	6	R1 lam cap	2.04	50.2	16.7	23.4	6.0	3.7	0
1222	6	R1	1.99	48.0	31.6	10.0	3.9	6.5	0
1223	6	R2	3.97	32.0	21.5	23.9	3.4	19.2	0
1224	6	R3	8.21	31.9	18.9	25.2	4.9	19.1	0.2
1227	15	Ccam	5.05	24.2	15.0	23.5	21.1	16.2	0
1228	15	R	3.05	3.0	22.5	71.7	1.6	1.2	0
1231	14	C1cam	6.19	22.1	62.4	0.2	1.2	14.1	0.4
1232	14	C2cam	4.82	13.4	46.6	31.1	2.8	6.1	0
1233	14	Ccam & R	5.74	5.7	30.5	46.9	3.2	13.7	0
1234	14	R	2.97	5.4	28.9	40.5	4.8	20.4	0
1237	9	C1cam	5.57	20.2	11.7	26.9	18.5	22.7	0.07
1238	9	C2cam	4.33	19.3	12.3	19.8	17.6	31.0	0.3
1239	9	C2cam	7.61	8.8	11.3	18.7	10.9	50.3	1.1
1240	9	R	1.30	13.3	19.1	24.0	12.8	30.8	0.3

Appendix G (Continued)

Lab #	Site	Horizon	% CO ₃ -free Residue	<.2µm	.2-2µm	2-20µm	20-50µm	50µm-2mm	%>2mm
1243	10	Ccam & A1	3.71	21.3	29.4	20.5	13.9	14.9	0.05
1244	10	Ccam lam cap	10.24	14.4	21.7	32.3	7.8	23.8	1.8
1245	10	Ccam & R	16.14	2.8	7.2	16.2	5.0	68.8	18.2
1246	10	R1	2.36	10.6	22.5	21.7	7.5	37.7	2.7
1247	10	C2cam	11.98	8.4	17.2	21.4	8.3	44.7	5.4
1248	10	R2	1.52	15.9	18.2	14.5	48.8	2.6	0
1251	12	Ccam	1.43	43.2	19.1	25.6	3.5	8.6	0
1252	12	Ccam lam cap	1.31	33.8	20.5	17.2	23.7	4.8	0
1253	12	R1ca	1.05	40.6	15.7	24.9	12.7	6.1	0
1254	12	R2	0.35	32.2	25.6	39.6	Tr	2.6	0
1257	13	A13 & Ccam	0.50	45.9	12.1	24.9	13.1	4.0	0
1258	13	Ccam	0.67	45.1	17.2	23.2	9.5	5.0	0
1259	13	Ccam	0.38	40.8	13.0	21.3	16.7	8.2	0
1266	11	R	0.49	19.5	23.5	29.0	3.2	24.8	12.1
1271	5	R upper	0.50	67.5	22.9	4.3	1.4	3.9	0
1272	5	R lower	0.38	62.9	26.1	0.5	3.5	7.0	0
1275-A	3	R1	0.26	59.9	19.3	10.1	9.5	1.2	0
1275-B	3	R1	0.62	37.4	30.1	9.0	20.2	3.3	0
1276	3	R2	0.65	18.2	6.6	2.8	71.3	1.1	0
1280	4	R	0.82	18.2	74.6	3.5	2.5	1.2	0
1285	1	R	38.80	0.8	1.9	13.5	6.6	77.2	263.0
1290 upper	8	R	1.22	58.2	23.8	12.7	3.6	1.7	0
1290 lower	8	R	0.13	20.6	54.2	20.1	Tr	5.1	0

† % by weight based on weight of <2mm fraction

APPENDIX H
LITERATURE CITED FOR APPENDICES

APPENDIX H

LITERATURE CITED FOR APPENDICES

- Baker, K. F., and R. J. Cook. 1974. Biological control of plant pathogens. W. H. Freeman and Co., San Francisco.
- Bottinga, Y. 1968. Calculation of fractionation factors for carbon and oxygen isotopic exchange in the system calcite-carbon dioxide-water. *J. Phys. Chem.* 72:800-808.
- Boynton, D., and W. Reuther. 1938. A way of sampling soil gas in dense subsoil and some of its advantages and limitations. *Soil Sci. Soc. Am. Proc.* 3:37-42.
- Bray, R. H. 1937. The significance of particle size within the clay fraction. *Amer. Ceramic Soc. J.* 20:257-261.
- Broecker, W. S., and V. M. Oversby. 1971. Chemical equilibria in the earth. McGraw Hill Co., New York. pp. 150-170.
- Craig, H. 1953. The geochemistry of the stable carbon isotopes. *Geochim. Cosmochim. Acta.* 3:53-92.
- Craig, H. 1957. Isotopic standards for carbon and oxygen and correction factors for mass-spectroscopic analysis of carbon dioxide. *Geochim. Cosmochim. Acta.* 12:133-149.
- Dreimanis, A. 1962. Quantitative gasometric determination of calcite and dolomite by using Chittick apparatus. *J. Sedimen. Petrol.* 32:520-529.
- Emrich, K. D., H. Ehalt, and J. C. Vogel. 1970. Carbon isotope fractionation during the precipitation of calcium carbonate. *Earth Planet. Sci. Let.* 8:363-371.
- Friedman, I., and J. R. O'Neil. 1977. Compilation of stable isotope fractionation factors of geochemical interest. USGS Prof. Paper 440 KK.
- Garrels, R. M., and C. L. Christ. 1965. Solutions, minerals and equilibria. Freeman, Cooper and Co., San Francisco. pp. 74-92.
- Gile, L. H., and R. B. Grossman. 1979. The desert project soil monograph: Soils and landscapes of a desert region astride the Rio Grande Valley near Las Cruces, New Mexico. SCS, USDA. U.S. Government Printing Office, Washington, D. C.
- Gile, L. H., F. F. Peterson, and R. B. Grossman. 1966. Morphological and genetic sequences of carbonate accumulation in desert soils. *Soil Sci.* 101:347-360.

- Glover, E. D. 1961. Method of solution of calcareous material using the complexing agent, EDTA. *J. Sediment. Petrol.* 31:622-626.
- Grim, R. E., J. E. Lamar, and W. F. Bradley. 1937. The clay minerals in Illinois limestones and dolomites. *J. Geol.* 45:829-843.
- Grossman, R. B., and J. L. Millet. 1961. Carbonate removal from soils by a modification of the acetate buffer method. *Soil Sci. Soc. Amer. Proc.* 25:325-326.
- Hendy, C. H. 1971. The isotopic geochemistry of speleothems. I. The calculation of the effects of different modes for formation on the isotopic composition of speleothems and their applicability as paleoclimatic indicators. *Geochim. Cosmochim. Acta.* 35:801-824.
- Hendy, C. H., T. A. Rafter, and N. W. G. MacIntosh. 1972. The formation of carbonate nodules in the soils of the Darling Downs, Queensland, Australia, and the date of the Talgai Cranium. *Proc. 8th. Int. Radiocarbon Dating Conf., Lower Hutt, New Zealand.* 417-437.
- Hoefs, J. 1980. *Stable isotope geochemistry.* Springer-Verlag, New York.
- Jackson, M. L. 1969. *Soil chemical analysis--advanced course.* 2nd. ed. Pub. by author, Dept. Soil Science, Univ. of Wisconsin, Madison.
- Junge, C. E., and R. T. Werby. 1958. The concentration of chloride, sodium, potassium, calcium, and sulfate in rainwater over the United States. *J. Meteor.* 15:417-425.
- Keeling, C. D. 1958. The concentration and isotopic abundance of carbon dioxide in rural areas. *Geochim. Cosmochim. Acta.* 13:322-334.
- Keith, M. L., and J. N. Weber. 1964. Isotopic composition and environmental classification of selected limestones and fossils. *Geochim. Cosmochim. Acta.* 28:1787-1816.
- Leamy, M. L., and T. A. Rafter. 1972. Isotope ratios preserved in pedogenic carbonate and their application in paleopedology. *Proc. 8th. Int. Radiocarbon Dating Conf., Lower Hutt, New Zealand.* 353-365.
- Lodge, J. P., Jr., J. B. Pate, W. Basbergill, G. S. Swanson, K. C. Hill, E. Lorange, and A. L. Lazrus. 1968. *Chemistry of United States precipitation: Final report on the national precipitation sampling network.* National Center for Atmospheric Research, Boulder, Colo.

- Lyda, S. D., and E. Burnett. 1975. The role of carbon dioxide in growth and survival of *Phymatotrichum omnivorum*. In G. W. Bruehl (ed.), *Biology and control of soil-borne plant pathogens*. The Amer. Phytopath. Soc., St. Paul, Minn.
- Magaritz, M., and A. J. Amiel. 1980. Calcium carbonate in a calcareous soil from the Jordan Valley, Israel: its origin as revealed by the stable carbon isotope method. *Soil Sci. Soc. Am. J.* 44:1059-1062.
- Magaritz, M., A. Kaufman, and D. H. Yaalon. 1981. Calcium carbonate nodules in soils: $^{18}\text{O}/^{16}\text{O}$ and $^{13}\text{C}/^{12}\text{C}$ ratios and ^{14}C contents. *Geoderma* 25:158-172.
- Ostrom, M. E. 1961. Separation of clay minerals from carbonate rocks by using acid. *J. Sediment. Petrol.* 31:123-129.
- Ray, S., H. R. Gault, and C. G. Dodd. 1957. The separation of clay minerals from carbonate rocks. *Am. Mineral.* 42:681-685.
- Rightmire, C. T., and B. B. Hanshaw. 1973. Relationship between the carbon isotope composition of soil CO_2 and dissolved carbonate species in groundwater. *Water Resources Res.* 9:958-967.
- Rubinson, M., and R. N. Clayton. 1969. Carbon-13 fractionation between aragonite and calcite. *Geochim. Cosmochim. Acta.* 33:997-1022.
- Salomons, W. 1975. Chemical and isotopic composition of carbonates in recent sediments and soils from western Europe. *J. Sediment. Petrol.* 45:440-449.
- Salomons, W., A. Goudie, and W. G. Mook. 1978. Isotopic composition of calcrete deposits from Europe, Africa, and India. *Earth Surf. Process.* 3:43-57.
- Salomons, W., and W. G. Mook. 1976. Isotope geochemistry of carbonate dissolution and reprecipitation in soils. *Soil Sci.* 122:15-24.
- Smith, R. M., P. C. Twiss, R. K. Krauss, and J. M. Brown. 1970. Dust deposition in relation to site, season, and climatic variables. *Soil Sci. Soc. Am. Proc.* 34:112-117.
- Soil Survey Staff. 1975. *Soil Taxonomy: A basic system of soil classification for making and interpreting soil surveys*. Agri. Handbook No. 436, SCS, USDA.
- Vogel, J. G., P. M. Grootes, and W. G. Mook. 1970. Isotopic fractionation between gaseous and dissolved carbon dioxide. *Zeitschr. Physik.* 230:225-238.

- Warn, G. F., and W. H. Cox. 1951. A sedimentary study of dust storms in the vicinity of Lubbock, Texas. *Am. J. Sci.* 249:553-568.
- Wendt, I. 1968. Fractionation of carbon isotopes and its temperature dependence in the system CO_2 -gas- CO_2 in solution and HCO_3 - CO_2 in solution. *Earth Planet. Sci. Let.* 4:64-68.
- Wilding, L. P., N. E. Smeck, and L. R. Drees. 1977. Silica in soils: Quartz, cristobalite, tridimite, and opal. pp 471-552. In J. B. Dixon and S. B. Weed (eds.), *Minerals in soil environments*. Soil Sci. Soc. Am., Madison, Wisconsin.